

**PL-TR-94-2196**

## **INFRARED PLASMA EMISSIONS**

**M.R. Hammond**

**J.V. Eccles**

**R.A. Armstrong**

**Mission Research Corporation**

**1 Tara Blvd., Suite 302**

**Nashua, NH 03062-2801**

**31 May 1994**

**Final Report**

**20 November 1989 - 31 May 1994**

**Approved for Public Release; Distribution Unlimited**

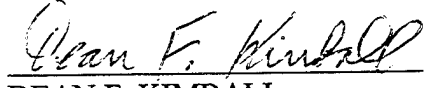


**PHILLIPS LABORATORY**  
**Directorate of Geophysics**  
**AIR FORCE MATERIEL COMMAND**  
**HANSCOM AIR FORCE BASE, MA 01731-3010**

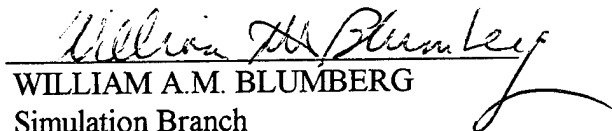
**19960404 045**

**DTIC QUALITY INSPECTED**

"This technical report has been reviewed and is approved for publication."



DEAN F. KIMBALL  
Contract Manager  
Simulation Branch



WILLIAM A.M. BLUMBERG  
Simulation Branch  
Optical Environment Division



ROGER A. VAN TASSEL, Director  
Optical Environment Division

This report has been reviewed by the ESC Public Affairs Office (PA) and is releasable to the National Technical Information Service (NTIS).

Qualified requestors may obtain additional copies from the Defense Technical Information Center (DTIC). All others should apply to the National Technical Information Service (NTIS).

If your address has changed, if you wish to be removed from the mailing list, or if the addressee is no longer employed by your organization, please notify PL/IM, 29 Randolph Road, Hanscom AFB, MA 01731-3010. This will assist us in maintaining a current mailing list.

Do not return copies of this report unless contractual obligations or notices on a specific document require that it be returned.

REPORT DOCUMENTATION PAGE			Form Approved OMB No. 0704-0188	
<p>Public reporting burden for this collection of information is estimated to average 1 hour per response, including the time for reviewing instructions, searching existing data sources, gathering and maintaining the data needed, and completing and reviewing the collection of information. Send comments regarding this burden estimate or any other aspect of this collection of information, including suggestions for reducing this burden, to Washington Headquarters Services, Directorate for Information Operations and Reports, 1215 Jefferson Davis Highway, Suite 1204, Arlington, VA 22202-4302, and to the Office of Management and Budget, Paperwork Reduction Project (0704-0188), Washington, DC 20503.</p>				
1. AGENCY USE ONLY (Leave blank)	2. REPORT DATE	3. REPORT TYPE AND DATES COVERED		
	31 May 1994	Final (20 November 1989-31 May 1994)		
4. TITLE AND SUBTITLE		5. FUNDING NUMBERS		
Infrared Plasma Emissions		PE: 61102F PR: 2310 TA G4 WU CC Contract: F19628-90-C-0025		
6. AUTHOR(S)		8. PERFORMING ORGANIZATION REPORT NUMBER		
M.R. Hammond, J.V. Eccles, R.A. Armstrong				
7. PERFORMING ORGANIZATION NAME(S) AND ADDRESS(ES)		9. SPONSORING/MONITORING AGENCY NAME(S) AND ADDRESS(ES)		
Mission Research Corporation One Tara Blvd., Suite 302 Nashua, NH 03062-2801		Phillips Laboratory 29 Randolph Road Hanscom AFB, MA 01731-3010 Contract Manager: Dean Kimball /GPOS		
10. SPONSORING/MONITORING AGENCY REPORT NUMBER PL-TR-94-2196				
11. SUPPLEMENTARY NOTES				
12a. DISTRIBUTION/AVAILABILITY STATEMENT		12b. DISTRIBUTION CODE		
Approved for public release; distribution unlimited				
13. ABSTRACT (Maximum 200 words)				
<p>In this final report, we present the infrared spectrum of a laser-produced oxygen plasma. We have focused on extending the spectral range of observation of OI Rydberg emissions to 13 <math>\mu\text{m}</math>. We report the first observations of OI Rydberg line emission in the 8-13 <math>\mu\text{m}</math> wavelength region. We also present observations of Bremsstrahlung emission that compare favorably with recent theoretical results of Lin.</p> <p>We have developed a model called APOSTLE which predicts the line-broadened emission spectrum from an OI plasma. We describe the theoretical and functional basis for the model. The model results are discussed and compared with the data obtained in the plasma experiment.</p>				
14. SUBJECT TERMS			15. NUMBER OF PAGES	
Plasma	Infrared	Emissions	Rydberg	128
Laser	Stark Broadening		Bremsstrahlung	
16. PRICE CODE				
17. SECURITY CLASSIFICATION OF REPORT		18. SECURITY CLASSIFICATION OF THIS PAGE	19. SECURITY CLASSIFICATION OF ABSTRACT	20. LIMITATION OF ABSTRACT
Unclassified		Unclassified	Unclassified	SAR

SECURITY CLASSIFICATION OF THIS PAGE

CLASSIFIED BY:

DECLASSIFY ON:

SECURITY CLASSIFICATION OF THIS PAGE

## TABLE OF CONTENTS

Chapter		Page
	PREFACE .....	vii
1.	INTRODUCTION .....	1
2.	LINUS ISSUES .....	4
3.	EXPERIMENTAL .....	5
	A. LINUS Experimental Platform .....	5
	B. Data Acquisition and Reduction .....	7
4.	OBSERVATIONS .....	8
	A. Line Emission .....	10
	B. Continuum .....	15
5.	BREMSSTRAHLUNG RADIATION .....	16
6.	APOSTLE LINE BROADENING MODEL .....	20
	A. Theory .....	20
	1. Ion Collisional Broadening .....	21
	2. Electron Impact Broadening .....	23
	3. Additional Approximations .....	28
	B. APOSTLE Model .....	29
7.	APOSTLE MODEL VS. DATA .....	36
	A. Collisionally Dominated Plasma .....	36
	B. ARCHON Chemical Kinetics Modeling .....	38
8.	SUMMARY AND CONCLUSIONS .....	40
	REFERENCES .....	43
	APPENDIX A-APOSTLE User's Manual .....	47
	APPENDIX B- Source Code .....	57
	APPENDIX C-APOSTLE Output .....	115

## LIST OF FIGURES

	Page
1. Experimental apparatus used for acquisition of a continuous 3.5-13.0 $\mu\text{m}$ emission spectrum from a laser produced oxygen plasma.....	6
2. Optical path of emission in the experiment .....	7
3. The short-dashed curve is the IR emission spectrum of the laser produced oxygen plasma at an aperture delay time of 20 $\mu\text{s}$ . The plasma was created from 110 torr O <sub>2</sub> and the measurement is at the center of the emission region. The medium-dashed curve is the continuum model and solid curve is the sum of the continuum and line emission models .....	9
4. The OI line emission spectrum was obtained by subtracting the power law fit to Lin's emissivity coefficients shown in figure 3 .....	11
5. Energy level diagram illustrating the major transitions observed in the line emission spectrum in the range 3.5-13.0 $\mu\text{m}$ .....	11
6. The electronic temperature is determined from a least squares fit to the plot of the left-hand side of eq. (5) against hcF/k. The least squares fit is shown as the solid line which is associated with an electronic temperature of $\pm 1000$ K, where the uncertainty reflects the standard deviation of the fit .....	14
7. Term diagram for the five transitions used for the electronic temperature determination and state population measurement .....	15
8. Comparison of EGG-22 and theoretical emissivity coefficients for free-free transitions in the field of neutral oxygen atom .....	19
9. Comparison of theoretical and empirical emissivity coefficients for free-free transitions in the field of a neutral oxygen atom. All values are for an electron temperature of 10,000 K. All values are relative to Lin's emissivity coefficients at 2 $\mu\text{m}$ .....	20
10. Modular design of the APOSTLE model .....	30
11. The APOSTLE calculated electric field probability distribution for ion-collisional broadening .....	31
12. Block structure of the APOSTLE <i>stark</i> module. ....	32

13.	Plot of gA as function of $\lambda$ as predicted by the APOSTLE model in the absence of collisional-Stark broadening . . . . .	33
14.	Block structure of the APOSTLE <i>linshape</i> module . . . . .	33
15.	Example of the effect of convolution of triangular instrumental line shape with a collisional-Stark broadened line. . . . .	35
16.	Comparison of the triplet Boltzmann state population distribution and the ARCHON calculation . . . . .	39
17.	Comparison of the APOSTLE predicted spectrum using collisionally-coupled state populations and the ARCHON calculated state populations. . . . .	40

## LIST OF TABLES

1.	Gratings and interference filters used to acquire a continuous infrared spectrum in the range 3.5-13.0 $\mu\text{m}$ . . . . .	5
2.	Observed line positions, assignments, calculated Einstein coefficients, and approximate line widths in LINUS IR plasma spectrum at 20 $\mu\text{s}$ . . . . .	12
3.	Measured relative populations. . . . .	14
4.	Bremsstrahlung emissivity coefficients for free-free in the field of a neutral at an electron temperature $T_e=10,000$ K. . . . .	18
5.	Bremsstrahlung emissivity coefficients for free-free in the field of a neutral at an electron temperature $T_e=25,000$ K. . . . .	18
6.	Bremsstrahlung emissivity coefficients for free-free in the field of a neutral at an electron temperature $T_e=50,000$ K. . . . .	18
7.	Model vs. Data comparison of band integrated intensities. . . . .	36
8.	ARCHON reaction set model . . . . .	38

## Preface

This final scientific report summarizes work performed for the period November 1989 to March 1994 under PL contract no. F-19628-90-C-0025. The objective of this contract was to enhance our understanding of nuclear induced atmospheric plasma processes which give rise to optical and infrared radiation emission which can impact target discrimination capabilities of surveillance acquisition and tracking systems. This objective was achieved through (1) the benchmarking of Defense Nuclear Agency's EGG-22 plasma emission code against experimental observations and recent theoretical continuum emissivity coefficients and (2) the development of the APOSTLE spectral line broadening model.

In 1980, the Air Force Phillips Laboratory (then the Geophysics Laboratory) initiated an investigation into the spectral characteristics of atmospheric plasmas. The first results were reported in Applied Optics<sup>1</sup>. It became clear with the early results that theoretical treatments for spectral line broadening in a plasma was not well developed. Thus, we developed the APOSTLE (Atmospheric Plasma Optical Spectral-Temporal Line Emission) code to describe the spectral emission characteristics of the plasmas. This code was developed in parallel with the experimental program and thus is well benchmarked against data. While subtle differences between the code predictions and the data persist, the overall agreement is excellent.

## 1. INTRODUCTION

The study of recombining laser-produced plasmas plays an important role in understanding the chemical dynamics and temporal behavior in ion-electron recombination processes in the disturbed upper atmosphere. During these processes, atomic oxygen is expected to be the strongest emitter since  $N^+$  will charge transfer with O due to its lower ionization energy. This charge transfer will then result in a persistence of a high  $O^+$  density for which recombination and radiative decay become important.

There have been few infrared spectroscopy studies of laser-produced atmospheric plasmas. Initial experiments<sup>1</sup> demonstrated that laser-produced plasmas can be used to achieve very high levels of atomic excitation. Additionally, laser produced plasmas have been shown to be strong sources of bremsstrahlung radiation.<sup>1,2</sup>

Spectral investigation of these plasmas began as early as 1964<sup>3</sup> and most of the work since then has been in the visible region.<sup>2</sup> In previous infrared studies , Laurie and Baird<sup>4</sup> and Lurie *et al.*<sup>5</sup> reported observations of IR line emission in the spectral range 1.80-3.10  $\mu m$  and 5.7-7.5  $\mu m$  from high-lying OI states (Rydberg) in a laser-produced recombining oxygen plasma. The observed OI spectral lines, particularly near 7.45  $\mu m$ , were unusually broad (0.04-0.17  $\mu m$ ) and originated from Rydberg states with the principal quantum number between 3 and 6. Brown *et al.*<sup>6</sup> measured OI transitions originating from  $n=6$  and 7 by laser absorption spectroscopy occurring at wavelengths as long as 12.35  $\mu m$ . Similarly, broad emission lines are observed by Winkelmann and Tilgner<sup>7</sup> for ArI at 4.6, 7.4, and 12.3  $\mu m$  in an argon plasma jet. These studies suggest a large Stark broadening effect for the hydrogen states, which give rise to these inter-Rydberg IR transitions. Studies of the Rydberg line emissions of alkali and alkaline-earth atoms have shown that the Stark shifts increase in magnitude as the principal quantum number of the initial energy level of the Rydberg atom increases.<sup>8</sup> In other words, as the size of the electron shell increases, the bond between the optical electron and the core becomes weaker, resulting in greater influence of the external electric fields. For an oxygen plasma, OI transition probabilities have been calculated<sup>9</sup> for  $n=7-6$  and 8-7 transitions near 12.35 and 19.1  $\mu m$ , but there are no prior published measurements.

Collisional-Stark broadening of emission lines from a relaxing plasma has been examined by a combination of spectroscopic techniques and theoretical treatments. Line shape analysis provides determinations of charged particle density and radiative transfer characteristics in stellar atmospheres, laser fusion plasmas, and laboratory discharges.<sup>10,11</sup> There is excellent agreement between experiment and theory with respect to the Stark-broadened lines of atomic hydrogen and it

is common practice to seed laboratory plasmas with hydrogen to determine electron densities.<sup>12,13</sup> Konjevic and Roberts<sup>14</sup> and Konjevic *et al.*<sup>15</sup> have critically reviewed and tabulated the experimental data of Stark widths and shifts of spectral lines of non-hydrogenic atoms. These data are compared with the extensive theoretical calculations of Griem<sup>10</sup> for the lighter elements up to Ca (as well as Cs) and with results of Dimitrijevic and Konjevic<sup>16</sup> for some heavier elements. In general, the agreement with these semi-classical calculations<sup>10,16</sup> is within 20%. For some of the heavier elements, the discrepancies are larger.

Several experiments have tested the predictions of Stark broadening theories for some plasma-broadened neutral oxygen lines.<sup>17,18,19,20,21,22,23,24</sup> Plasma sources used in these investigations include well-stabilized arcs, a gerdin-type generator, shock tubes, and RF discharges. For these LTE (local thermodynamic equilibrium) plasmas, the electronic temperature of the radiator is determined typically from absolute line intensity measurements and ranges from 10,000 K to 14,000 K. The electron density is in the range of  $(1-10)\times 10^{16}$  cm<sup>-3</sup> from H<sub>B</sub> line width measurements. There is generally good agreement (within 30%) between the experimental and calculated line widths and shifts. The comparisons for oxygen (OI) and other neutral atoms are almost entirely for spectral lines emitted in the near-UV and visible. There is little information available on Stark broadening of infrared spectral lines. Though, line widths and shifts have been measured for several ArI, NI, and SI lines in the near-IR,  $\lambda=1-2\mu\text{m}$ .<sup>21,22,23,24,25,26,27</sup> Typically these line widths are poorly predicted by theory. Stark broadening parameters have been calculated<sup>11</sup> for other non-hydrogenic atoms, particularly for isolated spectral lines of He and Na and for longer wavelengths,<sup>28</sup> but there are no experimental data with which to compare. Laboratory measurements of atomic oxygen emission line profiles between 1 and 3  $\mu\text{m}$  have been made by Assous<sup>21</sup> at an electron density of about  $3\times 10^{16}$  cm<sup>-3</sup> in an induction-heated oxygen plasma. The experimentally determined line widths and shifts are in poor to good agreement with different calculations depending on the theoretical method used. Baird and Alexiou<sup>29,30</sup> have performed Stark line broadening calculations for high angular momentum states of atomic oxygen, principally the  $n=6$  to 5 transitions near 7.45  $\mu\text{m}$ . These semi-classical calculations were used to investigate the sensitivity of the OI line widths to electron densities and temperatures.

The determinations of Stark electron-broadening parameters by existing semi-classical<sup>31,48,32,33,34</sup> or fully quantum mechanical<sup>34,35,36</sup> theoretical methods generally require heavy computational demands even for single line calculations. A large number of atomic inter-Rydberg transitions and nearby perturbing levels are required to calculate plasma broadened IR spectral line emission. To

interpret these data, an efficient, yet accurate, calculation method is needed. Due to the lack of Stark broadening parameters for OI IR transition with  $\lambda > 2 \mu\text{m}$ , a modified version of present theoretical methods is used to predict the IR spectrum of laser-produced oxygen plasma. First, the Anderson formalism<sup>37</sup> is used to produce an efficient model of electron collisional broadening. The impact approximation model is then coupled to a quasi-static model of Hooper<sup>38</sup> to account for ion collisional broadening. While previous efforts have concentrated in the visible and near-IR region of the spectrum, the present study predicts spectra over a wide spectral range. With increasing levels of approximation within the model one can obtain Stark broadened spectra over a large spectral range with decreasing computational demands.

In this final report we present the infrared spectrum of a laser-produced oxygen plasma. We have focused on extending the spectral range of observation of OI Rydberg emission to 13  $\mu\text{m}$ . We report here the first observations of OI Rydberg line emission in the wavelength region 8-13  $\mu\text{m}$ . Additionally, we present observations of Bremsstrahlung radiation that compare favorably in shape and magnitude with recent theoretical emissivity coefficients by Lin<sup>39</sup> for free-free transitions in the field of a neutral oxygen atom. The data are also compared to the continuum theories of John and Williams<sup>40</sup> and Geltman<sup>41</sup> as well as the empirical values of Taylor and Caledonia.<sup>42</sup>

We have developed a model to predict the plasma OI line emission spectrum. We describe here the theoretical basis and the functionality of the model. The line emission model is used in conjunction with Lin's<sup>39</sup> emissivity coefficients to characterize the plasma conditions. These results are compared to the data and discussed in the rest of this report. In Chapter 2, the issues addressed under this contract are described. In Chapter 3, the experimental apparatus used in this study is described and procedures for data reduction is outlined. The observations are presented in Chapter 4. In Chapters 5 and 6, we present the validation of EGG-22 through comparison with Lin's emissivity coefficients and we describe the APOSTLE line emission model. The results of line and continuum emission modelling are compared with the data in the Chapter 7. Finally, a user's manual for the model is included in Appendix A. In Appendix B, we list the source code and in Appendix C, we list APOSTLE predicted line positions and Einstein coefficients.

## 2. LINUS ISSUES

Previous work on the LINUS project motivated the need to extend the spectral range of observation to validate existing plasma radiance models. The extended range allowed us to investigate more completely the behavior of continuum emission from a laser produced oxygen plasma. This investigation was parallel to the development of new emissivity coefficients for electron-neutral collisions for atomic oxygen. The data reported herein is in good agreement with these new coefficients and provided benchmarking for the EGG-22 plasma radiance model.

The literature review also revealed a lack of information on the subject of collisional-Stark broadening of OI infrared lines. Thus we developed a computationally efficient model of collisional Stark broadening of line emissions from atomic oxygen within a laser-induced plasma. The model is based on a combination of earlier theories of Stark broadening and is in good agreement with previous experimental and theoretical works. The model was used to generate spectra for a wide range of parameters. The comparison of the many numerically computed spectra and the experimentally measured spectral emissions provided estimates of OI electronic temperature and electron density and temperature. Finally, application of the model to the LWIR region of the OI spectrum shows Stark broadening effects from collisional broadening in lower density plasmas ( $N_e \sim 10^{13} \text{ cm}^{-3}$ ).

The goal of this investigation was to validate the EGG-22 plasma radiance model. The data presented in this final report was acquired using the LINUS experiment at Phillips laboratory. In particular, the issues addressed in this contract were

1. Parametric Issues: The parameters used to characterize the plasma conditions are O-atom density, electron density, electron temperature, and emitter electronic temperature. The electronic temperature is derived from the continuum subtracted spectrum. In conjunction with Saha equilibrium, the simultaneous fit of the continuum and line emission models give the best parameter estimates that describe the plasma conditions.
2. Thermalization issues: OI Rydberg states are collisionally coupled when there are a sufficient number of thermalizing collisions. State populations are measured in the observed line emission spectrum. Complete Local thermodynamic equilibrium (LTE) is not expected to occur in the plasma but Saha equilibrium is expected. Spectral calculations were performed

using the ARCHON chemical kinetics code to model state populations of a recombination model where deviations from equilibrium are expected.

3. Validation of EGG22: The EGG-22 plasma radiance model is compared with Lin's theoretical emissivity coefficients for e-O collisional interactions. These new coefficients are also compared to data and to previous theories.
4. LWIR line emission observation: We have extended the spectral of OI line emission observation to 13  $\mu\text{m}$ . First observations of composite lines occurring at 10.4 and 12.35 are reported here.

### 3. EXPERIMENTAL

#### A. LINUS Experimental Platform

The apparatus used for this study is similar to that used by Lurie and Baird<sup>4</sup> and is illustrated in Figure 1. The apparatus was used to acquire a continuous infrared spectrum from 3.5-13.0  $\mu\text{m}$ . The beam from a Quanta-Ray Nd:YAG laser (model DCR 1A,  $\lambda=1.064$  mm, 10 ns fwhm multilongitudinal pulse, 10 Hz repetition rate) was propagated in the plane of the optical table, deflected vertically using a corner cube prism, and focused with a 51 mm focal length biconvex lens into a cubical cell fitted with uncoated ZnSe windows.

The radiation from the laser-produced plasma was collected at 90° to the laser beam axis and imaged onto the entrance slit of a 0.5 m f/6.9 grating monochromator (SPEX Industries Model 1870) using two 100 mm focal length uncoated ZnSe plano-convex lenses. Two gratings and three filters were used to cover the broad spectral range. The combinations are given in Table 1. The long-pass filters were used to block higher-order emissions.

Table 1. Gratings and interference filters used to acquire a continuous infrared spectrum across the spectral range 3.5-13.0  $\mu\text{m}$ .

Spectral Region ( $\mu\text{m}$ )	Long-pass Filter ( $\mu\text{m}$ )	Grating
3.5-6.3	3.3	150 grooves/mm
6.3-8.0	6.1	150 grooves/mm
6.3-13.0	6.1	75 grooves/mm
8.0-13.0	8.8	75 grooves/mm

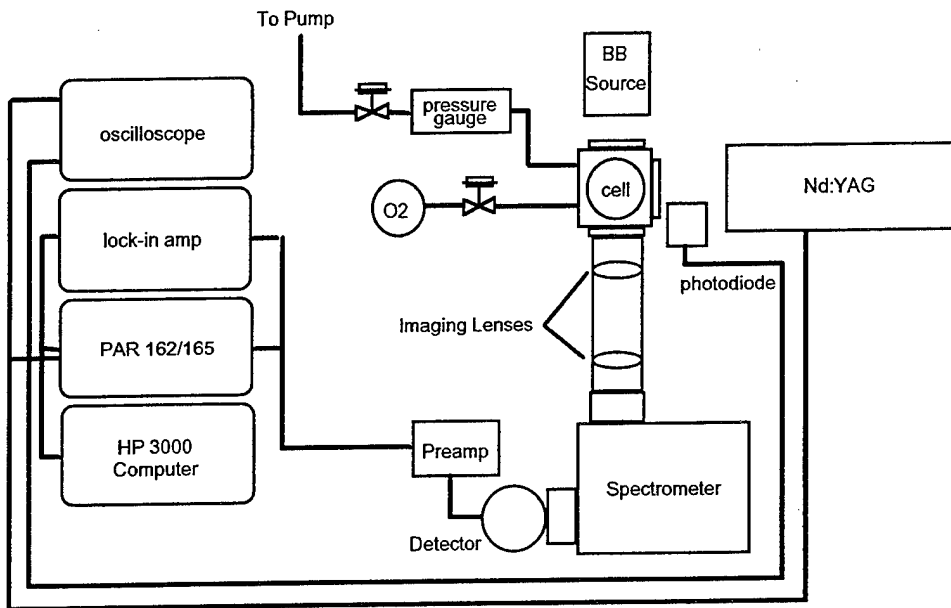


Figure 1. Experimental Apparatus used for acquisition of a continuous 3.5-13.0  $\mu\text{m}$  emission spectrum from a laser produced oxygen plasma.

A liquid nitrogen cooled HgCdTe detector (Santa Barbara Research Center, 5 mm square element) operated in the photo conductive mode with a matched preamplifier (SBRC Model A110, 80 db voltage gain) was used to detect the infrared emissions. The detector is well suited for use in the spectral range 3-13  $\mu\text{m}$  and has a detectivity of  $\sim 10^{10} \text{ cm Hz}^{-1/2} \text{ W}^{-1}$  near 6  $\mu\text{m}$  yielding an estimated NESR of  $\sim 10^{-6} \text{ W cm}^{-2} \text{ sr}^{-1} \mu\text{m}^{-1}$ . In the MWIR region (3.5-8.0  $\mu\text{m}$ ), the  $4\text{p}^5 \text{P}-3\text{d}^5 \text{D}$  transition near 6  $\mu\text{m}$  has a signal-to-noise ratio of  $\sim 40$ . In the LWIR region (8.0-13.0  $\mu\text{m}$ ), the 10.4  $\mu\text{m}$  line emission has a signal-to-noise ratio of  $\sim 15$ .

OI visible diagnostic information relating to energy deposition was monitored using a Hamamatsu photomultiplier tube fitted with a narrow band pass filter (20 nm) near 715.8 nm and a neutral density filter (O.D.=4.0). The line emission of interest in this window is the  $3\text{p}'(^1\text{D})-3\text{s}'(^1\text{D}^0)$  transition originating from a state with a Rydberg-like energy of  $116631 \text{ cm}^{-1}$  (Ionization potential =  $109837 \text{ cm}^{-1}$ ). Stability of the 715.8 nm signal during all data acquisition ensured stable energy deposition.

In this study, the plasma was produced from 110 torr high purity O<sub>2</sub> (Matheson, 99.995%). A laser pulse energy of 780 mJ created an estimated intensity of  $2 \times 10^{13} \text{ W cm}^{-2}$  in the focal plane. The resulting plasma emission region appeared cylindrically shaped and approximately 6 mm long and 2 mm in diameter. During all data acquisition, the entire optical path was enclosed in

plexiglass and purged with dry nitrogen to minimize CO<sub>2</sub> and H<sub>2</sub>O absorption effects on the measured plasma emissions.

## B. Data Acquisition and Reduction

Data acquisition was performed with a Princeton Applied Research model 162 boxcar averager operated in conjunction with a model 165 gated integrator using a 0.6  $\mu$ s aperture duration. Fifty laser shots were averaged per wavelength increment. Measurements were taken with an aperture delay time of 20  $\mu$ s. The output of the boxcar averager was sent to a HP Model 9000 series 310 computer which averaged 50 laser shots per wavelength increment.

The absolute spectral response of the system was determined with an Infrared Industries model 408 blackbody source operated at 1000°C where the signal processing of the blackbody emissions was done with a Stanford Research Systems lock-in amplifier. The wavelength accuracy of the system was calibrated using a HeNe laser in the sixth and higher orders.

Individual scans were recorded digitally on the HP computer and transferred to an IBM PC compatible computer at Mission Research Corporation. Information about the scan was recorded and used for the data reduction process. The spectral response of the system was then derived from a comparison of the observed blackbody emission spectra with the theoretical blackbody function. Figure 2 illustrates the optical path traversed by the emissions being studied.

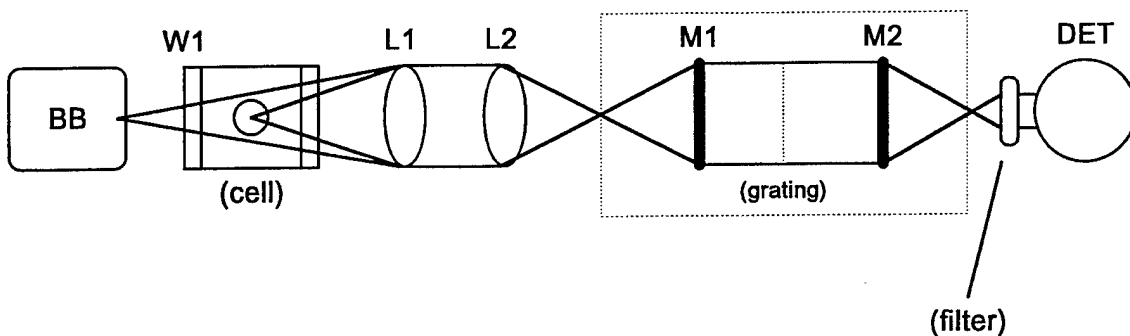


Figure 2. Optical path of emission in the experiment.

The measured voltage output of the detector (mV) for a given source spectral radiance,  $\Phi$  (W cm<sup>-2</sup> sr<sup>-1</sup>  $\mu$ m<sup>-1</sup>), is given by:<sup>67</sup>

$$S_p(\lambda) = R(\lambda) A_p \Omega_{L1} \frac{\Omega_{M1}\Omega_{DET}}{\Omega_{L2}\Omega_{M2}} T(\lambda) \int_{\lambda-\Delta\lambda}^{\lambda+\Delta\lambda} \Phi(\lambda) d\lambda \quad (1)$$

where,

$R$  = Instrument Spectral Response,

$\Omega_{L1}, \Omega_{L2}, \Omega_{M1}, \Omega_{M2}$ ,  $\Omega_{DET}$  = Solid angles subtended by mirrors 1 and 2, lenses 1 and 2, and the detector,

$A_p$  = Apparent disk of the spark,

$T(\lambda)$  = Total transmittance excluding window 1.

Using the theoretical blackbody function,  $N(\lambda, T)$ . The spectral response is written as,

$$R(\lambda) = \frac{S_{BB}(\lambda)}{A_{BB}\Omega_{BB} \frac{\Omega_{M1}\Omega_{DET}}{\Omega_{L2}\Omega_{M2}} T^*(\lambda) N(\lambda, T) \Delta\lambda_{BB}(\lambda)} \quad (2)$$

where,

$T^*(\lambda) = T_{W1}(\lambda)T(\lambda)$  is the total transmittance including window 1,

$\int_{\lambda-\Delta\lambda}^{\lambda+\Delta\lambda} \Phi(\lambda) d\lambda \cong \Phi(\lambda) \Delta\lambda_p(\lambda)$  and  $\Delta\lambda_p$  is the instrument resolution.

Substituting equation (28) into (27) yields the spectral radiance of the observed plasma emissions,

$$\Phi(\lambda) = \frac{A_B\Omega_B}{A_p\Omega_p} \frac{S_p(\lambda)}{S_B(\lambda)} \frac{\Delta\lambda_B(\lambda)}{\Delta\lambda_p(\lambda)} T_{W1}(\lambda) N(\lambda, T) = CalibrationFactor \frac{S_p(\lambda)}{\Delta\lambda_p(\lambda)} \quad (3)$$

#### 4. OBSERVATIONS

Figure 3 shows the IR spectrum of the laser-produced oxygen plasma. The spectrum can be described by the spectral sum of continuum radiation and collisionally broadened line emission. The plasma consists of excited and ionized atoms and electrons which radiate and recombine to

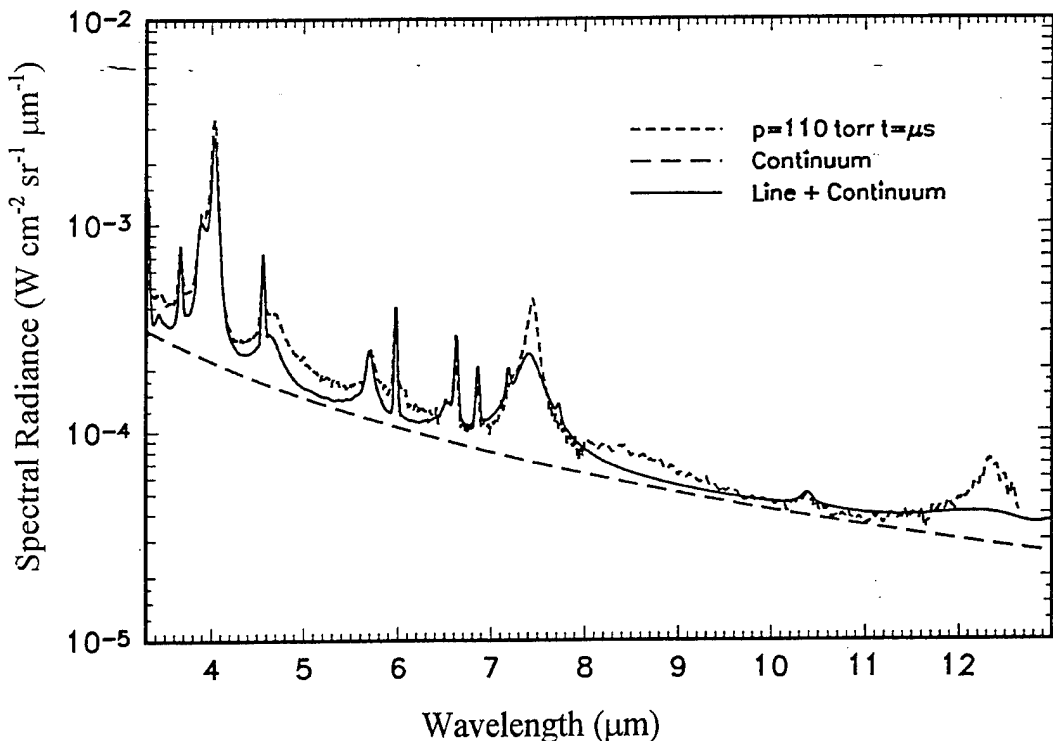


Figure 3. The short-dashed curve is the IR emission spectrum of the laser-produced oxygen plasma at an aperture time delay of 20  $\mu$ s. The plasma was created from 110 torr O<sub>2</sub> and the measurement is of the center of the emission region. The medium-dashed curve is the continuum model and the solid curve is the sum of the continuum and line emission models.

form electronically excited neutral atomic oxygen. Initially ( $\leq 1 \mu\text{s}$ ), infrared emission from the plasma is mostly recombination and continuum radiation which decreases rapidly as radiative and collisional relaxation processes progress. At 20  $\mu\text{s}$ , the major species are O, O<sup>+</sup>, and electrons with electron-to-neutral density ratio  $< 1\%$ .<sup>43</sup>

Significant continuum radiation persists throughout the plasma lifetime. Continuum radiation occurs through both electron recombination with ions (free-bound or recombination radiation), and electron collisions with ions and neutral atoms (free-free transitions or bremsstrahlung radiation). Since bremsstrahlung radiation from electron-neutral atom interactions is not a Coulombic process, the interaction is short-ranged. As such, bremsstrahlung radiation due to electron-atom interactions is expected to dominate only after  $\sim 10 \mu\text{s}$ ; prior to this electron-ion interactions dominate. The observed continuum spectrum is modelled using a theory for free-free transitions in the field of a neutral which is superposed with the line emission component of the spectrum.

The infrared line emission spectrum is produced by inter-Rydberg state transitions. These states are populated by recombination and collisional processes. Initial studies of the thermal

equilibration time between electrons and atoms suggest that thermalization is achieved in approximately 6  $\mu$ s.<sup>43</sup> Collisional coupling is then expected to occur for those Rydberg states within  $kT_e$  of the ionization potential. Consequently, Saha equilibrium is assumed to describe the Rydberg state population distribution. Emitter line profiles in a laser-produced plasma are broadened through the Stark effect by ions and collisions with electrons. Collisional-Stark broadening of spectral lines is significant even at low electron densities ( $10^{13}$  cm<sup>-3</sup>). We developed a collisional-Stark broadening model to predict the line emission spectrum. The model is described in detail in Chapter 6 and only pertinent information is reviewed here. The line emission model predicts the spectrum using electron density,  $N_e$ , electron temperature,  $T_e$ , ion temperature,  $T_i$ , and emitter electronic temperature,  $T_{el}$ , as free parameters. For this study, we set  $T_e = T_{el}$ , where the empirically derived temperature was used in the spectral calculation.

We examine the characteristics of the plasma by simultaneously fitting continuum and line emission models to the observed spectrum. The parameters used to characterize the plasma conditions are O-atom density, electron density, electron temperature, and emitter electronic temperature. The electronic temperature is derived from the continuum subtracted spectrum. In conjunction with Saha equilibrium, the simultaneous fit of the continuum and line emission models give the best parameter estimates that describe the plasma conditions. These results are discussed below. The line emission model fitting is described in further detail in Chapter 7.

### A. Line Emission

The continuum subtracted spectrum is shown in Figure 4. Table 2 is a listing of the line positions of the spectral features observed in the region 3.5 to 13  $\mu$ m, their transition assignments, predicted Einstein coefficients and observed line widths. The observed transitions are illustrated in energy-level diagrams in Figure 5. It should be noted that the line widths are to be interpreted only qualitatively since there is a high degree of spectral blending.

The feature near 10.4  $\mu$ m is given a composite line assignment dominated by 6d<sup>5</sup>D-6p<sup>5</sup>P and 5p<sup>3</sup>P-4d<sup>3</sup>D. The broad feature near 12.35  $\mu$ m occurs at the long wavelength edge of the detector responsivity and, therefore, the line shape of the feature is not entirely realized. This feature is predicted to be dominated by six transitions: 7 g,h,i<sup>3,5</sup> G,H,I -6f,g,h<sup>3,5</sup> F,G,H. This is the first reported observation of the 10.4 and 12.35  $\mu$ m emission from a laser produced plasma.

We have examined the integrated intensities of 5 transitions in the spectrum that exhibit the least blending with other features for state population and electronic temperature determination.

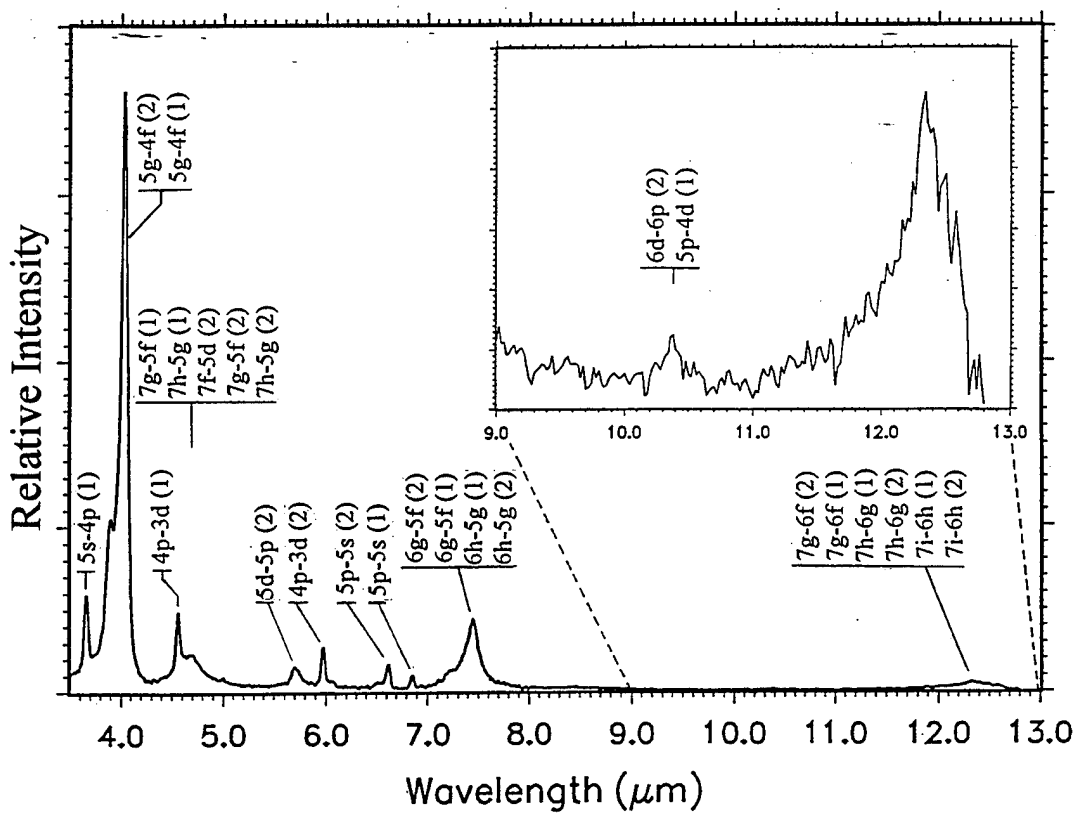


Figure 4. The OI line emission spectrum was obtained by subtracting the power law fit to Lin's emissivity coefficients shown in Figure 3.

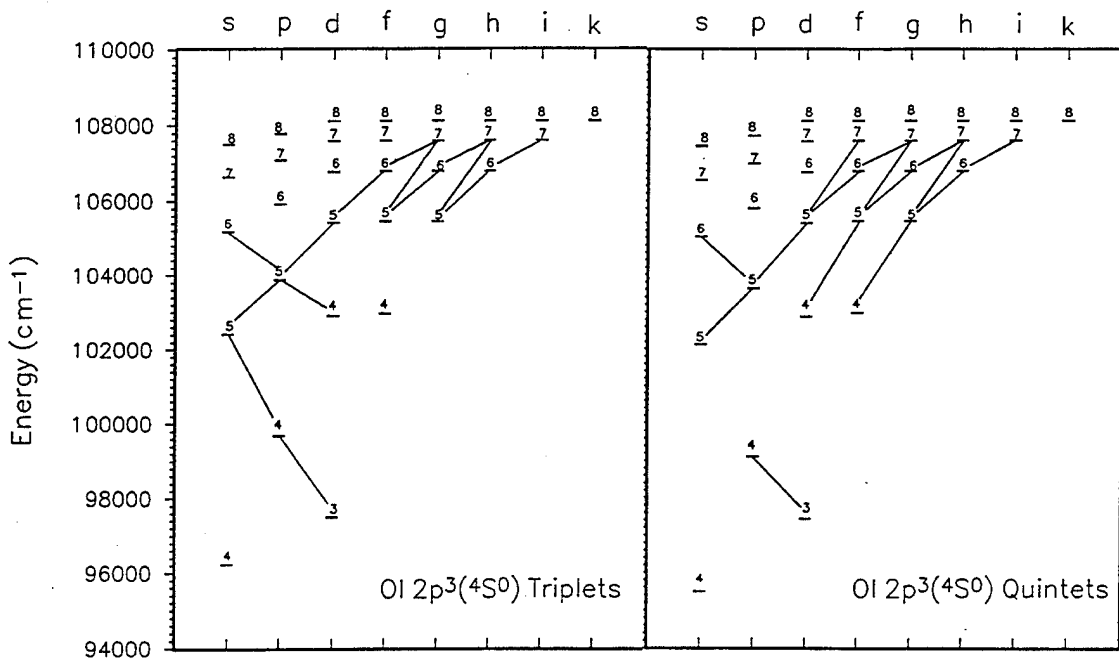


Figure 5. Energy level diagram illustrating the major transitions observed in the line emission spectrum from 3.5 to 13.0  $\mu\text{m}$ .

TABLE 2. Observed line positions, assignments, calculated Einstein coefficients, and approximate line widths in LINUS IR plasma spectra at 20  $\mu$ s.

Observed Feature ( $\mu$ m)	Wavelength <sup>a</sup> ( $\mu$ m)	Transition Assignment <sup>a</sup> (spin in parentheses)	$gA^a$ ( $s^{-1}$ )	approximate FWHM <sup>b</sup> ( $\mu$ m)
3.67	3.6618	5s-4p (1)	$1.227 \times 10^7$	0.04
3.89	3.8819	5f-4d (2)	$9.603 \times 10^7$	0.04
3.94	3.9474	5f-4d (1)	$5.794 \times 10^7$	0.02
4.04	4.0496	5g-4f (2)	$1.916 \times 10^8$	0.04
	4.0499	5g-4f (1)	$1.149 \times 10^8$	
4.56	4.5607	4p-3d (1)	$9.371 \times 10^6$	0.04
	4.6510	7g-5f (1)	$1.481 \times 10^7$	
	4.6511	7h-5g (1)	$1.680 \times 10^7$	
4.62	4.5254	7f-5d (2)	$1.585 \times 10^7$	0.2
	4.6507	7g-5f (2)	$2.469 \times 10^7$	
	4.6511	7h-5g (2)	$2.799 \times 10^7$	
5.69	5.6842	5d-5p (2)	$4.146 \times 10^7$	0.1
5.98	5.9773	4p-3d (2)	$7.405 \times 10^6$	0.04
6.51	6.4978	5d-5p (1)	$1.995 \times 10^7$	0.06
6.61	6.6249	5p-5s (2)	$1.514 \times 10^7$	0.05
6.86	6.8583	5p-5s (1)	$8.911 \times 10^6$	0.04
7.19	7.1786	6s-5p (2)	$8.170 \times 10^6$	---
	7.2664	6f-5d (1)	$1.615 \times 10^7$	
	7.4281	6g-5f (2)	$5.032 \times 10^7$	
7.44	7.4285	6g-5f (1)	$3.020 \times 10^7$	
	7.4556	6h-5g (1)	$5.431 \times 10^7$	0.15
	7.4556	6h-5g (2)	$9.052 \times 10^7$	
10.38	10.3859	6d-6p (2)	$1.408 \times 10^7$	0.2
	10.3995	5p-4d (1)	$3.435 \times 10^6$	
	12.3629	7g-6f (2)	$1.694 \times 10^7$	
	12.3644	7g-6f (1)	$1.017 \times 10^7$	
12.35	12.3648	7h-6g (1)	$1.757 \times 10^7$	0.5
	12.3648	7h-6g (2)	$2.929 \times 10^7$	
	12.3625 <sup>c</sup>	7i-6h (1)	$2.892 \times 10^7$	
	12.3625 <sup>c</sup>	7i-6h (2)	$4.821 \times 10^7$	

<sup>a</sup>Taken from Chung *et al.*<sup>12</sup>

<sup>b</sup>Only approximate since there is a high degree of blending associated with these features.

These transitions include:  $5s^3P$ - $4p^3S$ ,  $4p^3P$ - $3d^3D$ ,  $4p^5P$ - $3d^5D$ ,  $5p^5D$ - $5s^5P$ , and  $5p^3P$ - $5s^3S$ , occurring near 3.67, 4.56, 5.98, 6.61, and 6.86  $\mu$ m respectively. Assuming Saha equilibrium, the integrated intensity ( $Wcm^{-2} sr^{-1}$ ) of the spectral distribution of a transition is given by:

$$I = \frac{d}{4\pi} \frac{N_0}{Z} g \exp\left(-\frac{hcF}{kT}\right) A \frac{hc}{\lambda} \quad (4)$$

where  $N_0$  is the total atom density divided by the partition function,  $F$  the emitting state term value,  $T$  the electronic temperature,  $A$  the Einstein coefficient, and  $\lambda$  the transition wavelength. The degeneracy,  $g$  is given by  $(2l+1)(2s+1)$ . The path length,  $d$ , was calculated with a Lagrangian hydrodynamics model. The model predicted that the plasma emission region is approximately 6 mm long and 2 mm in diameter which is consistent with visual observation. Since the monochromator slit was perpendicular to the long axis of the emission region, a path length of 2 mm was used in the analysis of the data. Linearization of equation (4) yields the following relationship:

$$\ln\left[\frac{I}{gAhc/\lambda}\right] = -\frac{1}{T}\left(\frac{hcF}{k}\right) + \ln\left[\frac{dN_0}{4\pi Z}\right] \quad (5)$$

Figure 6 shows the results of the left hand side of equation (5) plotted against  $hcF/k$  for the five transitions. An electronic temperature of  $8000 \pm 1000$  K is derived from the slope of the least squares fit to the data. The intercept determined from the least squares, which reveals information about the absolute number density, is not used in the analysis since a large error bar is associated with that number. The uncertainty in the derived temperature is the standard deviation associated with the fit. The error bars on the data points were derived from the following sources: (1) signal-to-noise estimations near each feature which resulted in individual intensity errors varying across the range 4-9%, and (2) 10% estimated area in the total intensity of the spectrum based on repetitions of the same experiment. In the error analysis, linear detector response with respect to signal was assumed. The derived electronic temperature was then used in the line emission modelling to obtain an estimate of the electron density.

The five transitions used for electronic temperature estimation were also used to estimate state populations. By determining the ratio of the relative integrated line intensities, the relative emitting state populations are measured. Table 3 lists the ratios of the transition probabilities, observed intensities multiplied with their respective transition energies, measured upper state populations and energies. A term diagram is shown for the five transitions in figure 7.

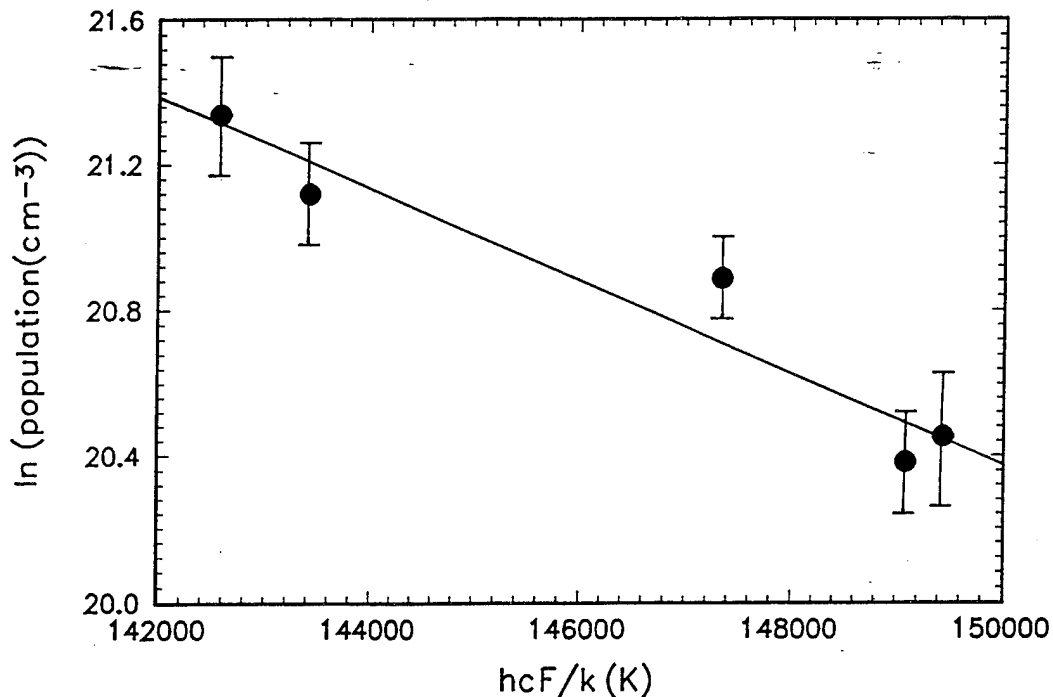


Figure 6. The electronic temperature is determined from a least squares fit to the plot of the left-hand side of equation (5) against  $hcF/k$ . The least squares fit is shown as the solid line which is associated with an electronic temperature of  $8000 \pm 1000$  K where the uncertainty reflects the standard deviation of the fit.

TABLE 3. Measured relative populations.

Upper State Ratio	Energies (cm⁻¹)	$N_i/N_j$	$g_i A_i/g_j A_j$	$I_i E_i/I_j E_i$
4p(1)/5s(1)	99681, 102412	$1.26 \pm 0.06$	0.763	0.964
4p(1)/4p(2)	99681, 99094	$0.80 \pm 0.05$	1.265	1.018
4p(1)/5p(2)	99681, 103626	$2.1 \pm 0.2$	0.619	1.290
4p(1)/5p(1)	99681, 103870	$2.0 \pm 0.2$	1.051	2.050
5s(1)/4p(2)	102412, 99094	$0.61 \pm 0.04$	1.657	1.056
5s(1)/5p(2)	102412, 103626	$1.6 \pm 0.1$	0.811	1.338
5s(1)/5p(1)	102412, 103870	$1.5 \pm 0.2$	1.377	2.126
4p(2)/5p(2)	99094, 103626	$2.6 \pm 0.2$	0.489	1.267
4p(2)/5p(1)	99094, 103870	$2.5 \pm 0.3$	0.831	2.013
5p(2)/5p(1)	103626, 103870	$1.2 \pm 0.1$	1.669	1.589

Inspection of Table 3 shows the measured populations to decrease with increasing state energy. This suggests that these states are collisionally coupled. Electronic population of the Rydberg states are associated with more loosely bound electrons and are thus more susceptible to external effects induced by the plasma. Under Saha equilibrium conditions, thermalization through

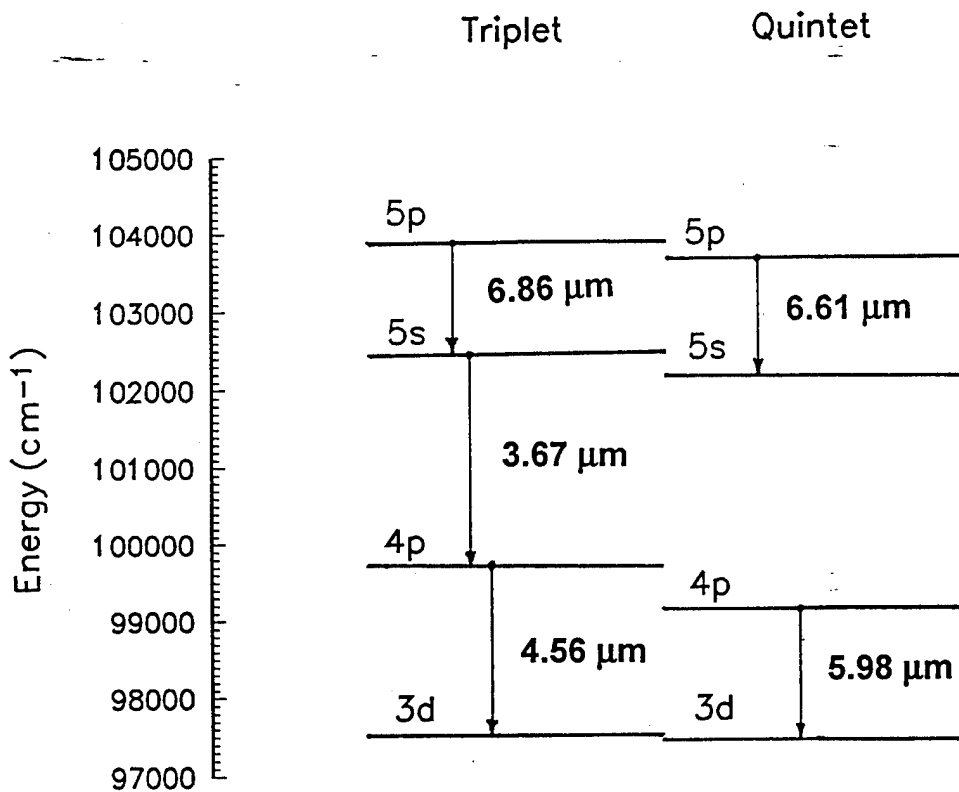


Figure 7. Term diagram for the five transitions used for the electronic temperature determination and state population measurement.

collisions with electrons determines the population distribution. The distribution reflects the electron temperature ( $T_{el} = T_e$ ). Specifically, those Rydberg states within  $kT_e$  of the ionization potential may display coupled electron and electronic temperatures.

### B. Continuum

The electron and atomic oxygen densities can be estimated from the continuum if the electron temperature is known, the plasma is collision dominated, and the form of the continuum is known. Figure 3 shows the power law fit to the theoretical emissivity coefficients of Lin.<sup>39</sup> The electron density was determined from the line emission modelling and the electronic temperature was measured from the spectroscopic analysis of integrated line intensities.

From the continuum fit, the product of the path length and electron and atomic oxygen densities can be determined by from:

$$\epsilon(\lambda, T) = dN_e N_o J(\lambda, T) \quad (6)$$

where  $J(\lambda, T)$  is the power law fit to Lin's emissivity coefficients.<sup>39</sup> The electron and atomic oxygen densities were uniquely determined using equation (6) and the Saha equilibrium condition. Saha equilibrium predicts the ratio of the square of the electron density to the oxygen density given the electron temperature:<sup>44</sup>

$$\frac{N_e^2}{N_o} = \left( \frac{2\pi m k T}{h^2} \right)^{3/2} \frac{2g_+}{g_o} e^{-(I-E_o)/kT} \quad (7)$$

where  $E_o$  is the multiplet averaged ground state energy,  $I$  is the ionization limit,  $T$  is electron temperature,  $m$  is the electron mass, and  $g_+$  and  $g_o$  are the multiplet average ground state degeneracies for the ion and neutral. Using the spectroscopically determined temperature, the electron and atomic oxygen densities are estimated to be  $8 \times 10^{15}$  and  $5 \times 10^{18}$  cm<sup>-3</sup> respectively. Using these values in eq. (6) results in an effective path length of 0.016 cm.

## 5. BREMSSTRAHLUNG RADIATION

Continuum emission in the laser-produced plasma is due to free-free (Bremsstrahlung) and free-bound processes. Continuum emission due to bremsstrahlung radiation by electron-ion collisions and recombination are well understood, and the reader is guided towards the previous LINUS final report for additional information. For bremsstrahlung radiation due to electron-neutral collisions (F-F(N)) we outline the theoretical developments that were concurrent with experimental program.

Bremsstrahlung radiation due to electron-neutral collisions in the EGG-22 plasma radiance model is based on the work by Zel'dovich and Raizer.<sup>45</sup> The expression for the F-F(N) emission coefficient may be expressed as,<sup>45</sup>

$$\epsilon_{FF} = \frac{32\pi e^2 \sigma}{3c^3} \left( \frac{2}{\pi m^3 k T} \right)^{1/2} \left[ 2(kT)^2 + 2h\nu k T + (h\nu)^2 \right] N_a N_e \exp\left(-\frac{h\nu}{kT}\right) \quad (8)$$

The formulation of equation (8) is not regarded as exact since different temperature and energy dependencies can be derived based on different representations of the electron-neutral atom interaction. This formulation is the one presently used in the EGG-22 plasma radiance model. The cross section for interaction is not well established here but has a direct impact on the coefficient.

EGG-22 uses cross sections derived from the experimental results of Taylor and Caledonia<sup>42</sup> which are expressed in terms of radiative absorption coefficients. However, the measurements were only made at 2, 3.5, and 5  $\mu\text{m}$  and at only one electron temperature. Thus, there is considerable uncertainty in extrapolating and interpolating these results to different wavelengths.

Lin's treatment<sup>39</sup> of the emissivity coefficient for free-free transitions in the field of a neutral oxygen atom is fully quantum mechanical and implements polarized orbitals. In Tables 4, 5, and 6, we list the values for Lin's emissivity coefficients<sup>39</sup> and the values predicted by EGG-22 for electron temperatures of 10000 K, 25000 K, and 50000 K in the wavelength range 1 to 30  $\mu\text{m}$ . Figure 8 is a plot the emissivity coefficients for each of the three temperatures. There is reasonably good agreement between Lin's coefficients<sup>39</sup> and EGG22 at 10000 K. However, there is markedly different behavior as the electron temperature is increased. The distinguishing characteristic is that Lin's coefficients<sup>39</sup> increase with increasing electron temperature whereas the prediction by EGG-22 shows just the opposite. This result is surprising since intuitively, Bremsstrahlung emission due to electron-neutral collisions should decrease due to the decreasing residence time of the electron near the atom decreases as the electron's effective temperature increases. Discussions with Lin<sup>39</sup> have indicated that the "intuitive" decrease with increasing temperature may be fallacious and the apparent increase is due to energetic wave- function overlap in this region. It is probably academic however, since at 50000 K, electron-neutral Bremsstrahlung emission is a minor source of radiance (the gas is nearly 100% ionized).

In figure 9, Lin's theoretical coefficients are compared with those of John and Williams<sup>40</sup>, Geltman<sup>41</sup>, and the empirical coefficients of Taylor and Caledonia.<sup>42</sup> The theories agree within a factor of two with one another. There is considerable disagreement however, between the theoretical and the empirical values.

TABLE 4. Bremsstrahlung emissivity coefficients for free-free in the field of a neutral at an electron temperature  $T_e=10000$  K.

$\lambda$	Chun Lin	EGG-22	Ratio
1	4.3(-36)	1.5(-35)	0.29
5	3.7(-37)	6.5(-37)	0.57
9	1.2(-37)	1.5(-37)	0.80
13	6.0(-38)	5.9(-38)	1.0
17	3.6(-38)	2.9(-38)	1.2
21	2.3(-38)	1.7(-38)	1.4
25	1.7(-38)	1.1(-38)	1.6
29	1.2(-38)	7.2(-39)	1.7

TABLE 5. Bremsstrahlung emissivity coefficients for free-free in the field of a neutral at an electron temperature  $T_e=25000$  K.

$\lambda$	Chun Lin	EGG-22	Ratio
1	2.4(-35)	2.3(-35)	1.0
5	1.3(-36)	4.9(-37)	2.7
9	4.0(-37)	1.1(-37)	3.6
13	1.9(-37)	4.0(-38)	4.8
17	1.1(-37)	1.9(-38)	5.8
21	7.3(-38)	1.1(-38)	6.6
25	5.2(-38)	7.0(-39)	7.4
29	3.8(-38)	4.7(-39)	8.1

TABLE 6. Bremsstrahlung emissivity coefficients for free-free in the field of a neutral at an electron temperature  $T_e=50000$  K.

$\lambda$	Chun Lin	EGG-22	Ratio
1	5.2(-35)	1.8(-35)	2.9
5	2.4(-36)	3.7(-37)	6.5
9	7.6(-37)	7.8(-38)	9.7
13	3.7(-37)	2.9(-38)	12
17	2.1(-37)	1.4(-38)	15
21	1.4(-37)	8.0(-39)	18
25	9.9(-38)	5.0(-39)	20
29	7.4(-38)	3.4(-39)	22

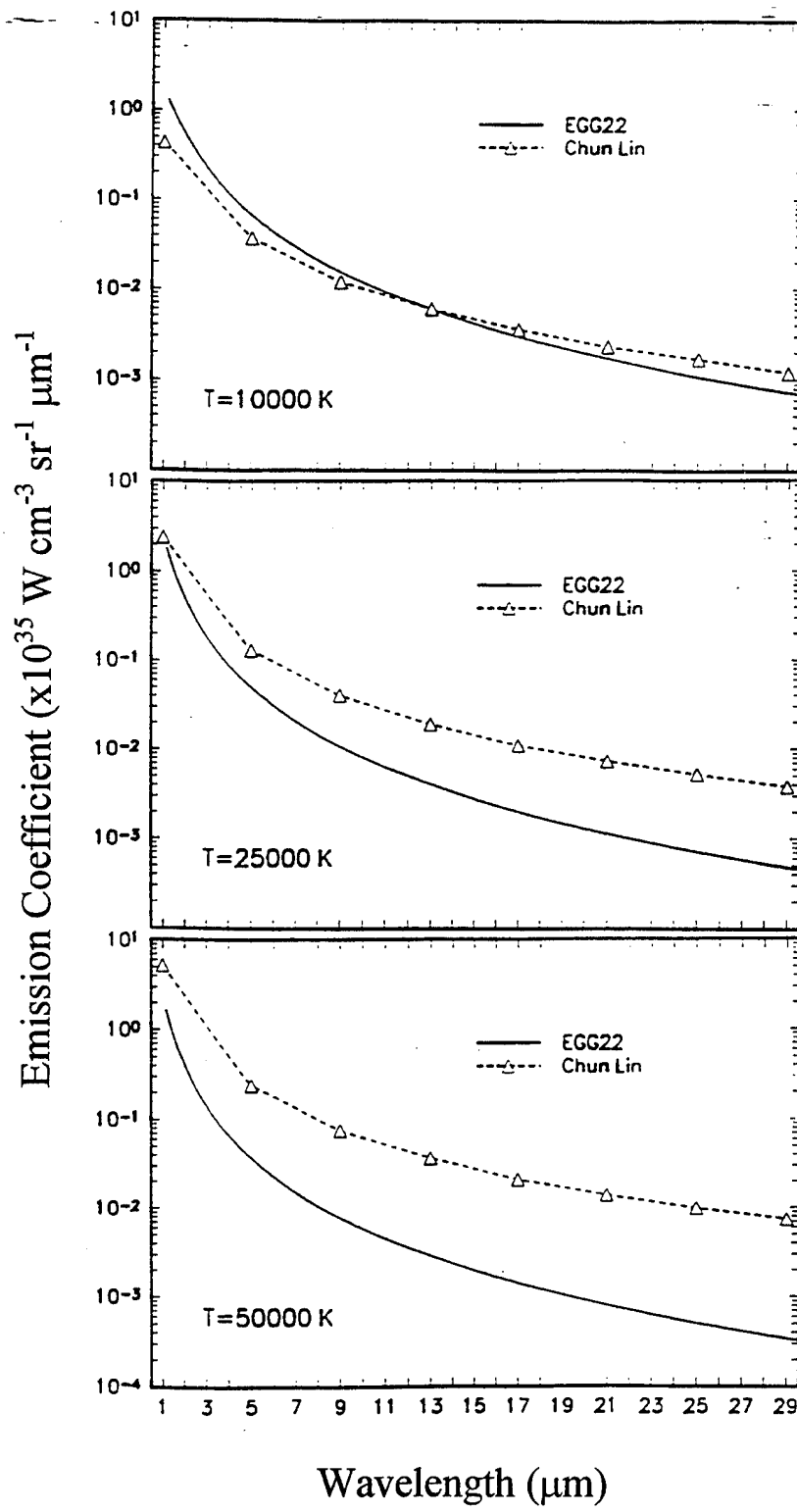


Figure 8. Comparison of EGG-22 and theoretical emissivity coefficients for free-free transitions in the field of a neutral oxygen atom.

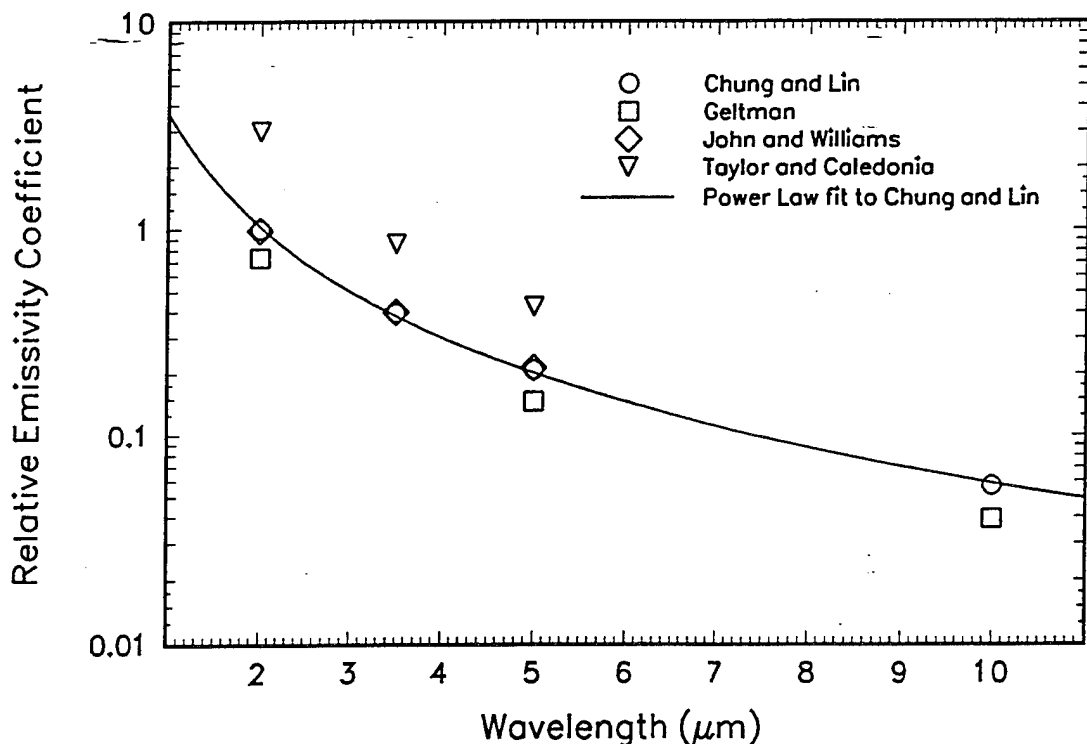


Figure 9. Comparison of theoretical and empirical emissivity coefficients for free-free transitions in the field of a neutral oxygen atom. All values are for an electron temperature of 10000 K. All values are relative Lin's emissivity coefficient at  $2\mu\text{m}$ .

## 6. APOSTLE LINE BROADENING MODEL

### A. Theory

A foundational work of pressure broadening of spectral lines was produced by Anderson<sup>37</sup> in 1949. Early treatments of pressure broadening assumed that collisions are adiabatic,<sup>60,65,66</sup> i.e., no energy transfer takes place during a collision. The adiabatic assumption is usually applicable in the optical regime because energy transfer in an electron-atom collision is insufficient to induce such transitions. Anderson<sup>37</sup> included inelastic collisions and, thus, the applicability of his theory can be extended to the microwave and infrared regions. By assuming that the colliding neutral particles follow classical paths, the line width and shift can be described in terms of a semi-classical scattering operator. The scattering operator matrix is then evaluated using a second-order expansion approximation.<sup>11,32,36,37</sup> These methods were further developed by Tsao and Curnutte<sup>46</sup> and Kolb and Griem<sup>47</sup>.

Most collisional-Stark broadening calculations<sup>31,32,34,35</sup> are performed using extensions of the classical path impact theory developed by Anderson<sup>37</sup> for self-broadening of neutral emitters. The theory has been adapted and extended to a radiating plasma by Griem, Baranger, Sahal-Brechot,

and Cooper and their co-workers.<sup>11,31,32, 33,48</sup> The theory of collisional broadening<sup>10,11</sup> encompasses two limiting cases: (1) the impact approximation based on instantaneous collisions where the collision is short in comparison to the time between collisions, and (2) the quasi-static approximation based on slowly moving perturbers. For a plasma, the impact approximation describes electron impact on the radiating atom and the quasi-static approximation describes the ion-radiator collision effects. The quasi-static approximation is used to statistically represent ion-collisional influences as external electric fields (microfields). The ion-produced microfields vary so slowly that their time-dependence can be neglected. In this case, the calculation reduces to that of the static Stark effect, taking into account the statistical distribution of the electric fields at the radiator. In plasmas with atoms excited to sufficiently high  $n$  states, the small energy differences between perturbing levels become comparable to the line widths (overlapping lines) and the quasi-static line splitting is significant.<sup>3</sup> For lower-lying Rydberg levels whose components of different orbital angular momentum are well-separated in energy (isolated lines), the line broadening is caused mainly by collisions with electrons. There is an increase in the electron-impact width with increasing  $n$  and  $l$  of the upper state for lines belonging to a spectral series.<sup>8</sup> In many plasmas the electric fields produced by electrons colliding with the radiators vary so rapidly (i.e., collisions are short in duration) that the corresponding line widths and shifts depend only on net changes in the radiator states.

The determination of collisionally broadened<sup>10,11</sup> linewidths is divided into the effects of low-frequency perturbers (ions) using the quasi-static approximation and of the high frequency perturbers (electrons) using the impact approximation. To develop a "fast" computational model of line broadening over a large spectral range, we use the approximations of Anderson<sup>37</sup> for electron collisional effects and the model of Hooper<sup>38</sup> for ion collisional effects. The approximation criteria are examined in detail as some spectral features fall outside the limits of model validity. Such cases are flagged as inappropriate estimates.

### **1. Ion Collisional Broadening**

The quasi-static approximation is valid if the splitting caused by the perturber field,  $\Delta\omega$ , is large compared to the inverse of the duration of the collision,  $1/\tau_p$ , or

$$\Delta\omega \gg \frac{1}{\tau_p} \approx \frac{u_p}{b_p} \quad (9)$$

where  $u_p$  is the velocity of the perturber and  $b_p$  is its characteristic impact parameter. For long range Coulomb interactions,  $b_p$  is limited by plasma shielding effects and can be approximated by the Debye length,  $\lambda_D$ .

The use of the quasi-static approximation for the ions is equivalent to representing the ions by a normalized distribution function,  $\mathcal{P}(E)$ , of static electric fields,  $E$ .  $\mathcal{P}(E)$  depends on the ion mass, density, and temperature. By adopting this physical picture for the ions, the standard quantum mechanical theory for Stark effect is applicable.

The Stark effect is described by the Stark Hamiltonian, which is the product of the electric dipole moment,  $er$ , and the electric field,  $E$ . The selection rules for electric dipole induced transitions are  $\Delta s=0$ ,  $\Delta l=+1,-1$ ,  $\Delta m_l=+1,0,-1$ . The presence of the Stark field has two effects. First, the energy levels of the  $m_l$  magnetic substates are shifted, *i.e.*, their degeneracy is lifted. For all atoms except hydrogen, the amount of energy shift is proportional to the square of  $m_l$ . Therefore, the line shifting is not symmetric about the unperturbed line. Second, lines forbidden by the electric dipole selection rules become allowed due to the mixing of states. The presence of an electric field results in spectra with split and broadened lines. The Stark shifted line positions,  $\omega_{ij}$ , and corresponding perturbed wave functions are determined by diagonalization of the Stark Hamiltonian. The electric dipole transition moments are calculated using the resulting wave functions and energies. After calculating the energy levels and wave functions for a particular field, the Einstein coefficients are calculated according to:<sup>49</sup>

$$A_{ij} = \frac{64\pi^4 \tilde{\omega}_{ij}^3}{3h} | \langle i | er | j \rangle |^2 \quad (10)$$

where  $h$  is Planck's constant, the transition frequency is in wavenumbers.

The basis set for the Stark Hamiltonian matrix assumes *L-S* coupling and is defined by the spin,  $s$ , the principal number,  $n$ , the orbital angular momentum,  $l$ , and the magnetic quantum number,  $m_l$ . The diagonal matrix elements of the Hamiltonian are the unperturbed energy levels for oxygen atom, the majority of which have been documented by Moore<sup>50</sup>. States not listed in Moore are calculated using the polarization formulas in Edlen<sup>51</sup> and the polarizability constants in Isberg<sup>52</sup>. The formulas are based on the theory of Born and Heisenberg<sup>53</sup> and of Waller<sup>54</sup>, who modifies the hydrogenic term formula for the interaction of the valence electron with the core electrons. The off-diagonal elements of the Stark Hamiltonian matrix are calculated by multiplying the dipole

moment matrix elements by the ion-induced field. The radial part of the dipole moment matrix element is obtained from the calculations of Chung *et al.*<sup>9</sup> and Lin.<sup>55</sup> These calculations employ a frozen core representation of the oxygen wave functions. For transitions higher than *h-g*, the radial matrix elements are calculated from the tables in Oertel and Shomo<sup>56</sup>, which are extensions of the Coulomb approximation calculations of Bates and Damgaard.<sup>57</sup> The signs of these matrix elements may differ from those of Lin<sup>55</sup> depending on whether *n'-n"* is even or odd because of a difference in the phase definition in the wave functions. Formulas for the angular component, consisting of direction cosine matrix elements, are based on the standard approach given by Condon and Shortley.<sup>49</sup>

The ion-induced field in the Stark Hamiltonian is given by Holtsmark<sup>58</sup> to be  $2.6eN_p^{2/3}$ . Since the temporal dependence of the ion field is difficult to characterize experimentally or theoretically, the accepted approach is to statistically simulate the effect of the quasi-static ions by a plasma microfield distribution. Using this approach, a microfield distribution has been calculated by Baranger and Mozer.<sup>59</sup> Hooper<sup>38</sup> further refined the theory by including correlation among all perturbers and allowing independent input for plasma density and ion and electron temperature. The microfield distribution used in the present model is based on Hooper's approach for the case of a low frequency electric microfield distribution at a neutral point.

## 2. Electron impact Broadening

Most theories on electron impact broadening are based on three assumptions: the classical path, impact, and binary assumptions. The classical path approximation assumes that the perturber path is straight for neutral radiators and hyperbolic for charged radiators. The impact approximation assumes that the duration of the collision is short compared to the time between collisions. The binary approximation assumes that a collision involves two species: the radiator and one perturber. These approximations allow one to express the interaction of the electron perturber and the neutral emitter as a definite function of time,  $H_1(t)$ . The classical path approximation is particularly useful in treating Stark broadening of spectral lines emitted in plasmas because the interparticle forces are long range Coulomb forces and the broadening is dominated by many weak collisions. The impact approximation can be invoked if the duration of a perturbing collision,  $\tau_p$ , is much shorter than the time between perturbing collisions,  $\tau_b$ , is small compared to the time between collisions. The duration of the collision can be approximated by dividing the largest impact parameter for

producing an emission disturbance,  $b_p$ , by the average perturber velocity,  $u_p$ . Therefore, the impact approximation can be used when

$$\tau_p \approx \frac{b_p}{u_p} \ll \tau_b \approx \frac{1}{N u_p \pi b_p^2} \quad (11)$$

This is essentially identical with the criterion for the binary collision approximation:

$$\frac{4}{3} \pi b_p^3 N_p \ll 1 \quad (12)$$

The impact approximation also implies the opposite of the criterion of the quasi-static approximation<sup>2</sup>, that is

$$\Delta\omega \ll \frac{u_p}{b_p} \quad (13)$$

where  $\Delta\omega$  defines the region around the line center that can be confidently modeled under impact approximation theory. The largest possible impact parameter for a perturbing collision is limited by the Debye length,  $\lambda_D$ . For electrons as perturbers with average velocity,  $u = (8kT_e / \pi m_e)^{1/2}$ , equation (13) can be reduced to  $\Delta\omega < \omega_{pe}$  where  $\omega_{pe}$  is the electron plasma frequency.

Anderson<sup>37</sup> states that the impact approximation is equivalent to assuming that all emission lines are either well resolved or not at all resolved when compared to the linewidth, i.e., degenerate levels. This simplification was removed by Kolb<sup>47</sup> who generalized Anderson's method to include overlapping lines. We return to Anderson's theory for reason of model efficiency. The comparison of the calculations with those using more complex theory and with experimental data will test the success of the approximations used.

Under the impact approximation, the spectral distribution of a single transition is Lorentzian<sup>60</sup>

$$L(\tilde{\omega} - \tilde{\omega}_{ij}) = \frac{\delta\tilde{\omega}_{ij} / \pi}{(\tilde{\omega} - \tilde{\omega}_{ij} - \Delta\tilde{\omega}_{ij})^2 + \delta\tilde{\omega}_{ij}^2} \quad (14)$$

where  $\delta\tilde{\omega}_{ij}$  is the half width at half the maximum line intensity and  $\Delta\tilde{\omega}_{ij}$  is the line shift due to electron impact. Once the electron collisional broadening width and shift are determined then equation (14) can be used to construct the total line emission spectrum through summation over all electric dipole allowed transitions.

The line broadening cross section,  $\sigma_b$  and line shift cross section,  $\sigma_s$ , for an electron-radiator collision are related to the linewidth and lineshift by

$$\delta\tilde{\omega}_{ij} = N_e u_e \sigma_b \quad (15)$$

$$\Delta\tilde{\omega}_{ij} = N_e u_e \sigma_s \quad (16)$$

The cross sections are calculated from Anderson's<sup>37</sup> equation (52)

$$\sigma = \sigma_b + i\sigma_s = \int_0^\infty 2\pi S(b) db \quad (17)$$

where  $b$  is the impact parameter and  $S(b)$  may be interpreted as the probability of an electron collision disturbing the emission of radiation.  $S(b)$  is written in terms of the time-development matrix,  $T(t)$ , which is approximated by<sup>37</sup>

$$T(t) = \frac{2\pi}{ih} \exp \left[ - \int_{-\infty}^t H_1(t') dt' \right] \quad (18)$$

where  $t$  is time and  $H_1$  is the interaction Hamiltonian. Additionally, the classical path, impact and binary approximations greatly simplify the Hamiltonian describing the interaction of the perturber and emitter. The interaction Hamiltonian for the electron-neutral interaction is:

$$H_1 = -\frac{e^2}{r_c} + \frac{e^2}{\sqrt{r_c^2 - 2r_c r_a + r_a^2}} \quad (19)$$

where the distances from the  $O^+$  nucleus to the perturbing and emitting electron are, respectively,  $r_c$  and  $r_a$ . The first term is the Coulomb attraction between the perturbing electron and the oxygen nucleus and the second term is the Coulomb repulsion between the perturbing electron and the emitting electron.

Expanding the second term in equation (19) in  $(r_a/r_c)$ , and retaining the first order terms, one obtains the point-dipole charge interaction Hamiltonian

$$H_1 = e^2 \cos\gamma \frac{r_a}{r_c^2} \quad (20)$$

with  $\gamma$  as the angle between vectors  $r_c$  and  $r_a$ . To express the interaction Hamiltonian in spherical coordinates  $(r, \theta, \phi)$ , we choose the electron-atom collision to occur in a plane with  $\phi_c = 0$  and define the relationship of collision parameters to  $r_c$  and  $\theta_c$  by invoking the classical path approximation through

$$\begin{aligned} \cos\theta_c &= \bar{u}t / r_c \\ \sin\theta_c &= b / r_c \\ r_c^2 &= b^2 + \bar{u}^2 t^2 \end{aligned} \quad (21)$$

where  $\bar{u}$  is average electron velocity,  $t$  is time,  $b$  is the impact parameter. By substituting the relations in equation (21) into equation (20) through

$$\cos\gamma = \cos\theta_a \cos\theta_c + \sin\theta_a \sin\theta_c \cos(\phi_a - \phi_c) \quad (22)$$

the Hamiltonian becomes

$$H_1 = \frac{e^2 r_a}{r_c^3} (\lambda_{za} \bar{u}t + \lambda_{xa} b) \quad (23)$$

where  $\lambda_{za} = \cos\theta_a$  and  $\lambda_{xa} = \sin\theta_a \cos\phi_a$  are direction cosines of the emitting electron. To obtain a tractable expression for  $T(t)$  of equation (18), it is expanded in terms of powers of a matrix,  $P$ ,

$$P = \frac{2\pi}{h} \int_{-\infty}^{\infty} H_1(t) dt \quad (24)$$

The expression for  $S(b)$  is then written in terms of powers of the matrix  $P$  which result from the expansion of  $T(t)$ :

$$S(b) = S_0 + S_1 + S_2 + \dots \quad (25)$$

$S_0$  is zero for all situations.<sup>33</sup> As stated in Anderson<sup>37</sup>, the first-order term,  $S_1$  is imaginary and, thus, the first "shift" term of the expansion. For the present problem  $S_1$  is also zero as it depends on the interaction matrix elements that are zero due to symmetry (Anderson's equation<sup>37</sup> (54b)).  $S_2$  has two types of second-order terms and are named in Anderson<sup>37</sup> as  $(S_2)_{middle}$  and  $(S_2)_{outer}$  (Anderson's equations<sup>37</sup> (54c',c'')).  $(S_2)_{middle}$  is zero for the same reason as  $S_1$ . The only non-zero term in the second-order approximation is  $(S_2)_{outer}$ .  $S(b)$  is subsequently expressed as

$$S(b) \approx S_2(b) = \frac{1}{2} \left[ \sum_{m_i} \frac{\langle i, m_i | P^2 | i, m_i \rangle}{2l_i + 1} + \sum_{m_f} \frac{\langle f, m_f | P^2 | f, m_f \rangle}{2l_f + 1} \right] \quad (26)$$

where  $|i\rangle = |n_i l_i\rangle$  and  $|f\rangle = |n_f l_f\rangle$  are the initial and final states. This term gives the probability of a transition being caused by a collision averaged over the initial and final states. The line shift cross section is zero for the second-order approximation. The  $P$ -matrix element is given by

$$\langle a | P | b \rangle = \frac{2\pi}{h} \int_{-\infty}^{+\infty} \exp(i\omega_{ab}t) \langle a | H_1(t) | b \rangle dt \quad (27)$$

where  $\omega_{ab}$  is the transition frequency. The states  $|a\rangle = |nlm\rangle$  and  $|b\rangle = |n'l'm'\rangle$  are the wave functions of the radiator with the primed states being the perturbing states. With  $H_1$  given by equation (23), the  $P$ -matrix element becomes

$$\langle a | P | b \rangle = \frac{4\pi e^2}{h} \left[ iM_{za} \int_0^{t_D} \frac{ut \sin(\omega_{ab}t) dt}{(b^2 + u^2 t^2)^{3/2}} + M_{xa} \int_0^{t_D} \frac{b \cos(\omega_{ab}t) dt}{(b^2 + u^2 t^2)^{3/2}} \right] \quad (28)$$

where  $M_{za} = \langle a | r_a \lambda_{za} | b \rangle$ ,  $M_{xa} = \langle a | r_a \lambda_{xa} | b \rangle$  and  $\lambda$ 's are the direction cosines. The computation of the P matrix element requires solution to the time integrals. To account for correlation effects between electrons that shield the perturbing electron's electric field, a cutoff in the scattering integration over impact parameter is applied at the Debye length,  $\lambda_D$ . The introduction of a collision operator cutoff sets the upper integration limit,  $t_D$ , at

$$t_D = \frac{1}{v} (\lambda_D^2 - b^2)^{1/2} \quad (29)$$

Once the matrix element of  $P$  for a particular impact parameter is calculated, then  $S(b)$  is obtained through equation (26). Because  $S(b)$  diverges at small  $b$  values, a strong-collision cutoff ( $b_{min}$ ) is applied to suppress the divergence in the integration.<sup>8,62,64</sup> A Lorentz-Weisskopf type term is used to approximate the contribution of strong collisions to the broadening cross section by assuming that the phase shifts and inelastic effects produced by the electron-atom collisions are so large that the scattering operator matrix elements either oscillate rapidly between +1 and -1 or approach 0. The maximum impact parameter,  $b_{max}$ , outside which  $S(b)$  is taken as zero, is determined by Debye shielding as mentioned earlier. Although Griem<sup>31</sup> and Chappell *et al.*<sup>62</sup> argue that the maximum impact parameter should be  $1.123 \lambda_D$  and  $0.682 \lambda_D$  respectively, little difference was observed in the calculated spectra when these values were used. The maximum impact parameter use here is  $1.0 \lambda_D$ . Only small errors are introduced into line width calculations by the above second-order expansion and impact parameter cutoff procedures.

### 3. Additional Approximations

The time integral (eq. (28)) is solved numerically using a weighted trapezoidal routine. Because the numerical solution to the integrals is time consuming, an approximate analytic solution is obtained by allowing  $t_D$  to go to infinity. The integral can then be expressed analytically in terms of modified Bessel functions of integer order.

The computational demands of spectral models have motivated the need for greater levels of approximation. Along with the above theoretical and numerical approximations, we have included the options to make the following additional approximations in calculating the spectral line widths: one may choose to use (1) unperturbed wave functions and energy levels, (2) ion-perturbed energy levels only, or (3) ion-perturbed wave functions and energy levels. These three approximation levels are termed the *unperturbed*, *semi-perturbed*, and *perturbed* cases, respectively. If the wave functions and energies are not perturbed significantly by the ions, then the calculations of electron broadened line widths can be simplified by using the unperturbed wave functions and energies. For the *unperturbed* case, the calculations are performed for transitions between two  $n, l$  states with no ion collisional effects incorporated into the solution. For the *semi-perturbed* and *perturbed* cases, the calculation of  $S(b)$  is performed for transitions between two  $n, l, m$  states. The summation over  $m_i$  and division by  $2l_i+1$  in equation (26) are omitted since the magnetic substates are treated explicitly. These approximations are only justified by comparison to data and published linewidth calculations.

The levels of approximation, perturbed, semi-perturbed and unperturbed were examined for computational efficiency and degrading effects. Computational efficiency depends on the number of microfield intervals, number of basis states, and the number of lines in a spectral range. However, the unperturbed calculations are about a factor of 10 faster than the semi-perturbed calculations. The fully perturbed calculations are from 10 to  $>1000$  times slower than the semi-perturbed calculations. From performing many unperturbed and semi-perturbed calculations, it is found that the unperturbed lines are sometimes 30% narrower than lines from semi-perturbed calculations. A fully perturbed calculation and a semi-perturbed calculation over the spectral range  $3.5\mu\text{m}$  to  $8\mu\text{m}$  showed very little difference in the structure. The semi-perturbed calculations were used in the comparisons presented below.

## B. APOSTLE Model

The APOSTLE model was designed for computational efficiency to provide calculated spectra over large spectral ranges. APOSTLE consists of three modules, executed sequentially: *mfd*, *stark*, and *linshape*. The objective of APOSTLE is to predict the characteristic nature of a collisionally broadened spectra arising from a laser induced plasma.

In essence, the approach of the APOSTLE model lies in the determination of the spectral Radiance ( $\text{Wcm}^{-3}\text{sr}^{-1}(\text{cm}^{-1})^{-1}$ ) of a collisional-Stark broadened line:

$$I(\tilde{\omega} - \tilde{\omega}_{ij}) = N_i A_{ij} \varepsilon_{ij} L(\tilde{\omega} - \tilde{\omega}_{ij}) \quad (30)$$

where  $A_{ij}$  is the Einstein coefficient,  $\varepsilon_{ij}$  is the energy of the transition and  $L(\tilde{\omega} - \tilde{\omega}_{ij})$  is given by equation (14). The upper state population,  $N_i$  is given by:

$$N_i = \frac{N_0 g_i}{Z} \exp\left(-\frac{hcF_i}{kT}\right) \quad (31)$$

Figure 10 shows the modular design of APOSTLE. The first module performs the task of computing the ion microfield probability distribution. This code is executed first for which its output used as the input for the second module, *stark*. *Stark* is the main module responsible for computing the line positions, Einstein coefficients, state populations, and spectral distribution half-widths. The output

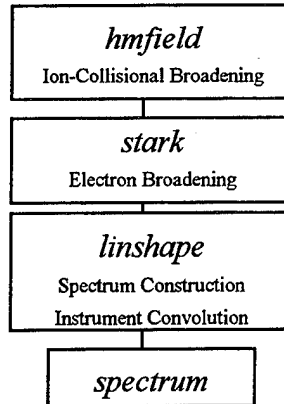


Figure 10. Modular design of the APOSTLE model.

of *stark* is then used in the third module, *linshape*, which constructs the spectrum according to equation (30), then convolves the spectrum with a user specified instrumental line shape.

The first code in the APOSTLE suite, *mfd*, is used to calculate the Stark effect on the oxygen Rydberg lines induced by the presence of ionic species. The computer code was written by C. F. Hooper<sup>72</sup> and it is used in the APOSTLE model in unmodified form. The only documentation available exists in the form of comments in the FORTRAN source code. The physical basis for the

code has been published by Hooper.<sup>58</sup> The output of *mfd* is a set of weighted electric field strengths with the corresponding probabilities of producing these field strengths. This output file, a graphical example of which is given in Figure 11, is used as an input file for the spectral-line-broadening code *stark*.

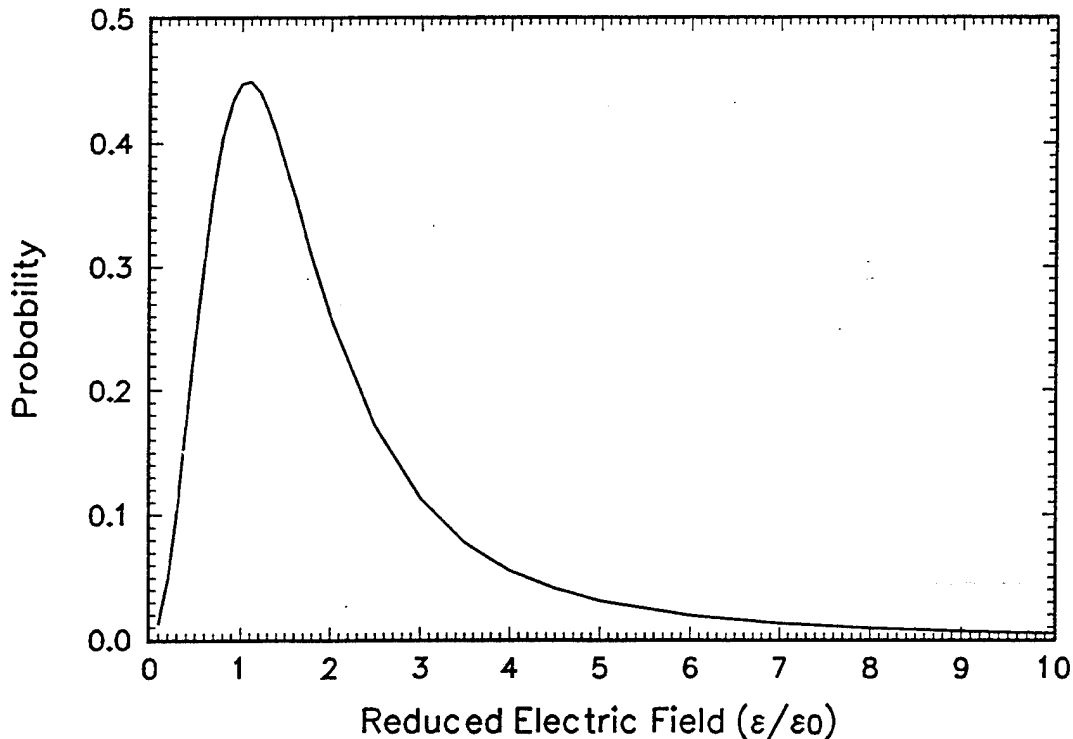


Figure 11. The APOSTLE calculated electric field probability distribution for ion-collisional broadening.

The effect of collisional-Stark broadening of the oxygen Rydberg spectral lines, by both ion and electron perturbers is calculated in *stark*. Figure 12 illustrates the block structure of the APOSTLE *stark* module. The *stark* module function is to calculate line positions, Einstein coefficients, state populations, and spectral line widths. The calculation is performed iteratively over the ion microfield distribution according to the basis set, microfield, spectral range, and parameters provided. State populations are calculated internally using to eq (24) according to the electronic temperature or will also accept populations calculated independently.

Figure 13 is a plot of  $gA$  with  $\lambda$  (product of the Einstein coefficient and upper state degeneracy) under unperturbed, zero-field conditions from 2-30  $\mu\text{m}$ . These values are tabulated in Appendix C. The figure shows a general tendency of decreasing values of  $gA$  with  $\lambda$  with  $gA$  varying over more than four orders of magnitude. However, five prominent groups of transitions can be readily

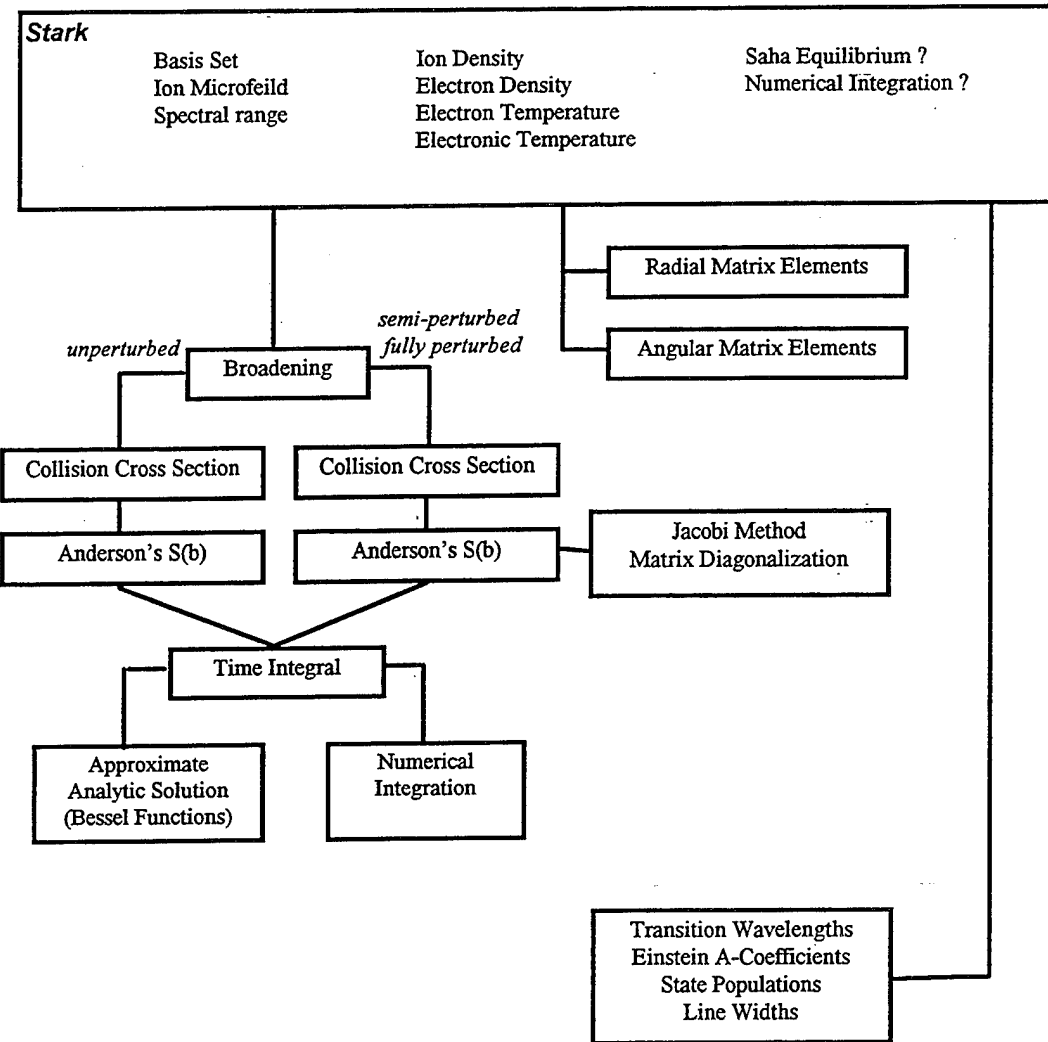


Figure 12. Block structure of the APOSTLE *stark* module.

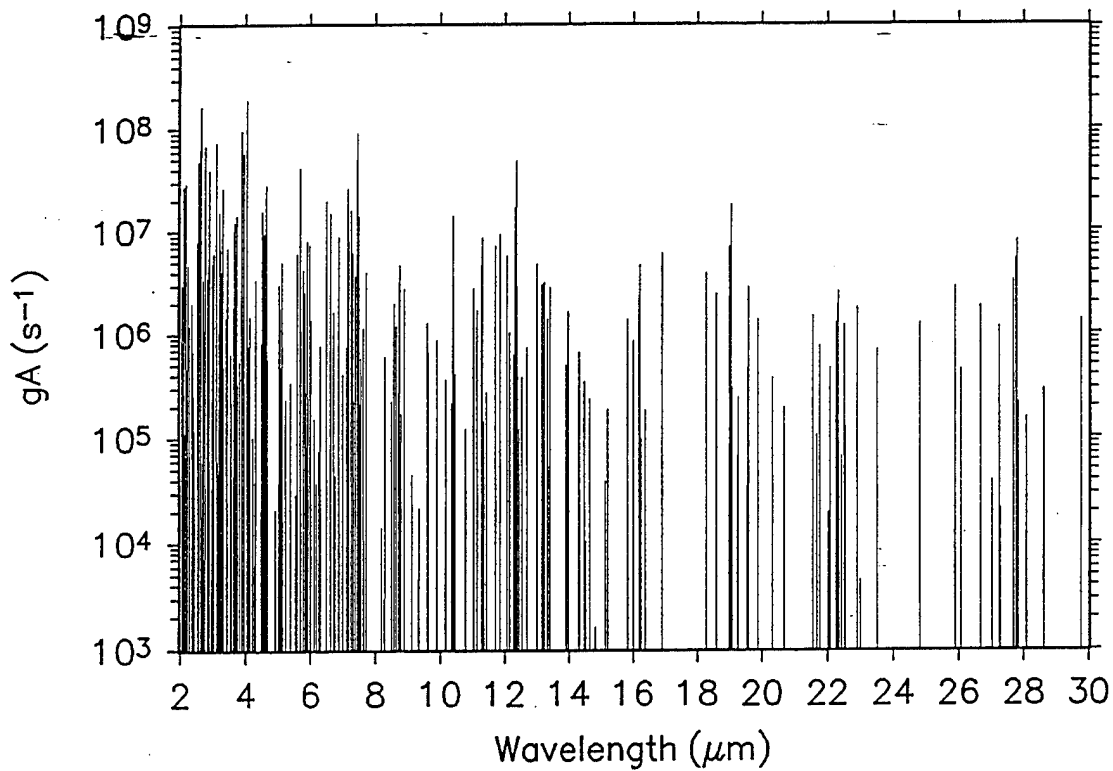


Figure 13. Plot of  $g_A$  as function of  $\lambda$  as predicted by the APOSTLE model in the absence of collisional-Stark broadening.

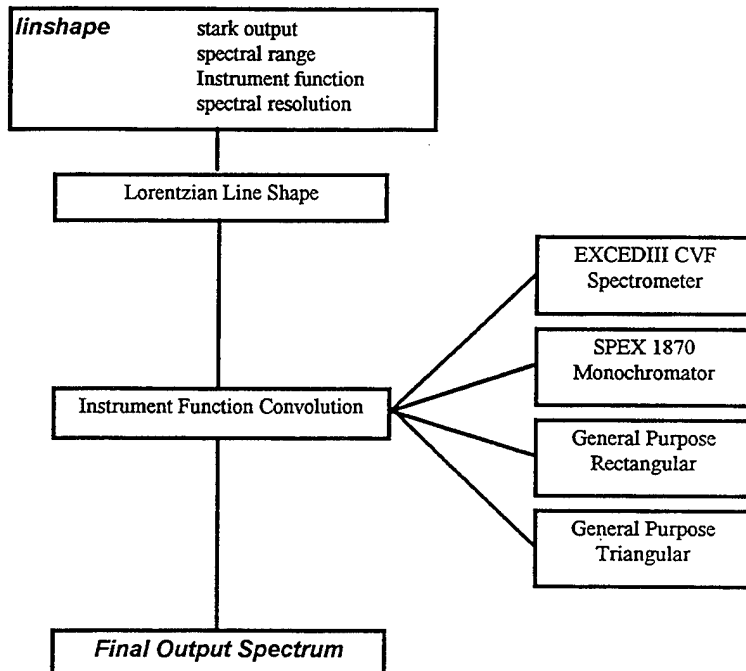


Figure 14. Block structure of the APOSTLE *linshape* module.

observed in the plot: 4.04  $\mu\text{m}$ , 7.45  $\mu\text{m}$ , 12.35  $\mu\text{m}$ , 19.0  $\mu\text{m}$ , and 27.8  $\mu\text{m}$ . The line position, Einstein coefficients, upper state populations, and electron-broadened half-widths define the output of *stark* which is used in the third APOSTLE module, *linshape*.

The third module in the APOSTLE model, *linshape*, performs the construction of the instrumentally convolved spectrum from the line-by-line broadening information from *stark*. This is accomplished in two steps: first, the Lorentzian spectral distribution is constructed for each transition from the line positions, Einstein coefficients, upper state populations, and spectral half-widths for each transition. Second, the spectrum is then convolved with an instrumental line shape (ILS) function which is user flexible and computed internally. Figure 14 illustrates the structure of *linshape*.

The total spectral radiance of the spectrum is obtained from the summation of eq (23) over all transitions. In wavelength space ( $\text{Wcm}^{-3}\text{sr}^{-1}\mu\text{m}^{-1}$ ) this is equal to,

$$I(\lambda) = \frac{1}{\lambda^2} \sum_{i,j} I(\tilde{\omega} - \tilde{\omega}_{ij}) \quad (32)$$

From this, the unconvolved spectrum is convolved with the ILS function,  $f(\lambda)$ :

$$I^*(\lambda) = \int I(\lambda') f(\lambda - \lambda') d\lambda' \quad (33)$$

Presently, options available include a function for a SPEX Industries model 1870 grating monochromator, EXCEDEIII CVF4 (circularly variable filter) spectrometer, and two general purpose ILS functions (triangular and rectangular) requiring user input resolution. Figure 15 illustrates a typical situation of the convolution of an unconvolved Lorentz distribution with the SPEX ILS function. In this figure, the ILS is characterized by a fwhm of  $\sim 0.032 \mu\text{m}$ .

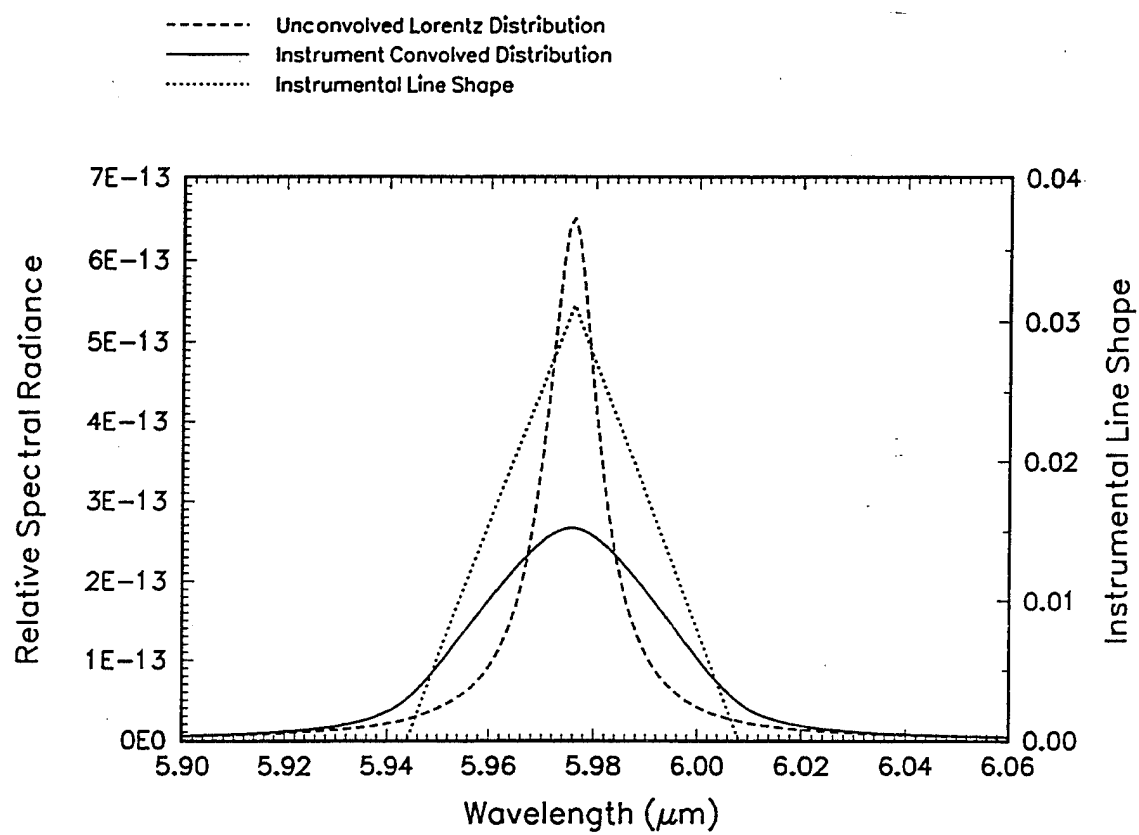


Figure 15. Example of the effect convolution of triangular instrumental line shape with a collisional-Stark broadened line.

## 7. APOSTLE MODEL VS. DATA

### A. Collisionally Dominated Plasma

The line emission model provides a spectral prediction to the laser-produced oxygen plasma IR spectrum in Chapter 4. The results of the fitting procedure are shown in figure 3. For the fitting procedure the parameter space ( $T_e$ ,  $T_{el}$ ,  $N_e$ ) of the line model was explored. The basis set consisted of 62 states (31 triplets and 31 quintets) with the highest principal quantum number,  $n=8$ . The plasma density was varied between  $2 \times 10^{15} \text{ cm}^{-3}$  to  $2 \times 10^{16} \text{ cm}^{-3}$ , and electron and electronic temperature parameters were varied between 5000K to 50,000K in 5000K intervals, and 5000K to 20,000K in 5000K intervals, respectively. The spectral calculations have been done with the semi-perturbed approximation of the model due to the computational demands of a fully perturbed calculation. A fully perturbed calculation was performed for a single set of parameters and compared to a semi-perturbed calculation at the same values. The results showed very little difference over the broad spectral range that was compared ( $3\mu\text{m} < \lambda < 12\mu\text{m}$ ).

The model was fit to the data using the empirically derived electronic temperature and atomic oxygen density. Using these values, an absolute Boltzmann state population distribution was generated. Stark broadening is relatively insensitive to electron temperature<sup>14</sup> but there are slight variations in shapes of some features. The fitting procedure was the variation of the electron density to give the best model-data agreement in the line widths of the  $4p^5P-3d^5D$  ( $5.976 \mu\text{m}$ ) and the  $5d^5D-5p^5P$  ( $5.6847 \mu\text{m}$ ) transitions. This resulted in an estimated electron density of  $8 \times 10^{15} \text{ cm}^{-3}$ .

In general, the agreement between model and data is good, although the model is excessively broadened for the  $7.45$  and  $12.35 \mu\text{m}$  emission features. Integrated band intensities over three spectral bands were calculated to investigate the discrepancy of the model prediction at  $7.45$  and  $12.35 \mu\text{m}$ . Table 7 lists the calculated integrated intensities for model and data.

TABLE 7. Model vs. Data comparison of band integrated intensities.

Wavelength Band ( $\mu\text{m}$ )	Data ( $\text{Wcm}^{-2} \text{ Sr}^{-1}$ )	APOSTLE( $\text{Wcm}^{-2} \text{ Sr}^{-1}$ )
3.8-4.3	$4 \times 10^{-4}$	$3 \times 10^{-4}$
6.9-8.0	$1 \times 10^{-4}$	$9 \times 10^{-5}$
10.8-12.35	$2 \times 10^{-5}$	$1 \times 10^{-5}$

Comparing the values in the first and second bands, the model prediction and experiment are in good agreement, thus suggesting only a line shape mismatch at 7.45  $\mu\text{m}$ . In third wavelength band, it is possible that the discrepancy observed may be due in part to the poor detector responsivity beyond 12.5  $\mu\text{m}$ . The disagreement of model and measurement for 7.45  $\mu\text{m}$  and 12.35  $\mu\text{m}$  features may be partly due to the fact that these features consist of strongly overlapping lines. The present model assumes that the lineshape for overlapping lines is the sum of the individual transition spectral distributions. Interference effects from overlapping lines may narrow the linewidth. To obtain a better agreement for multiplet lineshape, it is necessary to use the more complex expression for the lineshape of overlapping lines.<sup>47</sup>

Additionally, the plasma conditions may not be sufficiently described by Saha equilibrium. An examination of the constants of thermal equilibration suggests that equilibrium conditions between electron kinetic and other temperatures do not exist at early times within laser induced plasma emission region. The initial energy deposition of the laser beam into the focal region dissociates, fully ionizes and multiply ionizes the oxygen gas. Excess energy elevates the electron temperature. The ions quickly heat up and the plasma begins an expansion from the deposition region. Chemical kinetics calculations<sup>43</sup> indicate that recombination rapidly changes the gas from a fully ionized to partially ionized plasma within  $3 \times 10^{-7}$  s. At  $10^{-6}$  s, the ions should be in approximate equilibrium with the now dominant neutral O atoms due to the fast ion-neutral thermal transfer time constant ( $10^{-10}$  s). The equilibration time between the light electrons and heavy particles is significantly longer (about  $6 \times 10^{-6}$  s). Thus, the species kinetic temperatures may not be equal at the measurement time. This result is observed in modeling of a laser induced plasma done by Milroy et al. (1979)<sup>63</sup>.

Finally, it is worthwhile to examine the uncertainties in the calculations of the spectral emissions. The uncertainty in the plasma parameters is harder to quantify. Uncertainty in the electron density and temperature determinations is estimated to be from 30% to 50% based on changes in the spectra as the plasma parameters are varied. In addition, the model calculation is for spatially homogeneous conditions. The line-of-sight integration of the laser-induced plasma is most certainly not homogeneous. Given these uncertainties, the comparison of model with experiment is satisfactory.

## B. ARCHON Chemical Kinetics Modelling

At this juncture, the possibility of non-thermal state populations can now be investigated. This investigation was carried out with the use of the ARCHON chemical kinetics model. The reaction set model, along with rate coefficients is listed in Table 8.

TABLE 8. ARCHON reaction set model.

Reaction	Process Type	a	b	c
$O^{5+} + e + e \rightarrow O^{4+} + e$	three-body	$8.7 \times 10^{-18}$	-4.5	0
$O^{5+} + e \rightarrow O^{4+} + e$	dielectronic	$1.7 \times 10^{-10}$	-1.5	5.6
$O^{5+} + e \rightarrow O^{4+} + e$	radiative	$2.2 \times 10^{-9}$	-0.7	0
$O^{4+} + e + e \rightarrow O^{3+} + e$	three-body	$4.5 \times 10^{-18}$	-4.5	0
$O^{4+} + e \rightarrow O^{3+} + e$	dielectronic	$1.1 \times 10^{-10}$	-1.5	5.6
$O^{4+} + e \rightarrow O^{3+} + e$	radiative	$8.9 \times 10^{-10}$	-0.7	0
$O^{3+} + e + e \rightarrow O^{2+} + e$	three-body	$1.9 \times 10^{-18}$	-4.5	0
$O^{3+} + e \rightarrow O^{2+} + e$	dielectronic	$6.2 \times 10^{-11}$	-1.5	5.6
$O^{3+} + e \rightarrow O^{2+} + e$	radiative	$2.8 \times 10^{-11}$	-0.7	0
$O^{2+} + e + e \rightarrow O^{+} + e$	three-body	$5.6 \times 10^{-19}$	-4.5	0
$O^{2+} + e \rightarrow O^{+} + e$	dielectronic	$2.8 \times 10^{-11}$	-1.5	5.6
$O^{2+} + e \rightarrow O^{+} + e$	radiative	$5.6 \times 10^{-11}$	-0.7	0
$O^{+} + e + e \rightarrow O + e$	three-body	$7.4 \times 10^{-20}$	-4.5	0
$O^{+} + e \rightarrow O^{+} + e + e$	re-ionization	$3.9 \times 10^{-12}$	1.5	162
$O^{+} + e \rightarrow O^{2+} + e + e$	re-ionization	$1.2 \times 10^{-13}$	1.5	400
$O^{2+} + e \rightarrow O^{3+} + e + e$	re-ionization	$1.8 \times 10^{-14}$	1.5	640
$O^{3+} + e \rightarrow O^{4+} + e + e$	re-ionization	$4.7 \times 10^{-15}$	1.5	890
$O^{4+} + e \rightarrow O^{5+} + e + e$	re-ionization	$1.3 \times 10^{-15}$	1.5	1300
$O^{+} + e \rightarrow O(n=11,l)$	recombination	$1 \times 10^{-12}/g_i$	-1.5	5.6
$O(n_i, l_i) \rightarrow O(n_f, l_f) + h\nu$	radiative cascade			

The details of the calculation are discussed in the *Infrared Emissions Final Report*.<sup>43</sup> However only the pertinent details will be discussed here. It is to be noted here that the present calculation is preliminary. The reaction set does not include oxygen atom impact excitation or quenching reactions. Collision cross sections for the former are at present unavailable. The model was chosen only to illustrate the effect of electron recombination with singly-ionized oxygen on the IR plasma spectrum, particularly the 7.45  $\mu\text{m}$  emission feature. The initial conditions were chosen to match the initial cell conditions before the laser pulse, which were 110 torr  $\text{O}_2$ . The time dependence of the electron temperature was obtained from the earlier SALE calculations.<sup>43</sup>

Several calculations were made with different reaction set models, the results of which are not documented here. The desired result was to predict the 7.45  $\mu\text{m}$  spectral distribution.

The calculation yielded the recombination driven state populations which were subsequently used for APOSTLE spectral calculations. Figure 16 shows the resulting triplet state population distribution (the quintet state distribution is similar) compared to a Boltzmann distribution at 10000 K. Figure 17 shows the resulting synthetic spectrum, compared to the previously best fit thermal model spectrum and the experimental spectrum at 20  $\mu\text{s}$ . The normalization of the two model spectra were chosen to be coincident with the observed peak intensities of the 5.69, 5.98, 6.61, and 6.86  $\mu\text{m}$  features for the thermal model and the peak intensity of the 7.45  $\mu\text{m}$  feature for the non-thermal case. Although the spectral fit is poor for the 5.69, 5.98, 6.61, and 6.86  $\mu\text{m}$  features in the non-thermal case, the spectral distribution of the 7.45  $\mu\text{m}$  feature is reproduced with a much higher quality. It was also observed that the 4.04  $\mu\text{m}$  feature appears to be relatively insensitive to either thermal or non-thermal populations. It appears that some features are modelled well using an collisionally-coupled populations and others using a non-thermal model.

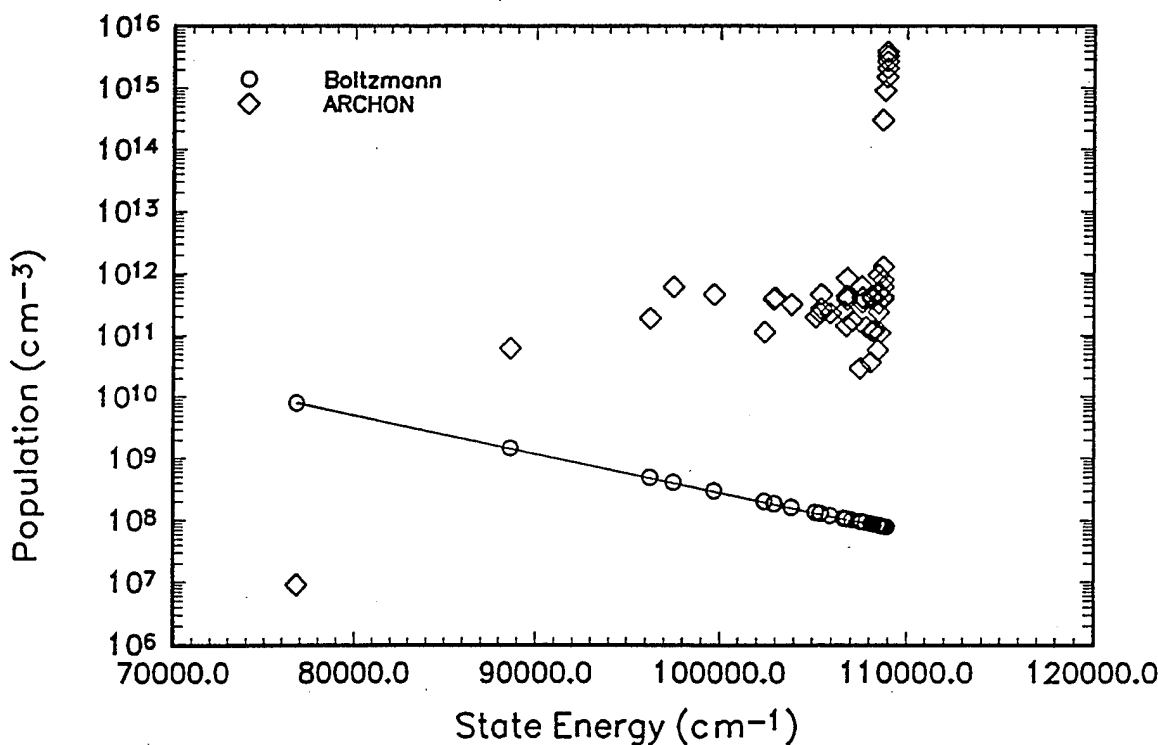


Figure 16. Comparison of the triplet Boltzmann state population distribution and the ARCHON calculation.

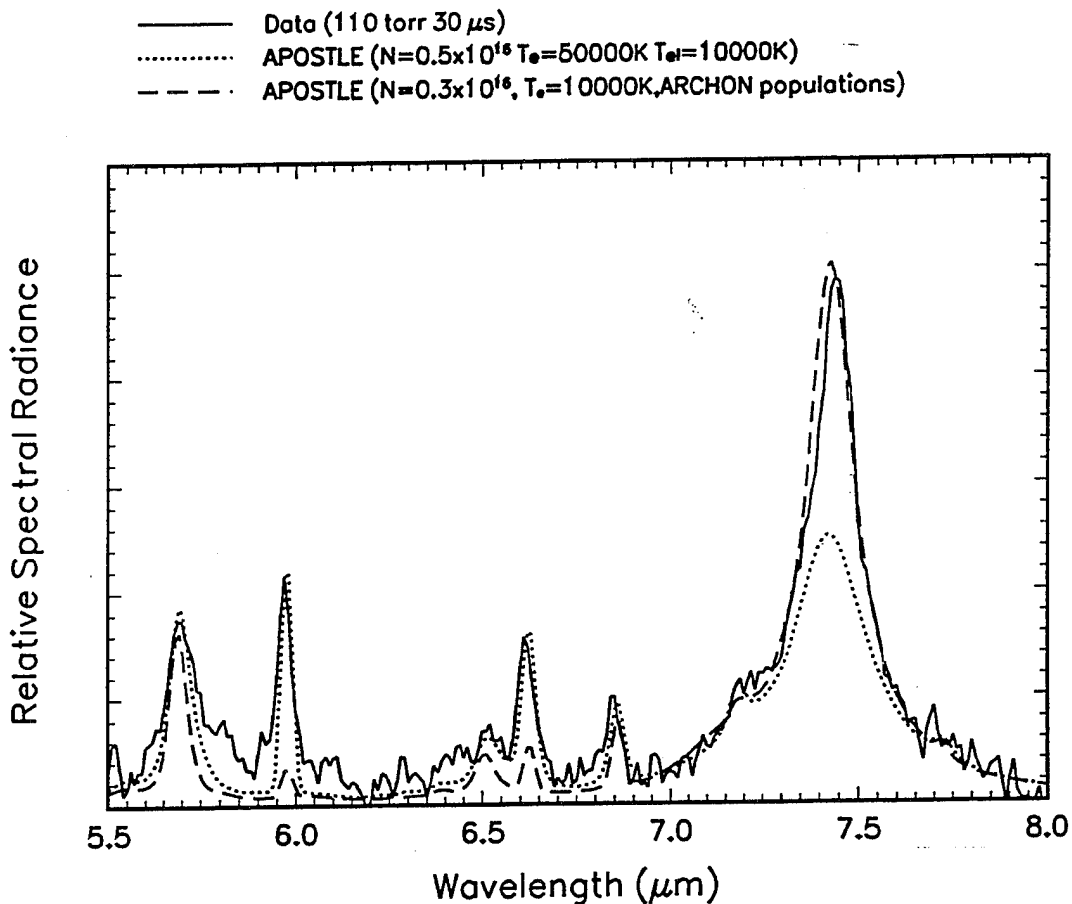


Figure 17. Comparison the APOSTLE predicted spectrum using collisionally-coupled state populations and the ARCHON calculated state populations.

## 8. SUMMARY AND CONCLUSIONS

We have obtained a time resolved infrared spectra from the center of a recombining laser produced oxygen plasma. Measurements were acquired in the spectral range from 3.5 to 13.0  $\mu\text{m}$  at an aperture delay time of 20  $\mu\text{s}$ . The transitions near 10.4, and 12.35  $\mu\text{m}$  are first reported observations in emission. The 10.4  $\mu\text{m}$  feature is a composite line dominated by the  $6d^5D$ - $6p^5P$  and  $5p^3P$ - $4d^3D$  transitions and the 12.35  $\mu\text{m}$  feature is dominated by the  $7g,h,i^{3,5}G,H,I$ - $6f,g,h^{3,5}F,G,H$  transitions.

In general, there is excellent agreement between line and continuum emission models and data. An electronic temperature of  $8000 \pm 1000$  K was derived from the spectroscopic analysis of the data. Using this value, the electron density was estimated at  $8 \times 10^{15} \text{ cm}^{-3}$  from the line emission

model. Lin's theoretical emissivity coefficients<sup>39</sup> were then used in conjunction with the assumption of Saha equilibrium to estimate the atomic oxygen density and the path length. The path length was derived to be 0.016 cm and the atomic oxygen density was estimated to be  $5 \times 10^{18} \text{ cm}^{-3}$  suggesting that the ionization level was <1%.

Although a single temperature was assumed to describe the state population distribution, this conclusion should not be interpreted rigorously since the plasma emission region may be inhomogeneous and inconsistent with collisional equilibrium conditions. However, the deduced temperature and density values were found to be in good agreement with the physical description of the plasma conditions given the experimental uncertainties.

The key issues surrounding the parametric characterization of the LINUS plasma include the temporal development of electron, ion, and neutral densities and temperature. These parameters determine the characteristic of the emission processes that unfold in the plasma relaxation. At early times, the observed radiance from the plasma is known to be continuum dominated, consisting mostly of Free-Free transitions in the field of an ion, Free-Bound processes, and Free-Free transitions in the field of a neutral. These processes are strongly dependent on the parameters densities and temperatures.

The present contract was coincident with the development of a new theoretical description for bremsstrahlung radiation due to electron-neutral collisions. This new model was compared to previous theories and the EGG-22 plasma radiance model. The agreement between EGG-22 and the new coefficients was good for an electron temperature of 10000 K thus validating EGG-22. The difference between Lin's coefficients and EGG-22 at higher temperatures is probably academic however, since at higher temperatures, the gas is nearly 100% ionized, and bremsstrahlung radiation due to F-F(N) becomes a minor source of radiation.

The present model of the Stark line broadening problem is based on the standard theory of Stark effect using the quasi-static approximation and impact theory of Anderson.<sup>37</sup> Many calculations in the four-dimensional parameter space ( $N_e$ ,  $T_e$ ,  $T_i$ ,  $T_{el}$ ) of the model were used to provide a best estimate of the plasma parameters within the measured spark region of a laser induced oxygen plasma. It is possible that the electron temperature departs from the OI electronic temperature during the early time of the spark ( $t < 10^{-5} \text{ s}$ ). However, the line spectrum is fairly insensitive to electron temperature and no estimates of  $T_e$  were obtained directly from lineshapes. The electron density and electronic temperature observed in the laser induced oxygen plasma were consistent with Saha equilibrium suggesting the plasma was collisionally dominated. These conclusions

compare favorably with previous atomic oxygen linewidth calculations and experimental studies of laser produced plasmas. The above favorable comparisons give confidence in the model results except for lines at  $7.45\mu\text{m}$  and  $12.45\mu\text{m}$  where approximation criteria failed. Although the present approach has been only applied to OI as radiator, the model should be applicable to emitters in a plasma that satisfy L-S coupling.

Two important issues related to the LINUS IR emission spectrum are homogeneity of the emission region and the attainment of local thermodynamic equilibrium. Thermal and non-thermal state population modelling was performed which was then used for APOSTLE spectral calculations. Non-thermal state populations were modelled with ARCHON using a reaction set model consisting primarily of three-body, dielectronic, and radiative recombination, and radiative decay. The  $7.45\mu\text{m}$  line shape was predicted with a much higher quality than that predicted using thermal populations. It was concluded that the different spectral character of the  $7.45\mu\text{m}$  emission could be due to at least two causes: insufficient treatment of overlapping lines or non-thermal state populations.

Spatial imaging of the LINUS plasma emission region was unfortunately not accomplished in the present study. This is a key issue important to understanding the plasma development and subsequent relaxation. The experimental observation of spatial information could also be used to benchmark the SALE hydrodynamic calculations<sup>43</sup>, as well as directly address the issues of homogeneity and collisional-radiative processes.

## REFERENCES

1. R.A. Armstrong, R.A. Lucht, W.T. Rawlins, Spectroscopic Investigation of Laser-Initiated Low Pressure Plasmas in Atmospheric Gases, *Appl. Optics*, 22, 10 (1983).
2. L.J. Radziemski and T.R. Loree, Laser-Induced Breakdown Spectroscopy: Time-Resolved Spectrochemical Applications, *Plasma Chem. And Plasma Proc.* 1(3), 281 (1981).
3. S.A. Ramsden and P. Slavic, A Radiative Detonation Model for the Development of a Laser-Induced Spark in Air, *Nature* 203, 1217 (1964).
4. J.B. Lurie and J.C. Baird, Medium Wavelength Infrared Emission from a Laser-Produced Oxygen Plasma: Observations of OI  $6h^{3,5}$  at 7.5  $\mu\text{m}$ , *Chem. Phys. Lett.* 125(4), 389 (1986).
5. J.B. Lurie, S.M. Miller, W.A.M. Blumberg, and R.A. Armstrong, Short Wavelength Infrared Line Emission in a Laser-Produced Plasma, *Chem. Phys. Lett.* 120, 481 (1985).
6. P.R. Brown, P.B. Davies, and S.A. Johnson, Infrared Laser Absorption Spectra of Rydberg Transitions of O-atoms, *Chem. Phys. Lett.* 133(3), 239 (1987).
7. G. Winkelmann and J. Tilgner, The Infrared Emission Spectrum of an Argon Plasma Jet Between 4 and 25 Microns, *Beitr. Plasmaphys.* 23(2), 193 (1983).
8. W.L. Wiese and N. Konjevic, Regularities and Similarities in Plasma-Broadened Spectral Line Widths (Stark Widths), *J. Quant. Spectrosc. Radiat. Transfer* 28(3), 185 (1982).
9. S. Chung, C.C. Lin, and E.T.P. Lee, Transition Probabilities of OI Spectral Lines, *J. Quant. Spectrosc. Radiat. Transfer*, 36, 19, (1986).
10. H.R. Griem, *Plasma Spectroscopy*, McGraw-Hill, New York, (1964).
11. H.R. Griem, *Spectral Line Broadening by Plasmas*, Academic Press, New York, (1974).
12. H.R. Griem, in *Advances in Atomic and Molecular Physics*, edited by D.R. Bates and B. Bederson, Academic Press, New York, (1975), Vol. 11, pp. 331-359.
13. H.R. Griem, in *Proceedings of the Eighteenth International Conference on Phenomena in Ionized Gases*, edited by W.Terry, Vol. 2, pp. 100, (1987).
14. N. Konjevic and J.R. Roberts, A Critical Review of the Stark Widths and Shifts of Spectral Lines from non-Hydrogenic Atoms, *J. Phys. Chem. Ref. Data* 5, 209 (1976).
15. N. Konjevic, M.S. Dimitrijevic, and W.L. Wiese, Experimental Stark Widths and Shifts for Spectral Lines of Neutral Atoms, *J. Phys. Chem. Ref. Data* 13, 619 (1984).
16. M.S. Dimitrijevic and N. Konjevic, Stark Broadening of Isolated Spectral Lines of Heavy Elements in Plasmas, *J. Quant. Spectr. Radiat. Transfer* 30, 45, (1983).
17. M. Jung, Broadening of Spectral Lines in Neutral Oxygen through a Microfield., *Z Astrophys.* 58, 93 (1963).

18. W.L. Wiese and P.W. Murphy, Shifts and Widths of Some Stark-Broadened Oxygen Lines in an Arc Plasma, *Phys. Rev.* 131(5), 2108 (1963).
19. K.R. Peschmann, Stark Effect of Oxygen Lines in an Arc, Emission Spectrum in the Spectral Range 5440-4050 A. *Z. Physik* 201, 79 (1967).
20. J.C. Morris and R.L. Garrison, Measurement of the Radiation Emitted *f*-Values and Stark Half-Widths for the Strong Vacuum Ultraviolet Lines of OI and NI. *Phys. Rev.* 188(1), 112 (1969).
21. R. Assous, The Width and Shift Caused by the Stark Effect for Lines of Neutral Atoms of Oxygen, *J. Quant. Spectr. Radiat. Transfer* 10, 975 (1970).
22. M.H. Miller and R.D. Bengtson, Measured Stark Widths and Shifts for Neutral Atomic Lines, *Phys. Rev. A* 1, 983 (1970).
23. A. Goly, D. Rakotoarijimy, and S. Weniger, Experimental Stark Parameters for Some Lines of Neutral Carbon, Oxygen and Sulfur, *J. Quant. Spectrosc. Radiat. Transfer*, 30, 417 (1983).
24. A. Goly and S. Weniger, Widths and Shifts of Some Plasma-Broadened Oxygen and Carbon Multiplets, *J. Quant. Spectrosc. Radiat. Transfer*, 38, 225 (1987).
25. R. Assous, Stark Effect in Infrared Lines in a Torch of Plasma Maintained at High Frequency, *J. Physique* 29, 877 (1968).
26. J.C. Morris, R.U. Krey, and R.L. Garrison, Radiation Studies of Arc-Heated Nitrogen, Oxygen and Argon Plasmas, *Air Force Space System Division, Report AVSSD-0049-68-RR* (1968).
27. J.M. Bridges and W.L. Wiese, Experimental Determination of Transition Probabilities and Stark Widths of SI and SII Lines, *Phys. Rev.* 159(1), 31 (1967).
28. M.S. Dimitrijevic and S. Sahal-Brechot, Stark Broadening of Neutral Helium Lines, *J. Quant. Spectrosc. Radiat. Transfer*, 31(1), 301 (1984); Stark Broadening of Na(I) Lines with the Principle Quantum Number of the Upper State Between 6 and 10, *J. Quant. Spectrosc. Radiat. Transfer*, 44, 421(1990); Stark Broadening of Li(I) Lines, *J. Quant. Spectrosc. Radiat. Transfer*, 46, 41, (1991).
29. J.C. Baird and S. Alexiou, Stark-Broadening in High Angular Momentum States of Atomic Oxygen - Application to Transitions Between 5.5  $\mu\text{m}$  and 8.0  $\mu\text{m}$ , *Chem. Phys. Lett.* 152(2-3), 124 (1988).
30. S. Alexiou and J.C. Baird, Emission Spectra of High Rydberg States in a Plasma: Stark Broadened Neutral Oxygen in the 7.5 Micron Region, *Phys. Rev. A* 42, 7413 (1990).
31. H.R. Griem, M. Baranger, A.C. Kolb, and G. Oertel, Stark Broadening of Neutral Helium Lines in a Plasma, *Phys. Rev.* 125(1), 177 (1962).

32. S. Sahal-Brechot, Stark Broadening of O VI Lines, *Astron. Astrophys.*, 1, 91 (1969); 2, 322 (1969).
33. L.A. Vainshtein and I.I. Sobel'man, Non-stationary Theory of the Stark Broadening of Spectral Lines in Plasmas, *Opt. Spectrosc.* 6, 279 (1959); R.J. Dyne and B.J. O'Mara, A Convergent Theory of Spectral Line Broadening in the Impact Approximation, *Astron. Astrophys.* 18, 363 (1972).
34. M. Baranger, Problem of Overlapping Lines in the Theory of Pressure Broadening, *Phys. Rev.* 111(2), 494 (1958).
35. M. Baranger, in *Atomic and Molecular Processes*, edited by D.R. Bates, Academic Press, New York, Vol. 13, pp. 493-548, (1962).
36. M. Baranger, Simplified Quantum Mechanical Theory of Pressure Broadening, *Phys. Rev.* 111(2), 481 (1958); 112, 855 (1958).
37. P.W. Anderson, Pressure Broadening in the Microwave and Infrared Regions, *Phys. Rev.*, 111, 76, 647 (1949).
38. C.F. Hooper Jr., Electric Microfield Distributions in Plasmas, *Phys. Rev.*, 149(1), 77 (1966); Low-Frequency Component Electric Microfield Distributions in Plasmas, *Phys. Rev.*, 165, 215 (1968); R.J. Tighe and C.F. Hooper Jr., Stark-Broadening in Laser-Produced Plasmas: A Two-Component, Two Temperature Formulation, *Phys. Rev. A*, 17, 410 (1978).
39. C. Lin, personal communication (1993).
40. T.L. John and R.J. Williams, Free-Free Absorption by N<sup>-</sup> and O<sup>-</sup>, *J. Quant. Spectrosc. Radiat. Transfer*, 17(2), 169 (1977).
41. S. Geltman, Free-Free Radiation in Electron-Neutral Atom Collisions, *J. Quant. Spectrosc. Radiat. Transfer*, 13, 601 (1973).
42. R.L. Taylor and G. Caledonia, Experimental Determination of the Cross Sections for Neutral Bremsstrahlung, *J. Quant. Spectrosc. Radiat. Transfer*, 9(5), 681 (1969).
43. P.C.F. Ip and R.A. Armstrong, Infrared Plasma Emissions, *Final Report, GL-TR-90-0131*, Air Force Geophysics Laboratory (1990).
44. R.W.P. McWhirter, in *Plasma Diagnostic Techniques*, Edited by R.H. Huddlestome and S.L. Leonard (Academic Press, New York 1965), chap. 5.
45. Y.B. Zel'dovich and Y.P. Raizer, in *Physics of Shock Waves and High-Temperature Hydrodynamic Phenomena*, edited by W.D. Hayes and R.F. Probstein, Academic Press, New York (1966), chap. V.
46. C.J. Tsao and B. Curnutte, Line Widths of Pressure Broadening in the Impact Approximation, *J. Quant. Spectrosc. Radiat. Transfer* 2, 41 (1962).

47. A.C. Kolb and H. Griem, Theory of Line Broadening in Multiplet Spectra, *Phys. Rev.* 111(2), 514 (1958).
48. J. Cooper and G.K. Oertel, Electron-Impact Broadening of Isolated Lines of Neutral Atoms in a Plasma, *Phys. Rev.* 180(1), 286 (1969).
49. E.U. Condon and G.H. Shortley, *The Theory of Atomic Spectra*, Cambridge University Press, (1963).
50. C.E. Moore, *Selected Tables of Atomic Spectra. Atomic Energy Levels and Multiplet Tables OI*, Nat. Stand. Ref. Data Ser., Natl. Bur. Stand. U.S. 3, Sec. 7, (1976).
51. B. Edlin, in *Handbuch der Physik*, edited by S. Flugge, Springer, Berlin, (1964), 27, pp. 80.
52. B. Isberg, Additions to the Normal Term System of the Spectrum of Atomic Oxygen, OI, *Arkiv Fysik* 35, 495 (1968).
53. M. Born and W. Heisenberg, Stark Effect in Hydrogen, *Z. Physik* 23, 338 (1924).
54. I. Waller, Second Order Stark Effect in Hydrogen and the Rydberg Correction of the spectra of He and Li<sup>+</sup>, *Z. Physik* 38, 635 (1926).
55. C. Lin, personal communication, (1992).
56. G.K. Oertel and L.P. Shomo, Tables for the Calculation of Radial Multipole Matrix Elements by the Coulomb Approximation, *Astrophys. J. Supp. Ser.* 16, 175 (1968).
57. D.R. Bates and A. Damgaard, The Calculation of the Absolute Strengths of Spectral Lines, *Phil. Trans. Roy. Soc. London Ser. A* 242, 101 (1949).
58. J. Holtsmark, On the Broadening of Spectral Lines, *Ann. Phys.* 58, 577 (1919).
59. M. Baranger and B. Mozer, Electric Field Distributions in an Ionized Gas, I. *Phys. Rev.* 115, 521 (1959); Electric Field Distributions in an Ionized Gas, II. *Phys. Rev.* 118, 626 (1960).
60. H.A. Lorentz, Stark Effect in Microfields, *Proc. Amst. Acad. Sci.* 8, 59 (1906).
61. C.F. Hooper Jr., Private Communication, (1989).
62. W.R. Chappell, J. Cooper, and E.W. Smith, Electron Correlations in Stark Broadening, *J. Quant. Spectrosc. Radiat. Transfer* 9(1), 149 (1969).
63. R.D. Milroy, C.E. Capjack, J.N. McMullin and C.R. James, Two-Dimensional Hydrodynamic Simulations of a Laser Heated Gas Target Plasma, *Can. J. Phys.* 57, 514 (1979).
64. L. Martin and W.F. Hornyak, eds., Methods of Experimental Physics, 8; (1969).
65. W. Lenz, Universal Theory of the Broadening of Spectral Lines, *Zeits. f. Physik.* 80, 423 (1933).
66. V.F. Weisskopf, Natural Line Broadening in a Beam of Harmonic Oscillators, *Phys. Zeits* 34, 1 (1933).
67. H.T. Betz and G.L. Johnson, in *Analytical Emission Spectroscopy Part I*, edited by E.L. Grove Marcel Dekker, Inc. New York (1971), chap. 5.

**APPENDIX A**

**APOSTLE USER'S MANUAL**

## I. INTRODUCTION

The APOSTLE computer code modules are written in FORTRAN 77 and are most efficiently executed on a computer with at least a i386 CPU with math coprocessor. The source code was developed as a three module program with Lahey and SVS brand compilers. In the past, the code has also executed successfully on SUN 386i workstation and the Apollo DN1000 computer. There is minimal "user-friendliness" code in the model. If a program execution is failing, it is advised to first check the input files for inconsistencies. If all parameters in the input files appear consistent, then one or more of those parameters may be outside the range of validity of the model.

The FORTRAN structure of each module is written compactly; that is, all subroutines and functions are contained in the source code module file. This design was meant to make source code compilation easier. Compilation is performed for each module, thus there should be three executables after compilation.

The APOSTLE program package should reside in one subdirectory. This is achieved by simply copying the source code, all of the input files, and external data files to a "C:\APOSTLE" subdirectory. A typical subdirectory listing may appear like:

```
Volume in drive C is MS-DOS 5
Volume Serial Number is 18E2-8248
Directory of C:\APOSTLE

.           <DIR>      04-21-94  8:36a
..          <DIR>      04-21-94  8:36a
README      3559  01-11-94  11:36a
M31S1       DAT      814  04-15-91  2:20p
M31S2       DAT      814  04-15-91  2:20p
M53S1       DAT     1387  09-20-91  11:40a
M53S2       DAT     1387  09-20-91  11:43a
M54S1       DAT     1415  04-07-93  8:48a
STARK        FOR    105430  06-24-94  11:55a
LINSHAPE    FOR    23126  05-23-94  11:57a
MFD          FOR    97707  01-09-94  11:34a
MFD          SET     362  01-07-94  11:22a
STARK1      SET     1194  06-24-94  11:46a
STARK2      SET     1194  06-24-94  11:47a
LINSHAPE    SET      796  05-23-94  10:16a
```

All files with the \*.set filename extensions are input files for the executables. These input files are edited manually before program execution. The information in the input files are commented and are meant to be self-explanatory. The format of the input files are structured as: parameters in column 1 and definitions/comments written in column 13. All data input is not formatted. The files M31S1.DAT, M31S2.DAT, M53S1.DAT, M53S2.DAT and

M54S1.DAT contain basis set information which is read in at the time of executables. The names of the \*.set files should never be changed since each program module searches the subdirectory for these files. Additionally, all input parameters in the input files should be in upper case. With these input files, a typical APOSTLE synthetic spectral calculation can be achieved in 4 steps:

- (1) edit input files
- (2) execute mfd.exe (microfield distribution) module
- (3) execute stark.exe (collisional stark broadening) module.
- (4) execute linshape.exe (line shape construction and instrument convolution) module

In the first step, the edited input files define the values of the parameters used by the model. These input files reside in the subdirectory where the output files will be written. It is useful to store the program executables in a "C:\BIN" subdirectory and including this subdirectory in the path statement of the AUTOEXEC.BAT file of the computer. The input files are edited using standard editors such as the MS-DOS editor "EDIT" or the Borland editor BRIEF. Once the input files are edited, program execution is carried out by typing the program module name at the DOS prompt. Program execution may also be carried out through the use of batch files.

In the second step, the mfd module is executed to create the microfield distribution. When the microfield distribution is created, the information is written to hard disk. In the third step, the stark module is executed. The calculation is looped over two iterations for spin 1 and spin 2. Thus there will be two output files from the stark module. The third and final step, is the construction of the spectrum from the line broadening information calculated by the stark module. Two files are written to hard disk: the instrument convolved spectrum and the unconvolved spectrum.

The following sections of this appendix describe the model I/O. Only partial output content is exemplified here due to the voluminous nature of the output files. The example input files may be used as a test case. The values of the input parameters for the test case have been chosen to reduce the program run time.

## II. MODULE I/O

### A. MFD

The first module executed is the ion microfield probability distribution module (mfd.exe). Figure A1 gives an example of the input file (mfd.set) for producing a microfield distribution

for an electron density of  $8 \times 10^{15} \text{ cm}^{-3}$  and an electron temperature of 10000 K. The output in this example is a single file (N8\_OT10.H15) consisting of a set of electric field strengths with the corresponding probabilities of producing these field strengths. There are a total of 51 sample points in the microfield distribution. The incremental spacing of this distribution is not constant.

<i>input</i>	<i>variable</i>	<i>description</i>
N8_OT10.H15	OUTFIL	OUTPUT FILENAME
0	IH	LOW FREQ.=0, HI FREQ.=1
0.8	EDENS	ELECTRON DENSITY XE16
10000.	TE	ELECTRON TEMP. IN K
1.1	ALPHA	INITIAL ESTIMATE (1.1)
0	R	RATIO OF TYPE 2 TO TYPE 1 PERTURBERS (0)
1.0	TRATIO	RATIO OF ELECTRON TO ION TEMPERATURE (1.0)
0	XI	NET RADIATOR CHARGE (0.0)
1	Z1	NET CHARGE OF TYPE 1 PERTURBER (1)
1	Z2	NET CHARGE OF TYPE 2 PERTURBER (1)
0.1	DALPHA1	VALUE FOR THE ALPHA-VALUE SEARCH (0.1)

Figure A1. The input file, mfd.set, is used to define the input parameters for the mfd module.

## B. STARK

The stark module calculates the line broadening information for spectrum construction. This output is used for the lineshape module. During execution, the information is written to the screen. The stark module reads in the input files (STARK1.SET and STARK2.SET), an example of which is given in Figure A2, and all the external files (M31S1.DAT, M31S2.DAT, N8\_OT10.H15, and possibly an externally calculated population file). In this example, a collisional-stark broadening calculation is performed for an electron density of  $8 \times 10^{15} \text{ cm}^{-3}$  and electron temperature of 10000 K.

<i>input</i>	<i>variable</i>	<i>description</i>
M31S1.DAT	NAMEIN	BASIS STATE FILENAME
0.8	XIDENS	ION DENSITY (1E16CM-3)
0.8	EDENS	ELECTRON DENSITY (1E16)
10000.	ETEMP	ELECTRON TEMPERATURE (K)
10000.	TEL	ELECTRONIC TEMPERATURE
4.0	WVMIN	MINIMUM WAVELENGTH
4.1	WVMAX	MAXIMUM WAVELENGTH
STARK1.DAT	NAMEOUT	OUTPUT FILENAME
N8_OT10.H15	NAMEFD	MICROFIELD FILENAME

51	NEPT	NUMBER OF ELECTRIC FIELD POINTS
5	NINC	SAMPLED INCREMENT
S	EBROAD	E-BROADENING: U,S,OR P?
C	ZEMAVG	IF U READ(R) OR CALCULATE(C)
NONE	NAMEWID	READ FROM FILE --->
Y	POPBOLTZ	POPULATION: BOLTZMANN? (Y/N)
N	NAMEPOP	IF N, READ FROM POP. FILE:
N	NAINT	NUMERICAL INTEGRATION?
10	NGAUSS	Quadrature intervals

Figure A2. The input file STARK1.SET used to define the input parameters for the stark module.

The input files (stark1.set and stark2.set) contains 18 lines each. The parameters in these files have the following definitions:

NAMEIN = name of the basis state filename  
 XIDENS = ion density in units of  $10^{16} \text{ cm}^{-3}$   
 EDENS = electron density in units of  $10^{16} \text{ cm}^{-3}$   
 ETEMP = electron temperature (K)  
 TEL = electronic temperature (K)  
 WVMIN = starting wavelength ( $\mu\text{m}$ )  
 WVMAX = ending wavelength of spectral range ( $\mu\text{m}$ )  
 NAMEOUT = name of the output file used in the linshape module  
 NAMEFD = name of the microfield distribution file  
 NEPT = number of points in the microfield distribution (51)  
 NINC = incremental sampling of the microfield distribution  
 EBROAD = electron broadening cases which have the following choices:  
     u - unperturbed energies and unperturbed wavefunctions  
     s - ion-perturbed energies and unperturbed wavefunctions  
     p - ion-perturbed energies and perturbed wavefunctions  
 ZEMAVG = for the unperturbed case, either [R]ead values of electron widths from a file or  
         [C]alculate the values  
 NAMEWID = if ZEMAVG=[R], file name to be read containing electron widths  
 POPBOLTZ = if[Y]es, then a relative Boltzmann distribution is calculated internally  
           according to the input electronic temperature

NAMEPOP = in POPBOLTZ=[N], the name of the file containing the state population distribution

NAINT = numerical integration [Y/N]

NGAUSS = if NAINT=[N], number of gaussian quadrature intervals

The first line is the basis state filename (m31s1.dat or m31s2.dat) and has the following format,

S
NBASIS
N1        L1     EN1L1    IGROUP1
N2        L2     EN2L2    IGROUP2
.
.
.

where the parameters in the basis state file have the following definitions:

S = spin angular momentum quantum number

NBASIS = number states in the file

N = principal quantum number

L = orbital angular momentum quantum number

ENL = term value of the unperturbed state ( $\text{cm}^{-1}$ )

IGROUP = group number

The order of the basis states in the basis state file is from large L to small L. Basis states which have the same group number can perturb one another if the electric dipole selection rules are obeyed.

Independently calculated state population distributions may be read by the stark module.

N1	L1	POPL1
N2	L2	POPL2
.	.	.
.	.	.

The program reads the first value of the microfield distribution, calculates the line broadening information for all transitions that lie in the input spectral range, then iterates to the next microfield distribution sample point. For example, if  $n_{inc}=5$ , then every fifth distribution sample point is used for the broadening calculation and there will be 11 iterations of the calculation.

Figure A3 shows partial output of the stark module. In the figure, the first three lines are the values for the electron density ( $\times 10^{16}$  ( $\text{cm}^{-3}$ )), the electron temperature (K), and electronic temperature (K). The next block of information is the line broadening information. The columns of numbers following the densities and temperatures are: 1) the wavelength of the transition ( $\mu\text{m}$ ), 2) Einstein coefficient ( $\text{s}^{-1}$ ), 3) population ( $\text{cm}^{-3}$ ), 4) halfwidth of the lorentzian distribution ( $\text{cm}^{-1}$ ), 5) weighted electric field strength probability, 6) product of the upper term value and  $hc/k$  (K), and 7) transition assignment. The line shape module only reads the first four columns of information. The last three contain extraneous information.

8.0000E-01
10000.0000
10000.0000
7.482 9.6503E+04 5.1219E+05 1.4340E+01 1.3550E-02 155566. 8j- 6h
3.768 5.2238E+04 1.7196E+07 4.8400E+01 4.5491E-01 155518. 8h- 5f
8.890 1.6921E+03 9.6574E+06 1.6519E+01 3.0673E-02 155008. 7h- 7s
4.401 5.8237E+04 2.8403E+06 1.6016E+01 5.0093E-03 154949. 8i- 5d
.
.
.
3.538 1.3098E+03 6.2842E+05 2.1680E+00 8.3124E-04 156984. 8j- 6h
4.775 2.5185E+04 2.1550E+05 1.5064E+01 2.8505E-04 156236. 8i- 7p
10.733 2.8651E+04 1.3376E+05 4.6791E+00 1.3553E-04 153029. 7i- 6g
-1. -1. -1. -1.
12565 0.408849E+01

Figure A3. Example information from the stark1.dat output file of the stark module.

### C. LINSHAPE

the linshape module constructs the spectrum from the line broadening information calculated by the stark module. The file in Figure A4 is an example of the input for the linshape module. There will be two such files; one for spin 1 information and one for spin 2 information. Typically, these are named stark1.dat and stark2.dat

<i>input</i>	<i>variable</i>	<i>description</i>
STARK1.DAT	NAMEIN1	CODE-B OUTPUT FOR SPIN 1
STARK2.DAT	NAMEIN2	CODE-B OUTPUT FOR SPIN 2
OUTPUT.SYN	ENAMEW	OUTPUT FILENAME (CONVOLVED SPECTRA
2.E+17	DENS	TOTAL ATOM DENSITY (CM <sup>-3</sup> )
1.0	PTHLEN	PATH LENGTH (CM) [0.6 CM FROM SALE RESULTS]
4.0	WVST	START WAVELENGTH (MICRONS)
4.1	WVEN	END WAVELENGTH (MICRONS)
0.001	R	INTERNAL RESOLUTION (MICRONS) (LINUS:0.001)
0.02	REXT	EXTERNAL RESOLUTION (MICRONS)
S	SPEC	N=NONE, S=SPEX, C=CVF
3.	SLIT	SLIT WIDTH IN MM
0.03	DELAMDA	MICRONS
T	INSTFNT	T=TRIANGULAR, R=RECTANGULAR

Figure A4. The input file, linshape.set used to define the input parameters for the linshape module.

The parameters in the linshape module input file have the following definitions,

- NAMEIN1 = name of the spin 1 output file from the stark module
- NAMEIN2 = name of the spin 2 output file from the stark module
- ENAMEW = name of the output file from the linshape module
- DENS = total atomic oxygen density (cm<sup>-3</sup>)
- PTHLEN = path length associated with the emission region
- WVST = starting wavelength of the spectral region (μm)
- WVEN = ending wavelength of the spectral region(μm)
- R = internal grid spacing(μm)
- REXT = external grid spacing(μm)
- SPEC = instrumental resolution (FWHM)
- SLIT = slit width in mm
- DELAMDA = if spex =[n], fwhm of the instrument resolution
- INSTFNT = shape of the resolution

There are two grid spacings associated with the output of the linshape module. The external grid spacing is design for hard space saving. If the external grid spacing is equal to the internal grid spacing, every spectral sample in the spectrum is included in the output file (output.syn). A note is

made here that too large of an internal grid-spacing will result in insufficient sampling of the spectral distribution which may lead to erroneous line shape construction and instrumental convolution. Additionally, the external grid spacing should never exceed the internal grid spacing.

**This Page Intentionally Left Blank.**

**APPENDIX B**  
**SOURCE CODE**

## CODE A: Ion microfield probability distribution

```
PROGRAM mfd
implicit real*8 (a-h,o-z)
character*12 outfil
common/freq/ih
common/micro/a,r,Tratio,xi,z1,z2,e(101),pe(101),alpha
common/lili2/r1(200),f11(200),f12(200),nl
parameter(pi=3.14159D+00)
parameter(ekb=1.38066D-16)
parameter(e0=4.8026D-10)
parameter(e02=e0*e0)

9000 format(3x,'edens  =',f8.2/3x,'Te      =',f8.2/3x,'alph   =',f8.2
&           /3x,'r      =',f8.2/3x,'Tratio =',f8.2/3x,'xi     =',f8.2
&           /3x,'z1     =',f8.2/3x,'z2     =',f8.2/3x,'dalph1 =',f8.2/)

      read(*,'(a)') outfil
      read(*,*) ih
      read(*,*) edens
      read(*,*) Te
      read(*,*) alph
      read(*,*) r
      read(*,*) Tratio
      read(*,*) xi
      read(*,*) z1
      read(*,*) z2
      read(*,*) dalph1

      open (7,file=outfil,status='unknown')
      write(*,9000) edens,Te,alph,r,Tratio,xi,z1,z2,dalph1

      edens=edens*(1.0D+16)
      rm1=3.0d0/(4.0d0*pi*edens)
      rm=(rm1)**(1./3.)
      elambda=sqrt((ekb*Te*rm1)/(3.0d0*e02))
      a=rm/elambda

      write(*,*) ' Computing microfield distribution...'

      call alser(alph,dalph1)
      call geni1
      call geni2
      call trans
      call afit

      close(1)
      stop
      end
```

## CODE B: Collisional Stark Broadening

```

C*****STARK.FOR*****
C
C      COLLISIONAL STARK BROADENING MODEL FOR ATOMIC OXYGEN
C
C          MISSION RESEARCH CORPORATION
C              1 TARA BLVD SUITE 302
C              NASHUA NH 03062-2801
C
C THIS IS THE MAIN PROGRAM IN THE STARK LINE BROADENING MODEL.
C SUCESFUL COMPILE AND LINKAGE WITH ASSOCIATED SUBROUTINES
C THE EXECUTABLE PROGRAM HANDLES FOUR TASKS:
C     1. READS IN INPUT PARAMETERS IN THE FORM OF AN INIT-FILE,
C     2. CALCULATES ION-PERTURBED ENERGY LEVELS AND WAVEFUNCTIONS,
C        TRANSITION WAVELENGTHS, TRANSITION PROBABILITIES, AND
C        RELATIVE POPULATIONS,
C     3. CALCULATES ELECTRON-BROADENED LINETHDS, AND
C     4. WRITES THE OUTPUT FILE.
C
C LOGICAL UNIT ASSIGNMENTS:
C
C      ( 2)      (NAMEOUT)      OUTPUT FILE: LINE, A-COEF, POP, E-BROAD
C      (14)      (NAMEPOP)      NAME OF NON-BOLTZMANN POP. FILE IF USED
C      (11)      (NAMEIN)      NAME OF BASIS STATE FILE
C      (21)      (NAMEFD)      NAME OF HOOVER MICROFIELD FILE
C      (22)      (NAMEWID)      NAME OF E-BROAD. FILE IF NOT CALC. THIS RUN
C      (31)      (OUTRANGE.DAT) NAME OF E-BROAD. FILE IF CALC. THIS RUN
C
C*****

```

```

PROGRAM STARK
IMPLICIT REAL*8 (A-H,O-Z)
PARAMETER (BK=1.3807D-16)
PARAMETER (PI=3.141592654D+00)
PARAMETER (A0=0.529177D-08)
PARAMETER (E0=4.80324D-10)
PARAMETER (EMASS=9.10953D-28)
PARAMETER (ECOUL=1.6D-19)
PARAMETER (C0=2.997925D+10)
PARAMETER (H0=6.6261961D-27)
PARAMETER (HBAR=1.05459D-34)
PARAMETER (COEFF=0.5D0*(2.D0*9.D11*A0*ECOUL**2/HBAR)**2)
PARAMETER (IDMN=55)
PARAMETER (INML=500)
PARAMETER (ITRN=12*INML)

CHARACTER*1 PERTURB, EBROAD, NAINT
CHARACTER*1 ZEMAVG, POPBOLTZ, ORB(0:8)
CHARACTER*24 NAMEIN, NAMEOUT, NAMEFD, NAMEWID, NAMEPOP

DATA ORB/'S','P','D','F','G','H','I','J','K'/

DIMENSION E(IDMN), PQN(IDMN), XLB(IDMN), IGROUP(IDMN)
DIMENSION RME(10,20,20)
DIMENSION ZNEW(INML, INML), EM(INML), PQNW(INML),
&           XLW(INML), XMW(INML), NEND(INML)
DIMENSION XG(100), WG(100)
DIMENSION A(IDMN, IDMN), WR(IDMN), Z(IDMN, IDMN)
DIMENSION XM(INML), EZWIDTH(IDMN, IDMN), XINDEW(INML)
DIMENSION AMP2(ITRN), WWRJ(ITRN), WWRJ(ITRN), XLAMB(ITRN)
DIMENSION XEF(102), PF(102), ELWIDTH(ITRN)
DIMENSION POP(IDMN, 0:IDMN)
DIMENSION IPQNW(ITRN), JPQNW(ITRN), IXLW(ITRN), JXLW(ITRN)

```

```

COMMON/CONSTANTS/EVELOC, DEBYELN, DEBROGLN
COMMON/ANS/PERTURB, EBROAD, NAINT
COMMON/EZPARAM/E, PQN, XLB, IGROUP, NBASIS
COMMON/RADIAL/RME
COMMON/PLASM/EDENS, ETEMP, SPIN
COMMON/IPARAM/NSTATE, NINIT, NFIN
COMMON/FPARAM/ZNEW, EM, PQNW, XLW, XMW, NEND
COMMON/GAUSS/ XG, WG, NGAUSS

1299 FORMAT(1X, 'K = ', I10, ' IS TOO LARGE', I10)
1301 FORMAT(1X, F7.3, 1P, 4(2X, E10.4), 2X, 0P, F7.0, 2X, I2, A, '-', I2, A)
2000 FORMAT(3X, '-1. -1. -1. -1.')
3000 FORMAT(1X, I10, 2X, E14.6)
9005 FORMAT(5X, I2, 3X, I2, 3X, 1P, E12.3, 3X, E12.3, 3X, E12.3)

DO 9999 ISPIN=1,2 ! END OF LOOP NEAR MAIN PROGRAM END STATEMENT

IF(ISPIN.EQ.1) THEN
  WRITE(*,*) ' STARK BROADENING - SPIN 1...'
  OPEN(7,FILE='STARK1.SET',STATUS='OLD')
ELSE IF (ISPIN.EQ.2) THEN
  WRITE(*,*) ' STARK BROADENING - SPIN 2...'
  OPEN(7,FILE='STARK2.SET',STATUS='OLD')
END IF

READ(7, '(A)') NAMEIN
READ(7,*) XIDENS
READ(7,*) EDENS
READ(7,*) ETEMP
READ(7,*) TEL
READ(7,*) WVMIN
READ(7,*) WVMAX
READ(7, '(A)') NAMEOUT
READ(7, '(A)') NAMEFD
READ(7,*) NEPT
READ(7,*) NINC
READ(7, '(A)') EBROAD
READ(7, '(A)') ZEMAVG
READ(7, '(A)') NAMEWID
READ(7, '(A)') POPBOLTZ
READ(7, '(A)') NAMEPOP
READ(7, '(A)') NAINT
READ(7,*) NGAUSS

CALL GAULEG(XG, WG, NGAUSS) ! SETUP GAUSSIAN INTEGRATION

NSTART=1
ISTOP=0
OPEN (2, FILE=NAMEOUT, STATUS='NEW')
WRITE(2, '(1PE12.4)') XIDENS
WRITE(2, '(F12.4)') ETEMP
WRITE(2, '(F12.4)') TEL
EDENS=EDENS*1.D16 ! ELECTRON DENSITY IN UNITS OF 1E16/CM3
NM=IDMN

IF (POPBOLTZ.EQ.'N') THEN
  OPEN(14,FILE=NAMEPOP,STATUS='OLD') ! USER SUPPLIED POPULATION
  DO 20 I=1,100
    READ(14,*) NPQN, NXL, POP(NPQN, NXL)
    IF (NPQN.EQ.3.AND.NXL.EQ.0) GO TO 21
20  CONTINUE
21  CONTINUE
ENDIF

EVCM=8065.479 ! CONSTANTS AND UNIT CONVERSION FACTORS
E02 = E0*E0
CONST3 = (H0*C0)

```

```

CONST5 = CONST3/BK      !CONST5 = 1/(0.695 CM-1/K)

DO 30 I = 1,102      ! INITIALIZATION OF MICROFIELD VARIABLES
    XEF(I) = 0.0
    PF(I) = 0.0
30  CONTINUE

DO 40 I = 1,IDMN      ! INITIALIZATION OF A(I,J)
DO 40 J = 1,IDMN
    A(I,J) = 0.0
    Z(I,J) = 0.0
40  CONTINUE
DO 41 I=1,ITRN
    ELWIDTH(I)=0.
41  CONTINUE

OPEN(11,FILE=NAMEIN, STATUS = 'OLD') ! INPUT BASIS STATES IN
READ(11,*)SPIN           ! ORDER OF DECREASING L
READ(11,*)NBASIS
DO 50 I=1,NBASIS
    READ(11,*)PQN(I),XLB(I),E(I),IGROUP(I)
50  CONTINUE
CLOSE(11)

IF (SPIN.EQ.1.) CALL RADMATX1      ! READ IN RADIAL
IF (SPIN.EQ.2.) CALL RADMATX2      ! MATRIX ELEMENTS
LMAX=INT(XLB(1))
MMAX=LMAX+1

DO 51 I=1,MMAX                  ! CALCULATE POSITIVE ML VALUES
    XM(I)=FLOAT(I-1)
51  CONTINUE

C STATIC ELECTRIC FIELDS DUE TO ION DENSITY, XIDENS=ION DENSITY IN
C UNITS OF 1E16 CM-3

IF (EDENS.EQ.0.) EBROAD='N'
IF (XIDENS.EQ.0.) THEN
    PF(1)=1.0
    XEF(1)=1.
    XEF(2)=2.
    NEPT=1
    NINC=1
ELSE
    EDN = XIDENS*(1.0D+16)
    RM1 = 0.75/(PI*EDN)
    RM = RM1** (1./3.)
    RM2 = RM**2
    ELAMBDA = BK*ETEMP
    ELAMBDA = ELAMBDA*RM1
    ELAMBDA = SQRT(ELAMBDA/(3.0*E02))
    AA = RM/ELAMBDA
    AA=AA
    EFO = ((300.0)*E0)/RM2      ! FIELD STRENGTH IN VOLTS/CM
    OPEN (21, FILE = NAMEFD, STATUS = 'OLD') ! INPUT HOOPER'S
    DO 60 KN=1,NEPT              ! MICROFIELD
        READ(21,*)XEF(KN),PF(KN)      ! DISTRIBUTION
60  CONTINUE
    CLOSE(21)
END IF
KH = ISTOP

C EVALUATE BROADENING: EVALUATE ELECTRON VELOCITY, DEBYE LENGTH,
C DEBROGLIE WAVELENGTH.

EVELOC=SQRT(8.*BK*ETEMP/(PI*EMASS))
DEBYELN=SQRT(BK*ETEMP/(4.*PI*EDENS*E0**2))

```

```

DEBROGLIN=H0 / (EMASS*EVELOC) / (2.*PI)

C EVALUATE ELECTRON WIDTH FOR UNPERTURBED CASE:

IF (EBROAD.EQ.'U') THEN
  IF (ZEMAVG.EQ.'R') THEN
    OPEN (22, FILE = NAMEWID, STATUS = 'OLD')
    DO 100 IE=1,NBASIS
    DO 100 JE=IE+1,NBASIS
      EZWIDTH(IE,JE)=0.
      READ(22,*) IDUM, JDUM, DUM, EZWIDTH(IE, JE)
      IDUM=IDUM ! SET DUMMY VARIABLES EQUAL TO SELF FOR
      JDUM=JDUM ! A CLEAN COMPILE
      DUM=DUM !
      EZWIDTH(JE, IE)=EZWIDTH(IE, JE)
100   CONTINUE
  ELSE IF (ZEMAVG.EQ.'C') THEN
    DO 110 IE=1,NBASIS
    DO 110 JE=IE+1,NBASIS
      IF (IE.NE.JE) THEN
        EZWIDTH(IE,JE)=0.
        NINIT=IE
        NFIN=JE
        CALL ELBAVG(EWIDTH,XSECT)
        EZWIDTH(IE, JE)=EWIDTH
        EZWIDTH(JE, IE)=EZWIDTH(IE, JE)
      END IF
110   CONTINUE
    ENDIF
  ENDIF

DO 1000 KN = NSTART,NEPT,NINC ! LOOP THRU QUASISTAT FIELD: FIND
      ! TRANSITIONS FOR EA FIELD VALUE
      NSTATE=0

      DO 1100 ML=1,MMAX ! BLOCK DIAGONALIZATION ACCORDING TO ML
      N=0
      DO 1105 I=1,NBASIS
        IF (XLB(I).LT.ABS(XM(ML))) GO TO 1106 ! DETERMINE
        ! SIZE OF
        ! MATRIX TO BE
        N=N+1
1105   CONTINUE
1106   CONTINUE ! DIAGONALIZED

C CALCULATE OFF-DIAGONAL MATRIX ELEMENTS (ANGULAR AND RADIAL)

      DO 1110 I=1,N
      DO 1110 J=I+1,N
        CALL ANGME(XLB(I),XM(ML),XLB(J),XM(ML),AME)
        IF (AME.EQ.0.) THEN
          A(I,J)=0.
        ELSE
          XLN1=XLB(I)
          XLN2=XLB(J)
          PN1=PQN(I)
          PN2=PQN(J)
          IF (XLN1.LT.XLN2) THEN
            XLN1=XLN2
            PTEMP=PN2
            PN2=PN1
            PN1=PTEMP
          END IF
          IXLN1=INT(XLN1)
          IPN1=INT(PN1)
          IPN2=INT(PN2)
          RADIALME=RME(IXLN1,IPN1,IPN2)
          IF (RADIALME.EQ.0.) THEN
            WRITE(2,*) IXLN1,IPN1,IPN2,RADIALME
          END IF
        END IF
      END IF
    END IF
  END IF
END IF

```

```

        A(I,J)=-AME*RADIALME*A0*XEF(KN)*EF0*EVCM
        END IF
        A(J,I)=A(I,J)
1110      CONTINUE

        DO 1120 I=1,N    ! DIAGONAL ELEMENTS ARE THE ZERO FIELD
        A(I,I)=E(I)    ! ENERGY LEVELS
1120      CONTINUE

        CALL JACOBI (A,N,NM,WR,Z,NROT)    ! MATRIX DIAGONALIZATION

C RELABEL ML STATES

        DO 1130 I=1,N
        NSTATE=NSTATE+1
        XINDEW(NSTATE)=FLOAT(I)
        NEND(NSTATE)=N
        EM(NSTATE)=WR(I)
        XMW(NSTATE)=XM(ML)
        PQNW(NSTATE)=PQN(I)
        XLW(NSTATE)=XLB(I)
        IF (N.EQ.1) THEN
            ZNEW(1,NSTATE)=Z(1,1)
        ELSE
            DO 1131 K=1,N
            ZNEW(K,NSTATE) = Z(K,I)
1131      CONTINUE
        ENDIF
1130      CONTINUE
1100      CONTINUE

```

C EVALUATED TRANSITION FREQUENCIES AND PROBABILITIES:

```

K=0
DO 1200 IM=1,NSTATE
DO 1200 JM=IM+1,NSTATE
    WWWX = ABS(XMW(IM)-XMW(JM))
    WWX = ABS(EM(IM)-EM(JM))
    XLAMBDA = 10000.0/MAX(100.0D0,WWX)
    IF (WWWX .LE. 1.     .AND.
&           WWX     .GE. 100.0 .AND.
&           XLAMBDA .LE. WVMAX .AND.
&           XLAMBDA .GE. WVMIN
& ) THEN

```

C EVALUATE DIPOLE MOMENT MATRIX ELEMENTS BETWEEN PERTURBED  
C WAVEFUNCTIONS FOR A DELTA ML=0,+1,-1 TRANSITION

```

TAMP=0.
DO 1210 II=1,NEND(IM)
DO 1210 JJ=1,NEND(JM)
    CALL ANGME(XLB(II),XMW(IM),XLB(JJ),XMW(JM),AME)
    IF (AME.NE.0.) THEN
        XLN1=XLB(II)
        XLN2=XLB(JJ)
        PN1=PQN(II)
        PN2=PQN(JJ)
        IF (XLN1.LT.XLN2) THEN
            XLN1=XLN2
            PTEMP=PN2
            PN2=PN1
            PN1=PTEMP
        END IF
        IXLN1=INT(XLN1)
        IPN1=INT(PN1)
        IPN2=INT(PN2)
        RADIALME=RME(IXLN1,IPN1,IPN2)

```

```

        IF (RADIALME.EQ.0.) THEN
          WRITE(2,*)SPIN,XLN1,PN1,PN2,RADIALME
        END IF
        TAMP=TAMP+ZNEW(II,IM)*ZNEW(JJ,JM)*AME*RADIALME
      END IF
1210    CONTINUE
      ZA=TAMP*E0*A0
      ZA2 = ZA**2
      ZA2 = ZA2*((WWX)**3)
      ZA2 = ZA2*(64*(PI**4)/(3*H0))

C ACCOUNT FOR ML=-ML DEGENERACY:

      IF ((XMW(IM).NE.0.) .OR. (XMW(JM).NE.0.)) ZA2=2.*ZA2
      IF (ZA2.LT.0.) WRITE(2,*) IM,JM,ZA2
      IF(ZA2 .GE. 1000.0) THEN
        K = K + 1
        XLAMB(K) = XLAMBDA
        WWRI(K) = EM(IM)
        WWRJ(K) = EM(JM)
        AMP2(K) = ZA2
        IPQNW(K)=PQN(WIM)
        JPQNW(K)=PQN(WJM)
        IXLW(K)=XLW(IM)
        JXLW(K)=XLW(JM)
        IF (EBROAD.EQ.'U') THEN
          ICOUNT=INT(XINDEW(IM))
          JCOUNT=INT(XINDEW(JM))
          ELWIDTH(K)=EZWIDTH(ICOUNT,JCOUNT)
        ELSE IF (EBROAD.EQ.'S') THEN
          PERTURB='N'
          NINIT=IM
          NFIN=JM
          CALL ELECBR(ELWIDTH)
          ELWIDTH(K)=ELWIDTH
        ELSE IF (EBROAD.EQ.'P') THEN
          PERTURB='Y'
          NINIT=IM
          NFIN=JM
          CALL ELECBR(ELWIDTH)
          ELWIDTH(K)=ELWIDTH
        ENDIF
      ENDIF
1200    CONTINUE
      IF (K.GT.ITRN) THEN
        OPEN(31,FILE='OUTRANGE.DAT',STATUS='UNKNOWN')
        WRITE(31,1299) K,KN
        CLOSE(31)
      ENDIF
      KH = KH + K
      AMP2SUM=0.

```

C DETERMINE THE UPPER LEVEL POPULATION OF A TRANSITION:

```

DO 1300 KI = 1,K
  IF (WWRI(KI) .GE. WWRJ(KI)) THEN
    WWE = WWRI(KI)
    DENP=POP(IPQNW(KI),IXLW(KI))
  ELSE
    WWE = WWRJ(KI)
    DENP=POP(JPQNW(KI),JXLW(KI))
  END IF
  ENERGY = WWE*CONST5
  DEN = (2.*SPIN+1)*EXP(-ENERGY/TEL)
  IF (POPBOLTZ.EQ.'N') DEN=DENP
  IF (KN.EQ.1) THEN

```

```

      DELX=(XEF(1+NINC)-XEF(1))
      ELSE IF ((NEPT-KN).LT.NINC) THEN
        DELX=XEF(KN)-XEF(KN-NINC)
      ELSE
        DELX=0.5*((XEF(KN)-XEF(KN-NINC))
                  +(XEF(KN+NINC)-XEF(KN)))
      & END IF
      DEN = DEN*PF(KN)*DELX          ! WEIGHT DENSITY BY
      IF (EDENS.EQ.0) ELWIDTH(KI)=-2. ! MF DISTRIB. P(E)DE

      IF (DEN.EQ.0.) GOTO 1290
      WRITE(2,1301) XLAMB(KI),AMP2(KI),DEN,ELWIDTH(KI),PF(KN),
      & ENERGY,IPQNW(KI),ORB(IXLW(KI)),JPQNW(KI),ORB(JXLW(KI))
      & WRITE(*,1301) XLAMB(KI),AMP2(KI),DEN,ELWIDTH(KI),PF(KN),
      & ENERGY,IPQNW(KI),ORB(IXLW(KI)),JPQNW(KI),ORB(JXLW(KI))
1290    CONTINUE

      AMP2SUM=AMP2SUM+AMP2(KI)
1300    CONTINUE
      WRITE(*,*) ' END OF PASS: ',KN
1000    CONTINUE

      WRITE(2,2000)
      WRITE(2,3000) KH,AMP2SUM/(1.D8)
      CLOSE(2)

9999  CONTINUE
      STOP
      END

      SUBROUTINE ELBAVG(EWIDTH,XSECT)
C***** ****
C
C THIS SUBROUTINE CALCULATES ELECTRON WIDTHS USING
C UNPERTURBED WAVEFUNCTIONS AND ENERGY LEVELS WITH
C WITH AN ANALYTICAL APPROXIMATION FOR THE INTEGRAL
C
C***** ****
      IMPLICIT REAL*8 (A-H,O-Z)
      PARAMETER(C0=2.997925D+10)
      PARAMETER(IDMN=55)           ! MUST BE > NBASIS
      PARAMETER(INML=500)          ! MUST BE > # OF M TRANSITIONS
      PARAMETER(ITRN=12*INML)      ! MUST > (L+1)*INML
      COMMON/CONSTANTS/EVELOC,DEBYELN,DEBROGLN
      COMMON/ANS/PERTURB,EBROAD,NAINT
      COMMON/EZPARAM/E,PQN,XLB,IGROUP,NBASIS
      COMMON/RADIAL/RME
      COMMON/PLASM/EDENS,ETEMP,SPIN
      COMMON/INTEGL/WAB,B,XMEXSUM2,XMEZSUM2
      COMMON/IPARAM/NSTATE,NINIT,NFIN
      CHARACTER*1 PERTURE,EBROAD,NAINT
      DIMENSION E(IDMN),PQN(IDMN),XLB(IDMN),IGROUP(IDMN)
      DIMENSION RME(10,20,20)
      DIMENSION XMEXSUM2(2, IDMN), XMEZSUM2(2, IDMN)
      DIMENSION XMW(IDMN), XMP(IDMN)
      EXTERNAL F3

C L=1 IS THE INITIAL STATE OF THE TRANSITION
C L=2 IS THE FINAL STATE OF THE TRANSITION
```

```

DO 1000 L=1,2
  IF (L.EQ.1) NTRANS=NINIT
  IF (L.EQ.2) NTRANS=NFIN
  DO 1100 MP=1,NBASIS
    XMEXSUM2(L,MP)=0.
```

```

XMEZSUM2(L,MP)=0.
IF (MP.NE.NTRANS .AND.
&     IGROUP(MP).EQ.IGROUP(NTRANS) .AND.
&     ABS( XLB(NTRANS)-XLB(MP) ).LE.1. .AND.
&     ABS( XLB(NTRANS)-XLB(MP) ).NE.0.) THEN
  XLN1=XLB(NTRANS)
  XLN2=XLB(MP)
  PN1=PQN(NTRANS)
  PN2=PQN(MP)
  IF (XLN1.LT.XLN2) THEN
    XLN1=XLN2
    PTEMP=PN2
    PN2=PN1
    PN1=PTEMP
  ENDIF
  IXLN1=INT(XLN1)
  IPN1=INT(PN1)
  IPN2=INT(PN2)
  MLEND=INT(XLB(NTRANS)+1.)
  MPLEND=INT(XLB(MP)+1.)
  IF (MLEND.GE.IDMN .OR. MPLEND.GE.IDMN) THEN
    WRITE(*,*) 'MLEND',MLEND,'MPLEND',MPLEND, IDMN
  ENDIF
  DO 1110 ML=1,MLEND
    XMW(ML)=XLB(NTRANS)-FLOAT(ML)+1.
    DO 1111 MPL=1,MPLEND
      XMP(MPL)=XLB(MP)-FLOAT(MPL)+1.
      XXXX = ABS(XMW(ML)-XMP(MPL))
      IF (XXXX.LE.1.) THEN
        IF (XXXX.EQ.1.) THEN
          CALL ANGXME(XLB(NTRANS),XMW(ML),XLB(MP),
&                      XMP(MPL),AME)
          CZ=2.
          XMEM=AME*RME(IXLN1,IPN1,IPN2)
          XMEMSUM2(L,MP)=XMEMSUM2(L,MP)+CZ*XMEM**2
        ELSE IF (XXXX.EQ.0.) THEN
          CALL ANGZME(XLB(NTRANS),XMW(ML),XLB(MP),
&                      XMP(MPL),AME)
          CZ=2.
          IF ((XMP(MPL).EQ.0.).AND.(XMW(ML).EQ.0.))
&          CZ=1.
          XMEM=AME*RME(IXLN1,IPN1,IPN2)
          XMEMSUM2(L,MP)=XMEMSUM2(L,MP)+CZ*XMEM**2
        ENDIF
      ENDIF
    1111      CONTINUE
    1110      CONTINUE
  1100      CONTINUE
  1000      CONTINUE

C INTEGRATE FROM SMALL B TO LARGE B

AA=0.0D0
BB=DEBYELN
CALL QGAUS(F3,AA,BB,XSECT)

C CALCULATION OF CROSS SECTION AND ELECTRON BROADENED LINE HALF-WIDTH
C IN WAVENUMBER

C      XSECTD=DEBROGLN**2
EWIDTH=EDENS*EVELOC*XSECT/C0 ! WHERE'S THE 2*PI ?
IF (EWIDTH.LT.1.E-4) EWIDTH=0.
RETURN
END

```

```

SUBROUTINE S2U(TD,S2C)
C*****
C THE FOLLOWING SUBROUTINE CALCULATES THE QUANTITY S2(B) *
C*****
IMPLICIT REAL*8 (A-H,O-Z)
PARAMETER(BK=1.3807D-16)
PARAMETER(PI=3.141592654D+00)
PARAMETER(A0=0.529177D-08)
PARAMETER(ECOUL=1.6D-19)
PARAMETER(C0=2.997925D+10)
PARAMETER(HBAR=1.05459D-34)
PARAMETER(COEFF=0.5D0*(2.D0*9.D11*A0*ECOUL**2/HBAR)**2)
PARAMETER(IDMN=55)      ! MUST BE > NBASIS
PARAMETER(INML=500)     ! MUST BE > # OF TRANSITIONS
PARAMETER(ITRN=12*INML) ! MUST BE > (L+1)*INML

COMMON/CONSTANTS/EVELOC,DEBYELN,DEBROGLN
COMMON/ANS/PERTURB,EBROAD,NAINT
COMMON/EZPARAM/E,PQN,XLB,IGROUP,NBASIS
COMMON/INTEGL/WAB,B,XMEXSUM2,XMEZSUM2
COMMON/IPARAM/NSTATE,NINIT,NFIN
CHARACTER*1 PERTURB,EBROAD,NAINT
DIMENSION E>IDMN, PQN>IDMN, XLB>IDMN, IGROUP>IDMN
DIMENSION XMEXSUM2(2, IDMN), XMEZSUM2(2, IDMN)
DIMENSION S2SUM(2)
EXTERNAL BESSK0,BESSK1,BESSI0,BESSI1,F1,F2

C L=1 IS THE INITIAL STATE OF THE TRANSITION
C L=2 IS THE FINAL STATE OF THE TRANSITION

XCO=2.*PI*C0
ZERO=0.D0
DO 100 L = 1,2
  IF (L.EQ.1) NTRANS=NINIT
  IF (L.EQ.2) NTRANS=NFIN
  S2SUM(L)=0.
  DO 110 MP=1,NBASIS
    IF (XMEXSUM2(L,MP).NE.0. .OR.
      & XMEZSUM2(L,MP).NE.0.) THEN
      WAB=ABS(E(MP)-E(NTRANS))*XCO
      IF (NAINT.EQ.'Y') THEN
        CALL QROMB(F1,ZERO,TD,X1T)
        CALL QROMB(F2,ZERO,TD,X2T)
      ELSE
        AVAR=B*WAB/EVELOC
        BK0=BESSK0(AVAR)
        IF (BK0.LT.1.E-30) BK0=0.
        X1T=AVAR*BK0/(B*EVELOC)
        BK1=BESSK1(AVAR)
        IF (BK1.LT.1.E-30) BK1=0.
        X2T=BK1*WAB/EVELOC**2
      ENDIF
      S2T=XMEZSUM2(L,MP)*X1T**2+XMEXSUM2(L,MP)*X2T**2
      S2SUM(L)=S2SUM(L)+S2T
    ENDIF
  110 CONTINUE
100  CONTINUE
  S2C=COEFF*(S2SUM(1)+S2SUM(2))
  RETURN
END

FUNCTION F1(TIME)
C*****
C TIME INTEGRANDS *
C*****

```

```

IMPLICIT REAL*8 (A-H,O-Z)

C MUST BE GREATER THAN NBASIS (55)
PARAMETER(IDMN=55)
COMMON/CONSTANTS/EVELOC,DEBYELN,DEBROGLN
COMMON/INTEGL/WAB,B,XMEXSUM2,XMEZSUM2
DIMENSION XMEXSUM2(2, IDMN), XMEZSUM2(2, IDMN)
F1TOP=EVELOC*TIME*SIN(WAB*TIME)
F1BOT=SQRT((B**2+(EVELOC*TIME)**2)**2)
F1=F1TOP/F1BOT
RETURN
END

FUNCTION F2(TIME)
IMPLICIT REAL*8 (A-H,O-Z)

PARAMETER(IDMN=55) ! MUST BE > NBASIS
COMMON/CONSTANTS/EVELOC,DEBYELN,DEBROGLN
COMMON/INTEGL/WAB,B,XMEXSUM2,XMEZSUM2
DIMENSION XMEXSUM2(2, IDMN), XMEZSUM2(2, IDMN)

F2TOP=B*COS(WAB*TIME)
F2BOT=SQRT((B**2+(EVELOC*TIME)**2)**2)
F2=F2TOP/F2BOT
RETURN
END

FUNCTION F3(CS)
IMPLICIT REAL*8 (A-H,O-Z)
PARAMETER(IDMN=55) ! MUST BE > NBASIS
COMMON/CONSTANTS/EVELOC,DEBYELN,DEBROGLN
COMMON/INTEGL/WAB,B,XMEXSUM2,XMEZSUM2
DIMENSION XMEXSUM2(2, IDMN), XMEZSUM2(2, IDMN)

B=CS
C IF (B.LT.DEBROGLN) THEN
  IF (B.LE.0.0D0) THEN
    F3 = 0.0D0
    RETURN
  ELSE
    HYPO=MAX(0.0D0,DEBYELN**2-B**2)
    TD=SQRT(HYPO)/EVELOC
    CALL S2U(TD,S2C)
    S2C = MIN(S2C,1.0D0)
    F3=S2C*B
    RETURN
  ENDIF
END

SUBROUTINE ELECBR(EWIDTH)
C*****
C THIS SUBROUTINE CALCULATES ELECTRON WIDTHS FOR THE SEMI-PERTURBED *
C AND FULLY-PERTURBED CASES WITH AN ANALYTICAL APPROXIMATION FOR THE *
C INTEGRAL *
C*****
IMPLICIT REAL*8 (A-H,O-Z)
PARAMETER(PI=3.141592654D+00)
PARAMETER(C0=2.997925D+10)
PARAMETER(IDMN=55) ! MUST BE > NBASIS
PARAMETER(INML=500) ! MUST BE > INML
PARAMETER(ITRN=12*INML) ! MUST BE > (L+1)*INML
COMMON/CONSTANTS/EVELOC,DEBYELN,DEBROGLN
COMMON/ANS/PERTURB,EBROAD,NAINT
COMMON/FPARAM/ZNEW,EM,PQNW,XLW,XMW,NEND

```

```

COMMON/INTEGL/WAB,B,XMEXSUM2,XMEZSUM2
COMMON/IPARAM/NSTATE,NINIT,NFIN
COMMON/PLASM/EDENS,ETEMP,SPIN
CHARACTER*1 PERTURB,EBROAD,NAINT
DIMENSION ZNEW(INML,INML),EM(INML),PQNW(INML),XLW(INML),
& XMW(INML),NEND(INML)
DIMENSION XMEXSUM2(2,IDMN),XMEZSUM2(2,IDMN)
EXTERNAL F4

C UNITS

C      AA=DEBROGLN
C      BB=DEBYELN
C      CALL QGAUS(F4,AA,BB,XSECT)
C      XSECT=XSECT+PI*DEBROGLN*DEBROGLN
AA=0.0D0
BB=DEBYELN
CALL QGAUS(F4,AA,BB,XSECT)

C CALCULATION OF CROSS SECTION AND ELECTRON HALF-WIDTH IN WAVENUMBER

C      XSECTD=PI*DEBROGLN**2
EWIDTH=EDENS*EVELOC*XSECT/C0
IF (EWIDTH.LT.1.E-4) EWIDTH=0.
RETURN
END

SUBROUTINE S2SPBESS(TD,S2)
C*****
C THE FOLLOWING SOUBROUTINE CALCULATES THE QUANTITY S2(B) *
C*****
IMPLICIT REAL*8 (A-H,O-Z)
PARAMETER(PI=3.141592654D+00)
PARAMETER(A0=0.529177D-08)
PARAMETER(ECOUL=1.6D-19)
PARAMETER(C0=2.997925D+10)
PARAMETER(HBAR=1.05459D-34)
PARAMETER(COEFF=0.5D0*(2.D0*9.D11*A0*ECOUL**2/HBAR)**2)
PARAMETER(IDMN=55) ! MUST BE > NBASIS
PARAMETER(INML=500) ! MUST BE > # OF TRANSITIONS
PARAMETER(ITRN=12*INML) ! MUST BE > (L+1)*INML
COMMON/CONSTANTS/EVELOC,DEBYELN,DEBROGLN
COMMON/ANS/PERTURB,EBROAD,NAINT
COMMON/EZPARAM/E,PQN,XLB,IGROUP,NBASIS
COMMON/FPARAM/ZNEW,EM,PQNW,XLW,XMW,NEND
COMMON/RADIAL/RME
COMMON/INTEGL/WAB,B,XMEXSUM2,XMEZSUM2
COMMON/IPARAM/NSTATE,NINIT,NFIN
COMMON/PLASM/EDENS,ETEMP,SPIN
CHARACTER*1 PERTURB,EBROAD,NAINT
DIMENSION E(IDMN),PQN(IDMN),XLB(IDMN),IGROUP(IDMN)
DIMENSION ZNEW(INML,INML),EM(INML),PQNW(INML),XLW(INML),
& XMW(INML),NEND(INML)
DIMENSION RME(10,20,20)
DIMENSION XMEXSUM2(2,IDMN),XMEZSUM2(2,IDMN)
DIMENSION S2SUM(2)
EXTERNAL BESSK0,BESSK1,BESSIO,BESSI1,F1,F2

C L=1 IS THE INITIAL STATE OF THE TRANSITION
C L=2 IS THE FINAL STATE OF THE TRANSITION

XCO=2.*PI*C0
ZERO=0.0D0
DO 1000 L=1,2
  IF (L.EQ.1) NTRANS=NINIT
  IF (L.EQ.2) NTRANS=NFIN

```

```

S2SUM(L)=0.
DO 1100 M=1,NSTATE
    IF (M.NE.NTRANS) THEN

```

C ION-PERTURBED STATES AND ENERGIES

```

IF (PERTURB.EQ.'Y') THEN
    WAB=ABS(EM(NTRANS)-EM(M))*XCO
    IF (NAINT.EQ.'Y') THEN
        CALL QROMB(F1,ZERO,TD,X1T)
        CALL QROMB(F2,ZERO,TD,X2T)
    ELSE
        AVAR=B*WAB/EVELOC
        BK0=BESSK0(AVAR)
        IF (BK0.LT.1.E-30) BK0=0.
        X1T=AVAR*BK0/(B*EVELOC)
        BK1=BESSK1(AVAR)
        IF (BK1.LT.1.E-30) BK1=0.
        X2T=BK1*WAB/EVELOC**2
    ENDIF
    DO 1110 II=1,NEND(NTRANS)
        IF (ABS(ZNEW(II,NTRANS)).GT.0.01) THEN
            DO 1111 JJ=1,NEND(M)
                IF (ABS(ZNEW(JJ,M)).GT.0.01) THEN
                    CALL ANGZME(XLB(II),XMW(NTRANS),
                                XLB(JJ),XMW(M),AZME)
                    CALL ANGXME(XLB(II),XMW(NTRANS),
                                XLB(JJ),XMW(M),AXME)
                &
                &
                IF ((AZME.NE.0.).OR.(AXME.NE.0.)) THEN
                    XLN1=XLB(II)
                    XLN2=XLB(JJ)
                    PN1=PQN(II)
                    PN2=PQN(JJ)
                    IF (XLN1.LT.XLN2) THEN
                        XLN1=XLN2
                        PTEMP=PN2
                        PN2=PN1
                        PN1=PTEMP
                    ENDIF
                    IXLN1=INT(XLN1)
                    IPN1=INT(PN1)
                    IPN2=INT(PN2)
                    RADIALME=RME(IXLN1,IPN1,IPN2)
                    IF (RADIALME.NE.0.) THEN
                        XMEZM=AZME*RADIALME*ZNEW(II,NTRANS)
                        *ZNEW(JJ,M)
                        XMEXM=AXME*RADIALME*ZNEW(II,NTRANS)
                        *ZNEW(JJ,M)
                    &
                    &
                    CZ=1.
                    IF ((XMW(M).NE.0.).OR.
                        (XMW(NTRANS).NE.0.)) CZ=2.
                    S2T= CZ*(XMEZM**2)*X1T**2
                    + 2.* (XMEXM**2)*X2T**2
                    S2SUM(L)=S2SUM(L)+S2T
                ENDIF
            ENDIF
        1111      CONTINUE
    ENDIF
    1110      CONTINUE
ELSE

```

C SEMI-PERTURBED CASE: UNPERTURBED WAVEFUNCTIONS AND PERTURBED ENERGIES

```

CALL ANGME(XLW(NTRANS),XMW(NTRANS),
            XLW(M      ),XMW(M      ),AME)
&           IF (AME.NE.0.) THEN

```

```

        CALL ANGZME (XLW(NTRANS) , XMW(NTRANS) ,
&                               XLW(M) , XMW(M) , AZME)
&                               CALL ANGXME (XLW(NTRANS) , XMW(NTRANS) ,
&                               XLW(M) , XMW(M) , AXME)
XLN1=XLW(NTRANS)
XLN2=XLW(M)
PN1=PQNW(NTRANS)
PN2=PQNW(M)
IF (XLN1.LT.XLN2) THEN
    XLN1=XLN2
    PTEMP=PN2
    PN2=PN1
    PN1=PTEMP
ENDIF
IXLN1=INT(XLN1)
IPN1=INT(PN1)
IPN2=INT(PN2)
XMEZM = AZME*RME(IXLN1,IPN1,IPN2)
XMEXM = AXME*RME(IXLN1,IPN1,IPN2)
WAB=ABS(EM(M)-EM(NTRANS))*XCO
IF (NAINT.EQ.'Y') THEN
    CALL QROMB(F1,ZERO,TD,X1T)
    CALL QROMB(F2,ZERO,TD,X2T)
ELSE
    AVAR=B*WAB/EVELOC
    BK0=BESSK0(AVAR)
    IF (BK0.LT.1.E-30) BK0=0.
    X1T=AVAR*BK0/(B*EVELOC)
    BK1=BESSK1(AVAR)
    IF (BK1.LT.1.E-30) BK1=0.
    X2T=BK1*WAB/EVELOC**2
ENDIF
CZ=1.
IF ((XMW(M).NE.0.).OR.(XMW(NTRANS).NE.0.))CZ=2.
S2T=CZ*(XMEZM**2)*X1T**2 + 2.* (XMEXM**2)*X2T**2
S2SUM(L)=S2SUM(L)+S2T
ENDIF
ENDIF
1100    CONTINUE
1000    CONTINUE
S2=COEFF*(S2SUM(1)+S2SUM(2))
RETURN
END

FUNCTION F4(CS)
IMPLICIT REAL*8 (A-H,O-Z)
PARAMETER(IDMN=55) ! MUST BE > NBASIS
COMMON/CONSTANTS/EVELOC, DEBYELN, DEBROGLN
COMMON/INTEGL/WAB, B, XMEXSUM2, XMEZSUM2
DIMENSION XMEXSUM2(2, IDMN), XMEZSUM2(2, IDMN)

B=CS
C    IF (B.LE.0) THEN
    IF (B.LE.DEBROGLN) THEN
        F4 = 0.
        RETURN
    ELSE
        HYPO=MAX(0.D0,DEBYELN**2-B**2)
        TD=SQRT(HYPO)/EVELOC
        CALL S2SPBESS(TD,S2C)
        S2C = MIN(S2C,1.D0)
        F4=S2C*B
        RETURN
    ENDIF
END

```

```

SUBROUTINE ANGME(XL1,XM1,XL2,XM2,AME)
C*****ANGULAR MATRIX ELEMENT FORMULAS FROM CHUN LIN*****
C
IMPLICIT REAL*8 (A-H,O-Z)
DELL=XL2-XL1
DELM=XM2-XM1
AME=0.
IF (DELL.EQ.1) THEN
  IF (DELM.EQ.1) THEN
    AME = -SQRT((XL1+XM1+1.)*(XL1+XM1+2.))
    /((2.0*(2.*XL1+1.)*(2.*XL1+3.)))
  ELSE IF (DELM.EQ.-1.) THEN
    AME = SQRT((XL1-XM1+1.)*(XL1-XM1+2.))
    /((2.0*(2.*XL1+1.)*(2.*XL1+3.)))
  ELSE IF (DELM.EQ.0.) THEN
    AME = SQRT((XL1-XM1+1.)*(XL1+XM1+1.))
    /((2.*XL1+1.)*(2.*XL1+3.)))
  ENDIF
ELSE IF (DELL.EQ.-1.) THEN
  IF (DELM.EQ.1.) THEN
    AME = SQRT((XL1-XM1)*(XL1-XM1-1.))
    /((2.0*(2.*XL1-1.)*(2.*XL1+1.)))
  ELSE IF (DELM.EQ.-1.) THEN
    AME = -SQRT((XL1+XM1)*(XL1+XM1-1.))
    /((2.0*(2.*XL1-1.)*(2.*XL1+1.)))
  ELSE IF (DELM.EQ.0.) THEN
    AME = SQRT((XL1+XM1)*(XL1-XM1))
    /((2.*XL1-1.)*(2.*XL1+1.)))
  ENDIF
ENDIF
RETURN
END

SUBROUTINE ANGZME(XL1,XM1,XL2,XM2,AME)
C*****Z-DIRECTION COSINES ANGULAR MATRIX ELEMENT FORMULAS FROM CHUN LIN*****
C
IMPLICIT REAL*8 (A-H,O-Z)

DELL=XL2-XL1
DELM=XM2-XM1
AME=0.
IF (DELL.EQ.1.) THEN
  IF (DELM.EQ.0.) THEN
    AME = SQRT((XL1-XM1+1.)*(XL1+XM1+1.))
    /((2.*XL1+1.)*(2.*XL1+3.)))
  ENDIF
ELSE IF (DELL.EQ.-1.) THEN
  IF (DELM.EQ.0.) THEN
    AME = SQRT((XL1+XM1)*(XL1-XM1))
    /((2.*XL1-1.)*(2.*XL1+1.)))
  ENDIF
ENDIF
RETURN
END

SUBROUTINE ANGXME(XL1,XM1,XL2,XM2,AME)
C*****X-DIRECTION COSINES ANGULAR MATRIX ELEMENT FORMULAS FROM CHUN LIN*****
C
IMPLICIT REAL*8 (A-H,O-Z)

```

```

DELL=XL2-XL1
DELM=XM2-XM1
AME=0.
IF (DELL.EQ.1.) THEN
  IF (DELM.EQ.1.) THEN
    AME = -0.5*SQRT((XL1+XM1+1.)*(XL1+XM1+2.))
  &   /((2.*XL1+1.)*(2.*XL1+3.)))
  ELSE IF (DELM.EQ.-1.) THEN
    AME = 0.5*SQRT((XL1-XM1+1.)*(XL1-XM1+2.))
  &   /((2.*XL1+1.)*(2.*XL1+3.)))
  ENDIF
ELSE IF (DELL.EQ.-1.) THEN
  IF (DELM.EQ.1.) THEN
    AME = 0.5*SQRT((XL1-XM1)* (XL1-XM1-1.))
  &   /((2.*XL1-1.)*(2.*XL1+1.)))
  ELSE IF (DELM.EQ.-1.) THEN
    AME = -0.5*SQRT((XL1+XM1)* (XL1+XM1-1.))
  &   /((2.*XL1-1.)*(2.*XL1+1.)))
  ENDIF
ENDIF
RETURN
END

```

```

*****
C FUNCTION INTEGRATOR FROM NUMERICAL RECIPES [PRESS ET AL.].
C
C RETURNS AS SS THE INTEGRAL OF THE FUNCTION FUNC FROM A TO B.
C INTEGRATION IS PERFORMED BY ROMBERG'S METHOD OF ORDER 2K, WHERE,
C E.G., K=2 IS SIMPSON'S RULE.
*****

```

```

SUBROUTINE QROMB(FUNC,A,B,SS)
*****
C HERE EPS IS THE FRACTIONAL ACCURACY DESIRED, AS DETERMINED BY THE *
C EXTRAPOLATION ERROR ESTIMATE; JMAX LIMITS THE TOTAL NUMBER OF STEPS; *
C K IS THE NUMBER OF POINTS USED IN THE EXTRAPOLATION. THE S AND H * *
C PARAMETERS STORE THE SUCCESSIVE TRAPEZOIDAL APPROXIMATIONS *
C AND THEIR RELATIVE STEP-SIZES. *
C*****
IMPLICIT REAL*8 (A-H,O-Z)
PARAMETER (EPS=1.E-3, JMAX=150, JMAXP=JMAX+1, K=2, KM=K-1)

```

```

DIMENSION S(JMAXP), H(JMAXP)
EXTERNAL FUNC
H(1)=1.
DO 11 J=1,JMAX
  CALL TRAPZD(FUNC,A,B,S(J),J)
  IF (J.GE.K) THEN
    CALL POLINT(H(J-KM),S(J-KM),K,0.,SS,DSS)
    IF (ABS(DSS).LT.EPS*ABS(SS)) RETURN
  ENDIF
  S(J+1)=S(J)

C THE FOLLOWING IS A KEY STEP. THE FACTOR IS 0.25 EVEN THOUGH THE
C STEP-SIZE IS DECREASED BY ONLY 0.5. THIS MAKES THE EXTRAPOLATION
C A POLYNOMIAL IN H**2 AS ALLOWED BY EQUATION (4.2.1), NOT JUST A
C POLYNOMIAL IN H.

```

```

11   H(J+1)=0.25*H(J)
      CONTINUE
      WRITE(*,*) J,DSS,EPS*SS
      WRITE(*,*) 'TOO MANY STEPS.'
      RETURN
END

```

```

SUBROUTINE TRAPZD(FUNC,A,B,S,N)
C*****
C THIS ROUTINE COMPUTES THE N'TH STAGE OF REFINEMENT OF AN EXTENDED *
C TRAPEZOIDAL RULE. FUNC IS INPUT AS THE NAME OF THE FUNCTION TO BE   *
C INTEGRATED BETWEEN LIMITS A AND B, ALSO INPUT. WHEN CALLED WITH N=1,   *
C THE ROUTINE RETURNS AS S THE CRUDEST ESTIMATE OF THE INTEGRAL OF F(X). *
C SUBSEQUENT CALLS WITH N=2,3,... (IN THAT SEQUENTIAL ORDER) WILL IMPROVE*
C THE ACCURACY OF S BY ADDING 2** (N-2) ADDITIONAL INTERIOR POINTS.    *
C S SHOULD NOT BE MODIFIED BETWEEN SEQUENTIAL CALLS.                  *
C*****
IMPLICIT REAL*8 (A-H,O-Z)

EXTERNAL FUNC
IF (N.EQ.1) THEN
S=0.5*(B-A)*(FUNC(A)+FUNC(B))

C IT IS THE NUMBER OF POINTS TO BE ADDED ON THE NEXT CALL.

IT=1
ELSE
TNM=FLOAT(IT)

C DEL IS THE SPACING OF THE POINTS TO BE ADDED

DEL=(B-A)/TNM
X=A+0.5*DEL
SUM=0.
DO 11 J=1,IT
SUM=SUM+FUNC(X)
X=X+DEL
11 CONTINUE

C THE FOLLOWING REPLACES S BY ITS REFINED VALUE.

S=0.5*(S+(B-A)*SUM/TNM)
IT=2*IT
ENDIF
RETURN
END

SUBROUTINE POLINT(XA,YA,N,X,Y,DY)
C*****
C GIVEN ARRAYS XA AND YA, EACH OF LENGTH N, AND GIVEN A VALUE X,        *
C THIS ROUTINE RETURNS A VALUE Y, AND AN ERROR ESTIMATE DY.            *
C IF P(X) IS THE POLYNOMIAL OF DEGREE N-1 SUCH THAT P(XAI)=YAI,        *
C I=1,...,N, THEN THE RETURNED VALUE Y=P(X).                         *
C*****
IMPLICIT REAL*8 (A-H,O-Z)
PARAMETER (NMAX=50)
DIMENSION XA(N), YA(N), C(NMAX), D(NMAX)

NS=1
DIF=ABS(X-XA(1))
DO 11 I=1,N
DIFT=ABS(X-XA(I))
IF (DIFT.LT.DIF) THEN
NS=I
DIF=DIFT
ENDIF
C(I)=YA(I)
D(I)=YA(I)
11 CONTINUE
Y=YA(NS)
NS=NS-1
DO 13 M=1,N-1
DO 12 I=1,N-M

```

```

      HO=XA(I)-X
      HP=XA(I+M)-X
      W=C(I+1)-D(I)
      DEN=HO-HP
      IF (DEN.EQ.0.) PAUSE
      DEN=W/DEN
      D(I)=HP*DEN
      C(I)=HO*DEN
12     CONTINUE
      IF (2*NS.LT.N-M) THEN
         DY=C(NS+1)
      ELSE
         DY=D(NS)
      NS=NS-1
      ENDIF
      Y=Y+DY
13     CONTINUE
      RETURN
END

```

```

FUNCTION BESSK0(X)
C*****C*****C*****C*****C*****C*****C*****C*****C*****C*****
C  RETURNS THE MODIFIED BESSEL FUNCTION K0(X) FOR POSITIVE REAL X *
C  EVALUATION OF THE MODIFIED BESSEL FUNCTION TAKEN FROM NUMERICAL   *
C  RECIPES [PRESS ET AL.].                                         *
C*****C*****C*****C*****C*****C*****C*****C*****C*****C*****
IMPLICIT REAL*8 (A-H,O-Z)
DATA P1,P2,P3,P4,P5,P6,P7
& /-0.57721566D+00,+0.42278420D+00,+0.23069756D+00,
& +0.34885900D-01,+0.26269800D-02,+0.10750000D-03,
& +0.74000000D-05/
DATA Q1,Q2,Q3,Q4,Q5,Q6,Q7
& /+1.25331414D+00,-0.78323580D-01,+0.21895680D-01,
& -0.10624460D-01,+0.58787200D-02,-0.25154000D-02,
& +0.53208000D-03/
IF (X.LE.2.0) THEN
Y=X*X/4.0
BESSK0=(-LOG(X/2.0)*BESSI0(X)+(P1+Y*(P2+Y*(P3+
& Y*(P4+Y*(P5+Y*(P6+Y*P7)))))))
ELSE
Y=(2.0/X)
BESSK0=(EXP(-X)/SQRT(X))*(Q1+Y*(Q2+Y*(Q3+
& Y*(Q4+Y*(Q5+Y*(Q6+Y*Q7))))))
ENDIF
RETURN
END

```

```

FUNCTION BESSK1(X)
C*****C*****C*****C*****C*****C*****C*****C*****C*****C*****
C  RETURNS THE MODIFIED BESSEL FUNCTION K1(X) FOR POSITIVE REAL X *
C*****C*****C*****C*****C*****C*****C*****C*****C*****C*****
IMPLICIT REAL*8 (A-H,O-Z)
DATA P1,P2,P3,P4,P5,P6,P7
& /+1.00000000D+00,+0.15443144D+00,-0.67278579D+00,
& -0.18156897D+00,-0.19194020D-01,-0.11040400D-02,
& -0.46860000D-04/
DATA Q1,Q2,Q3,Q4,Q5,Q6,Q7
& /+1.25331414D+00,+0.23498619D+00,-0.36556200D-01,
& +0.15042680D-01,-0.78035300D-02,+0.32561400D-02,
& -0.68245000D-03/
IF (X.LE.2.0) THEN
Y=X*X/4.0
BESSK1=(LOG(X/2.0)*BESSI1(X)+(1.0/X)*(P1+Y*(P2+
& Y*(P3+Y*(P4+Y*(P5+Y*(P6+Y*P7)))))))

```

```

ELSE
  Y=(2.0/X)
  BESSK1=(EXP(-X)/SQRT(X))*(Q1+Y*(Q2+Y*(Q3+
&           Y*(Q4+Y*(Q5+Y*(Q6+Y*Q7))))))
ENDIF
RETURN
END

FUNCTION BESSI0(X)
C*****C RETURNS THE MODIFIED BESSEL FUNCTION I0(X) FOR ANY REAL X *****
C*****
IMPLICIT REAL*8 (A-H,O-Z)
DATA P1,P2,P3,P4,P5,P6,P7
& /+1.0000000D+00,+3.5156229D+00,+3.0899424D+00,
& +1.20674920D+00,+0.2659732D+00,+0.3607680D-01,
& +0.45813000D-02/
DATA Q1,Q2,Q3,Q4,Q5,Q6,Q7,Q8,Q9
& /+0.39894228D+00,+0.1328592D-01,+0.2253190D-02,
& -0.15756500D-02,+0.9162810D-02,-0.2057706D-01,
& +0.26355370D-01,-0.1647633D-01,+0.3923770D-02/
IF (ABS(X).LT.3.75) THEN
  Y=(X/3.75)**2
  BESSI0=P1+Y*(P2+Y*(P3+Y*(P4+Y*(P5+Y*(P6+Y*P7))))))
ELSE
  AX=ABS(X)
  Y=(3.75/AX)
  BESSI0=(EXP(AX)/SQRT(AX))*(Q1+Y*(Q2+Y*(Q3+Y*(Q4+
&           Y*(Q5+Y*(Q6+Y*(Q7+Y*(Q8+Y*Q9)))))))
ENDIF
RETURN
END

FUNCTION BESSI1(X)
C*****C RETURNS THE MODIFIED BESSEL FUNCTION I1(X) FOR ANY REAL X *****
C*****
IMPLICIT REAL*8 (A-H,O-Z)
DATA P1,P2,P3,P4,P5,P6,P7
& /+0.5000000D+00,+0.87890594D+00,+0.51498869D+00,
& +0.15084934D+00,+0.26587330D-01,+0.30153200D-02,
& +0.32411000D-03/
DATA Q1,Q2,Q3,Q4,Q5,Q6,Q7,Q8,Q9
& /+0.39894228D+00,-0.39880240D-01,-0.36201800D-02,
& +0.16380100D-02,-0.10315550D-01,+0.22829670D-01,
& -0.28953120D-01,+0.17876540D-01,-0.42005900D-02/
IF (ABS(X).LT.3.75) THEN
  Y=(X/3.75)**2
  BESSI1=X*(P1+Y*(P2+Y*(P3+Y*(P4+Y*(P5+Y*(P6+Y*P7))))))
ELSE
  AX=ABS(X)
  Y=(3.75/AX)
  BESSI1=(EXP(AX)/SQRT(AX))*(Q1+Y*(Q2+Y*(Q3+Y*(Q4+
&           Y*(Q5+Y*(Q6+Y*(Q7+Y*(Q8+Y*Q9)))))))
ENDIF
RETURN
END

SUBROUTINE JACOBI(A,N,NP,D,V,NROT)
C*****C MATRIX DIAGONALIZATION FROM NUMERICAL RECIPES [PRESS ET AL.] *****
C   USING THE JACOBI METHOD

```

```

C*****
      IMPLICIT REAL*8 (A-H,O-Z)
      PARAMETER(NMAX=100)
      DIMENSION A(NP,NP),D(NP),V(NP,NP),B(NMAX),Z(NMAX)
      DO 12 IP=1,N
         DO 11 IQ=1,N
            V(IP,IQ)=0.
11      CONTINUE
            V(IP,IP)=1.
12      CONTINUE
         DO 13 IP=1,N
            B(IP)=A(IP,IP)
            D(IP)=B(IP)
            Z(IP)=0.
13      CONTINUE
      NROT=0
      DO 24 I=1,50
         SM=0.
         DO 15 IP=1,N-1
            DO 14 IQ=IP+1,N
               SM=SM+ABS(A(IP,IQ))
14      CONTINUE
15      CONTINUE
      IF (SM.EQ.0.) RETURN
      IF (I.LT.4) THEN
         TRESH=0.2*SM/N**2
      ELSE
         TRESH=0.
      ENDIF
      DO 22 IP=1,N-1
         DO 21 IQ=IP+1,N
            G=100.*ABS(A(IP,IQ))
            IF ((I.GT.4).AND.(ABS(D(IP))+G.EQ.ABS(D(IP)))
& .AND.(ABS(D(IQ))+G.EQ.ABS(D(IQ)))) THEN
               A(IP,IQ)=0.
            ELSE IF (ABS(A(IP,IQ)).GT.TRESH) THEN
               H=D(IQ)-D(IP)
               IF (ABS(H)+G.EQ.ABS(H)) THEN
                  T=A(IP,IQ)/H
               ELSE
                  THETA=0.5*H/A(IP,IQ)
                  T=1./(ABS(THETA)+SQRT(1.+THETA**2))
                  IF (THETA.LT.0.) T=-T
               ENDIF
               C=1./SQRT(1.+T**2)
               S=T*C
               TAU=S/(1.+C)
               H=T*A(IP,IQ)
               Z(IP)=Z(IP)-H
               Z(IQ)=Z(IQ)+H
               D(IP)=D(IP)-H
               D(IQ)=D(IQ)+H
               A(IP,IQ)=0.
            DO 16 J=1,IP-1
               G=A(J,IP)
               H=A(J,IQ)
               A(J,IP)=G-S*(H+G*TAU)
               A(J,IQ)=H+S*(G-H*TAU)
16      CONTINUE
            DO 17 J=IP+1,IQ-1
               G=A(IP,J)
               H=A(J,IQ)
               A(IP,J)=G-S*(H+G*TAU)
               A(J,IQ)=H+S*(G-H*TAU)
17      CONTINUE
            DO 18 J=IQ+1,N
               G=A(IP,J)

```

```

        H=A(IQ,J)
        A(IP,J)=G-S*(H+G*TAU)
        A(IQ,J)=H+S*(G-H*TAU)
18      CONTINUE
        DO 19 J=1,N
          G=V(J,IP)
          H=V(J,IQ)
          V(J,IP)=G-S*(H+G*TAU)
          V(J,IQ)=H+S*(G-H*TAU)
19      CONTINUE
        NROT=NROT+1
      ENDIF
21      CONTINUE
22      DO 23 IP=1,N
        B(IP)=B(IP)+Z(IP)
        D(IP)=B(IP)
        Z(IP)=0.
23      CONTINUE
24      CONTINUE
      RETURN
    END

```

```

      SUBROUTINE QGAUS(FUNC,A,B,SS)
C*****SUBROUTINE QGAUS(FUNC,A,B,SS) RETURNS AS SS THE INTEGRAL OF THE FUNCTION, FUNC,
C QGAUS(FUNC,A,B,SS) RETURNS AS SS THE INTEGRAL OF THE FUNCTION, FUNC, *
C BETWEEN A AND B, BY TEN POINT GAUSSIAN LEGENDRE INTEGRATION: THE *  

C FUNCTION IS EVALUATED EXACTLY TEN TIMES AT INTERIOR POINTS IN THE *  

C RANGE OF INTEGRATION. *
C
C WITH THE LOWER AND UPPER LIMITS OF INTEGRATION AND GIVEN N, GAULEG *
C RETURNS ARRAYS X AND W OF LENGTH N, CONTAINING THE ABSCISSAS AND *
C WEIGHTS OF THE GAUSS-LEGENDRE N-POINT QUADRATURE FORMULA *
C*****
C IMPLICIT REAL*8 (A-H,O-Z)
COMMON/GAUSS/ X,W,N
PARAMETER (NN=100)
C DIMENSION YY(NN),XX(NN)
DIMENSION X(NN),W(NN)
EXTERNAL FUNC

XR=B-A
SS=0
DO 100 J=1,N
  DX=XR*X(J)
  SS=SS+W(J)*FUNC((A+DX))
C   XX(J)=X(J)
C   YY(J)=FUNC((A+DX))
100 CONTINUE
SS=SS*XR
C   DO 12 J=1,N
C   WRITE(*,*)XX(J),YY(J)
C12  CONTINUE
      RETURN
    END

      SUBROUTINE GAULEG(X,W,N)
IMPLICIT REAL*8 (A-H,O-Z)
COMMON/ANS/PERTURB,EBROAD,NAINT
CHARACTER*1 PERTURB,EBROAD,NAINT
DIMENSION X(N),W(N)

XINT=1.
IF (NAINT.EQ.'N') THEN
  N=MIN(10,N)

```

```

W(N)=XINT/2.
X(N)=1.-W(N)/2.
DO 110 I=1,N-2
    W(N-I)=W(N-I+1)/2.
    X(N-I)=X(N-I+1)-W(N-I+1)/2.-W(N-I)/2.
110  CONTINUE
    W(1)=W(2)
    X(1)=X(2)-W(2)/2.-W(1)/2.
ELSE
    DX=XINT/FLOAT(N)
    W(1)=DX
    X(1)=DX/2.
    DO 120 I=2,N
        W(I)=W(1)
        X(I)=X(I-1)+W(I)/2.+W(I-1)/2.
120  CONTINUE
ENDIF
RETURN
END

```

```

*****
C THE FOLLOWING TWO SUBROUTINES CONTAIN THE RADIAL MATRIX. *
C ELEMENTS FOR OXYGEN CALCULATED BY CHUN LIN FOR SPIN 1 (TRIPLET) *
C AND SPIN 2 (QUINTET) *
*****

```

```

SUBROUTINE RADMATX1
IMPLICIT REAL*8 (A-H,O-Z)
COMMON/RADIAL/RME1
DIMENSION RME1(10,20,20)

C THE DATA FORMAT IS RME1(L1,PN1,PN2); L1-L2=+1

```

C P-S TRANSITION:

```

RME1(1, 3, 3) = -5.69980E+00
RME1(1, 4, 3) = -1.32130E-01
RME1(1, 5, 3) = 5.70950E-03
RME1(1, 6, 3) = 2.18900E-02
RME1(1, 7, 3) = 2.24800E-02
RME1(1, 8, 3) = 2.03440E-02
RME1(1, 9, 3) = 1.79130E-02
RME1(1,10, 3) = 1.57220E-02
RME1(1,11, 3) = 1.38520E-02
RME1(1,12, 3) = 1.22820E-02
RME1(1,13, 3) = 1.09640E-02
RME1(1,14, 3) = 9.85310E-03
RME1(1,15, 3) = 8.90960E-03
RME1(1, 3, 4) = 4.33920E+00
RME1(1, 4, 4) = -1.25200E+01
RME1(1, 5, 4) = -6.49010E-01
RME1(1, 6, 4) = -1.62430E-01
RME1(1, 7, 4) = -6.06670E-02
RME1(1, 8, 4) = -2.67710E-02
RME1(1, 9, 4) = -1.26120E-02
RME1(1,10, 4) = -5.85800E-03
RME1(1,11, 4) = -2.35970E-03
RME1(1,12, 4) = -4.47990E-04
RME1(1,13, 4) = 6.28850E-04
RME1(1,14, 4) = 1.24150E-03
RME1(1,15, 4) = 1.58520E-03
RME1(1, 3, 5) = 1.10210E+00
RME1(1, 4, 5) = 9.95550E+00
RME1(1, 5, 5) = -2.17500E+01
RME1(1, 6, 5) = -1.39390E+00
RME1(1, 7, 5) = -4.24680E-01
RME1(1, 8, 5) = -1.97530E-01

```

RME1(1, 9, 5) = -1.12670E-01  
RME1(1, 10, 5) = -7.25610E-02  
RME1(1, 11, 5) = -5.06750E-02  
RME1(1, 12, 5) = -3.74970E-02  
RME1(1, 13, 5) = -2.89740E-02  
RME1(1, 14, 5) = -2.31520E-02  
RME1(1, 15, 5) = -1.89980E-02  
RME1(1, 3, 6) = 5.86310E-01  
RME1(1, 4, 6) = 2.29000E+00  
RME1(1, 5, 6) = 1.74950E+01  
RME1(1, 6, 6) = -3.34100E+01  
RME1(1, 7, 6) = -2.35630E+00  
RME1(1, 8, 6) = -7.71360E-01  
RME1(1, 9, 6) = -3.81740E-01  
RME1(1, 10, 6) = -2.29910E-01  
RME1(1, 11, 6) = -1.55340E-01  
RME1(1, 12, 6) = -1.13150E-01  
RME1(1, 13, 6) = -8.68770E-02  
RME1(1, 14, 6) = -6.93560E-02  
RME1(1, 15, 6) = -5.70160E-02  
RME1(1, 3, 7) = 3.87520E-01  
RME1(1, 4, 7) = 1.18020E+00  
RME1(1, 5, 7) = 3.80550E+00  
RME1(1, 6, 7) = 2.69780E+01  
RME1(1, 7, 7) = -4.75060E+01  
RME1(1, 8, 7) = -3.53100E+00  
RME1(1, 9, 7) = -1.19830E+00  
RME1(1, 10, 7) = -6.09970E-01  
RME1(1, 11, 7) = -3.75860E-01  
RME1(1, 12, 7) = -2.58760E-01  
RME1(1, 13, 7) = -1.91440E-01  
RME1(1, 14, 7) = -1.48930E-01  
RME1(1, 15, 7) = -1.20200E-01  
RME1(1, 3, 8) = 2.84040E-01  
RME1(1, 4, 8) = 7.69880E-01  
RME1(1, 5, 8) = 1.91670E+00  
RME1(1, 6, 8) = 5.65600E+00  
RME1(1, 7, 8) = 3.84140E+01  
RME1(1, 8, 8) = -6.40400E+01  
RME1(1, 9, 8) = -4.91670E+00  
RME1(1, 10, 8) = -1.70370E+00  
RME1(1, 11, 8) = -8.80780E-01  
RME1(1, 12, 8) = -5.49260E-01  
RME1(1, 13, 8) = -3.81740E-01  
RME1(1, 14, 8) = -2.84600E-01  
RME1(1, 15, 8) = -2.22810E-01  
RME1(1, 3, 9) = 2.21200E-01  
RME1(1, 4, 9) = 5.61350E-01  
RME1(1, 5, 9) = 1.23580E+00  
RME1(1, 6, 9) = 2.79890E+00  
RME1(1, 7, 9) = 7.84300E+00  
RME1(1, 8, 9) = 5.18060E+01  
RME1(1, 9, 9) = -8.30120E+01  
RME1(1, 10, 9) = -6.51240E+00  
RME1(1, 11, 9) = -2.28680E+00  
RME1(1, 12, 9) = -1.19330E+00  
RME1(1, 13, 9) = -7.46390E-01  
RME1(1, 14, 9) = -5.23640E-01  
RME1(1, 15, 9) = -3.92070E-01  
RME1(1, 3, 10) = 1.79280E-01  
RME1(1, 4, 10) = 4.36520E-01  
RME1(1, 5, 10) = 8.95540E-01  
RME1(1, 6, 10) = 1.78620E+00  
RME1(1, 7, 10) = 3.82690E+00  
RME1(1, 8, 10) = 1.03670E+01  
RME1(1, 9, 10) = 6.71580E+01  
RME1(1, 10, 10) = -1.04420E+02

RME1(1,11,10) = -8.31800E+00  
RME1(1,12,10) = -2.94700E+00  
RME1(1,13,10) = -1.54720E+00  
RME1(1,14,10) = -9.75820E-01  
RME1(1,15,10) = -6.84070E-01  
RME1(1, 3,11) = 1.49490E-01  
RME1(1, 4,11) = 3.53970E-01  
RME1(1, 5,11) = 6.94220E-01  
RME1(1, 6,11) = 1.28650E+00  
RME1(1, 7,11) = 2.42090E+00  
RME1(1, 8,11) = 5.00070E+00  
RME1(1, 9,11) = 1.32280E+01  
RME1(1,10,11) = 8.44680E+01  
RME1(1,11,11) = -1.28270E+02  
RME1(1,12,11) = -1.03330E+01  
RME1(1,13,11) = -3.68400E+00  
RME1(1,14,11) = -1.94200E+00  
RME1(1,15,11) = -1.22820E+00  
RME1(1, 3,12) = 1.27340E-01  
RME1(1, 4,12) = 2.95600E-01  
RME1(1, 5,12) = 5.62180E-01  
RME1(1, 6,12) = 9.93600E-01  
RME1(1, 7,12) = 1.73350E+00  
RME1(1, 8,12) = 3.13950E+00  
RME1(1, 9,12) = 6.32030E+00  
RME1(1,10,12) = 1.64270E+01  
RME1(1,11,12) = 1.03740E+02  
RME1(1,12,12) = -1.54560E+02  
RME1(1,13,12) = -1.25570E+01  
RME1(1,14,12) = -4.49770E+00  
RME1(1,15,12) = -2.37760E+00  
RME1(1, 3,13) = 1.10300E-01  
RME1(1, 4,13) = 2.52310E-01  
RME1(1, 5,13) = 4.69360E-01  
RME1(1, 6,13) = 8.02860E-01  
RME1(1, 7,13) = 1.33370E+00  
RME1(1, 8,13) = 2.23630E+00  
RME1(1, 9,13) = 3.94190E+00  
RME1(1,10,13) = 7.78570E+00  
RME1(1,11,13) = 1.99630E+01  
RME1(1,12,13) = 1.24970E+02  
RME1(1,13,13) = -1.83280E+02  
RME1(1,14,13) = -1.49910E+01  
RME1(1,15,13) = -5.38780E+00  
RME1(1, 3,14) = 9.68160E-02  
RME1(1, 4,14) = 2.19020E-01  
RME1(1, 5,14) = 4.00780E-01  
RME1(1, 6,14) = 6.69510E-01  
RME1(1, 7,14) = 1.07500E+00  
RME1(1, 8,14) = 1.71420E+00  
RME1(1, 9,14) = 2.79450E+00  
RME1(1,10,14) = 4.82790E+00  
RME1(1,11,14) = 9.39680E+00  
RME1(1,12,14) = 2.38360E+01  
RME1(1,13,14) = 1.48160E+02  
RME1(1,14,14) = -2.14460E+02  
RME1(1,15,14) = -1.76330E+01  
RME1(1, 3,15) = 8.59250E-02  
RME1(1, 4,15) = 1.92710E-01  
RME1(1, 5,15) = 3.48190E-01  
RME1(1, 6,15) = 5.71410E-01  
RME1(1, 7,15) = 8.94980E-01  
RME1(1, 8,15) = 1.37800E+00  
RME1(1, 9,15) = 2.13460E+00  
RME1(1,10,15) = 3.40800E+00  
RME1(1,11,15) = 5.79760E+00  
RME1(1,12,15) = 1.11540E+01

RME1(1,13,15) = 2.80470E+01  
RME1(1,14,15) = 1.73320E+02  
RME1(1,15,15) = -2.48060E+02

C D-P TRANSITION:

RME1(2, 3, 3) = -7.15410E+00  
RME1(2, 4, 3) = -1.39930E+00  
RME1(2, 5, 3) = -6.29180E-01  
RME1(2, 6, 3) = -3.76330E-01  
RME1(2, 7, 3) = -2.58990E-01  
RME1(2, 8, 3) = -1.93390E-01  
RME1(2, 9, 3) = -1.52230E-01  
RME1(2, 10, 3) = -1.24280E-01  
RME1(2, 11, 3) = -1.04220E-01  
RME1(2, 12, 3) = -8.91940E-02  
RME1(2, 13, 3) = -7.75690E-02  
RME1(2, 14, 3) = -6.83390E-02  
RME1(2, 15, 3) = -6.08530E-02  
RME1(2, 3, 4) = 8.55100E+00  
RME1(2, 4, 4) = -1.33950E+01  
RME1(2, 5, 4) = -2.95390E+00  
RME1(2, 6, 4) = -1.40360E+00  
RME1(2, 7, 4) = -8.65420E-01  
RME1(2, 8, 4) = -6.07120E-01  
RME1(2, 9, 4) = -4.59440E-01  
RME1(2, 10, 4) = -3.65270E-01  
RME1(2, 11, 4) = -3.00580E-01  
RME1(2, 12, 4) = -2.53700E-01  
RME1(2, 13, 4) = -2.18310E-01  
RME1(2, 14, 4) = -1.90750E-01  
RME1(2, 15, 4) = -1.68750E-01  
RME1(2, 3, 5) = 6.36840E-01  
RME1(2, 4, 5) = 1.78280E+01  
RME1(2, 5, 5) = -2.12180E+01  
RME1(2, 6, 5) = -4.84580E+00  
RME1(2, 7, 5) = -2.34510E+00  
RME1(2, 8, 5) = -1.46100E+00  
RME1(2, 9, 5) = -1.03180E+00  
RME1(2, 10, 5) = -7.84600E-01  
RME1(2, 11, 5) = -6.26200E-01  
RME1(2, 12, 5) = -5.16990E-01  
RME1(2, 13, 5) = -4.37600E-01  
RME1(2, 14, 5) = -3.77540E-01  
RME1(2, 15, 5) = -3.30670E-01  
RME1(2, 3, 6) = 2.93510E-01  
RME1(2, 4, 6) = 1.21350E+00  
RME1(2, 5, 6) = 2.96800E+01  
RME1(2, 6, 6) = -3.06380E+01  
RME1(2, 7, 6) = -7.08620E+00  
RME1(2, 8, 6) = -3.45110E+00  
RME1(2, 9, 6) = -2.15720E+00  
RME1(2, 10, 6) = -1.52660E+00  
RME1(2, 11, 6) = -1.16280E+00  
RME1(2, 12, 6) = -9.29310E-01  
RME1(2, 13, 6) = -7.68240E-01  
RME1(2, 14, 6) = -6.51090E-01  
RME1(2, 15, 6) = -5.62430E-01  
RME1(2, 3, 7) = 1.85080E-01  
RME1(2, 4, 7) = 5.38970E-01  
RME1(2, 5, 7) = 1.85100E+00  
RME1(2, 6, 7) = 4.41860E+01  
RME1(2, 7, 7) = -4.16630E+01  
RME1(2, 8, 7) = -9.67780E+00  
RME1(2, 9, 7) = -4.72020E+00  
RME1(2, 10, 7) = -2.95140E+00  
RME1(2, 11, 7) = -2.08870E+00  
RME1(2, 12, 7) = -1.59090E+00

RME1(2,13, 7) = -1.27170E+00  
RME1(2,14, 7) = -1.05150E+00  
RME1(2,15, 7) = -8.91480E-01  
RME1(2, 3, 8) = 1.32810E-01  
RME1(2, 4, 8) = 3.35450E-01  
RME1(2, 5, 8) = 7.93510E-01  
RME1(2, 6, 8) = 2.54910E+00  
RME1(2, 7, 8) = 6.13660E+01  
RME1(2, 8, 8) = -5.42960E+01  
RME1(2, 9, 8) = -1.26230E+01  
RME1(2,10, 8) = -6.15250E+00  
RME1(2,11, 8) = -3.84280E+00  
RME1(2,12, 8) = -2.71690E+00  
RME1(2,13, 8) = -2.06780E+00  
RME1(2,14, 8) = -1.65190E+00  
RME1(2,15, 8) = -1.36540E+00  
RME1(2, 3, 9) = 1.02290E-01  
RME1(2, 4, 9) = 2.39580E-01  
RME1(2, 5, 9) = 4.86770E-01  
RME1(2, 6, 9) = 1.05730E+00  
RME1(2, 7, 9) = 3.30630E+00  
RME1(2, 8, 9) = 8.12280E+01  
RME1(2, 9, 9) = -6.85380E+01  
RME1(2,10, 9) = -1.59220E+01  
RME1(2,11, 9) = -7.74810E+00  
RME1(2,12, 9) = -4.83120E+00  
RME1(2,13, 9) = -3.41070E+00  
RME1(2,14, 9) = -2.59260E+00  
RME1(2,15, 9) = -2.06920E+00  
RME1(2, 3,10) = 8.23880E-02  
RME1(2, 4,10) = 1.84310E-01  
RME1(2, 5,10) = 3.45340E-01  
RME1(2, 6,10) = 6.39150E-01  
RME1(2, 7,10) = 1.32980E+00  
RME1(2, 8,10) = 4.12150E+00  
RME1(2, 9,10) = 1.03770E+02  
RME1(2,10,10) = -8.43920E+01  
RME1(2,11,10) = -1.95770E+01  
RME1(2,12,10) = -9.50710E+00  
RME1(2,13,10) = -5.91650E+00  
RME1(2,14,10) = -4.16970E+00  
RME1(2,15,10) = -3.16520E+00  
RME1(2, 3,11) = 6.84510E-02  
RME1(2, 4,11) = 1.48550E-01  
RME1(2, 5,11) = 2.64870E-01  
RME1(2, 6,11) = 4.50120E-01  
RME1(2, 7,11) = 7.92440E-01  
RME1(2, 8,11) = 1.61050E+00  
RME1(2, 9,11) = 4.99410E+00  
RME1(2,10,11) = 1.29000E+02  
RME1(2,11,11) = -1.01860E+02  
RME1(2,12,11) = -2.35870E+01  
RME1(2,13,11) = -1.14300E+01  
RME1(2,14,11) = -7.09850E+00  
RME1(2,15,11) = -4.99390E+00  
RME1(2, 3,12) = 5.81860E-02  
RME1(2, 4,12) = 1.23600E-01  
RME1(2, 5,12) = 2.13230E-01  
RME1(2, 6,12) = 3.43860E-01  
RME1(2, 7,12) = 5.53800E-01  
RME1(2, 8,12) = 9.46510E-01  
RME1(2, 9,12) = 1.89970E+00  
RME1(2,10,12) = 5.92330E+00  
RME1(2,11,12) = 1.56920E+02  
RME1(2,12,12) = -1.20930E+02  
RME1(2,13,12) = -2.79520E+01  
RME1(2,14,12) = -1.35160E+01

RME1(2,15,12) = -8.37730E+00  
 RME1(2, 3,13) = 5.03360E-02  
 RME1(2, 4,13) = 1.05270E-01  
 RME1(2, 5,13) = 1.77400E-01  
 RME1(2, 6,13) = 2.76250E-01  
 RME1(2, 7,13) = 4.21220E-01  
 RME1(2, 8,13) = 6.36380E-01  
 RME1(2, 9,13) = 1.10130E+00  
 RME1(2,10,13) = 2.19680E+00  
 RME1(2,11,13) = 6.90900E+00  
 RME1(2,12,13) = 1.87530E+02  
 RME1(2,13,13) = -1.41620E+02  
 RME1(2,14,13) = -3.26740E+01  
 RME1(2,15,13) = -1.57660E+01  
 RME1(2, 3,14) = 4.41560E-02  
 RME1(2, 4,14) = 9.12600E-02  
 RME1(2, 5,14) = 1.51170E-01  
 RME1(2, 6,14) = 2.29610E-01  
 RME1(2, 7,14) = 3.37560E-01  
 RME1(2, 8,14) = 4.96980E-01  
 RME1(2, 9,14) = 7.57900E-01  
 RME1(2,10,14) = 1.25680E+00  
 RME1(2,11,14) = 2.50180E+00  
 RME1(2,12,14) = 7.95070E+00  
 RME1(2,13,14) = 2.20810E+02  
 RME1(2,14,14) = -1.63920E+02  
 RME1(2,15,14) = -3.77520E+01  
 RME1(2, 3,15) = 3.91790E-02  
 RME1(2, 4,15) = 8.02320E-02  
 RME1(2, 5,15) = 1.31170E-01  
 RME1(2, 6,15) = 1.95600E-01  
 RME1(2, 7,15) = 2.80130E-01  
 RME1(2, 8,15) = 3.97070E-01  
 RME1(2, 9,15) = 5.71090E-01  
 RME1(2,10,15) = 8.58310E-01  
 RME1(2,11,15) = 1.41300E+00  
 RME1(2,12,15) = 2.81460E+00  
 RME1(2,13,15) = 9.04840E+00  
 RME1(2,14,15) = 2.56790E+02  
 RME1(2,15,15) = -1.87830E+02

C F-D TRANSITION:

RME1(3, 4, 3) = 1.01970E+01  
 RME1(3, 5, 3) = 3.32020E+00  
 RME1(3, 6, 3) = 1.80170E+00  
 RME1(3, 7, 3) = 1.19090E+00  
 RME1(3, 8, 3) = 8.71790E-01  
 RME1(3, 9, 3) = 6.78720E-01  
 RME1(3,10, 3) = 5.50490E-01  
 RME1(3,11, 3) = 4.59680E-01  
 RME1(3,12, 3) = 3.92290E-01  
 RME1(3,13, 3) = 3.40480E-01  
 RME1(3,14, 3) = 2.99530E-01  
 RME1(3,15, 3) = 2.66430E-01  
 RME1(3, 4, 4) = -1.58900E+01  
 RME1(3, 5, 4) = 1.39800E+01  
 RME1(3, 6, 4) = 5.16890E+00  
 RME1(3, 7, 4) = 2.92980E+00  
 RME1(3, 8, 4) = 1.97770E+00  
 RME1(3, 9, 4) = 1.46600E+00  
 RME1(3,10, 4) = 1.15120E+00  
 RME1(3,11, 4) = 9.39850E-01  
 RME1(3,12, 4) = 7.88960E-01  
 RME1(3,13, 4) = 6.76310E-01  
 RME1(3,14, 4) = 5.89260E-01  
 RME1(3,15, 4) = 5.20160E-01  
 RME1(3, 4, 5) = 1.69840E+00

RME1(3, 5, 5) = -3.00270E+01  
RME1(3, 6, 5) = 1.84360E+01  
RME1(3, 7, 5) = 7.06310E+00  
RME1(3, 8, 5) = 4.06580E+00  
RME1(3, 9, 5) = 2.76790E+00  
RME1(3, 10, 5) = 2.06300E+00  
RME1(3, 11, 5) = 1.62660E+00  
RME1(3, 12, 5) = 1.33230E+00  
RME1(3, 13, 5) = 1.12160E+00  
RME1(3, 14, 5) = 9.63850E-01  
RME1(3, 15, 5) = 8.41730E-01  
RME1(3, 4, 6) = 5.77150E-01  
RME1(3, 5, 6) = 3.73100E+00  
RME1(3, 6, 6) = -4.68020E+01  
RME1(3, 7, 6) = 2.35480E+01  
RME1(3, 8, 6) = 9.11450E+00  
RME1(3, 9, 6) = 5.27190E+00  
RME1(3, 10, 6) = 3.59870E+00  
RME1(3, 11, 6) = 2.68730E+00  
RME1(3, 12, 6) = 2.12220E+00  
RME1(3, 13, 6) = 1.74070E+00  
RME1(3, 14, 6) = 1.46740E+00  
RME1(3, 15, 6) = 1.26270E+00  
RME1(3, 4, 7) = 3.13170E-01  
RME1(3, 5, 7) = 1.28370E+00  
RME1(3, 6, 7) = 6.40080E+00  
RME1(3, 7, 7) = -6.64540E+01  
RME1(3, 8, 7) = 2.93100E+01  
RME1(3, 9, 7) = 1.13570E+01  
RME1(3, 10, 7) = 6.56990E+00  
RME1(3, 11, 7) = 4.48460E+00  
RME1(3, 12, 7) = 3.34900E+00  
RME1(3, 13, 7) = 2.64520E+00  
RME1(3, 14, 7) = 2.17040E+00  
RME1(3, 15, 7) = 1.83040E+00  
RME1(3, 4, 8) = 2.05950E-01  
RME1(3, 5, 8) = 6.97910E-01  
RME1(3, 6, 8) = 2.21520E+00  
RME1(3, 7, 8) = 9.72160E+00  
RME1(3, 8, 8) = -8.90490E+01  
RME1(3, 9, 8) = 3.57170E+01  
RME1(3, 10, 8) = 1.38040E+01  
RME1(3, 11, 8) = 7.96990E+00  
RME1(3, 12, 8) = 5.43260E+00  
RME1(3, 13, 8) = 4.05300E+00  
RME1(3, 14, 8) = 3.19920E+00  
RME1(3, 15, 8) = 2.62400E+00  
RME1(3, 4, 9) = 1.50080E-01  
RME1(3, 5, 9) = 4.58710E-01  
RME1(3, 6, 9) = 1.20440E+00  
RME1(3, 7, 9) = 3.37440E+00  
RME1(3, 8, 9) = 1.36980E+01  
RME1(3, 9, 9) = -1.14620E+02  
RME1(3, 10, 9) = 4.27690E+01  
RME1(3, 11, 9) = 1.64610E+01  
RME1(3, 12, 9) = 9.47720E+00  
RME1(3, 13, 9) = 6.44660E+00  
RME1(3, 14, 9) = 4.80220E+00  
RME1(3, 15, 9) = 3.78650E+00  
RME1(3, 4, 10) = 1.16470E-01  
RME1(3, 5, 10) = 3.33970E-01  
RME1(3, 6, 10) = 7.90460E-01  
RME1(3, 7, 10) = 1.83300E+00  
RME1(3, 8, 10) = 4.76130E+00  
RME1(3, 9, 10) = 1.83310E+01  
RME1(3, 10, 10) = -1.43160E+02  
RME1(3, 11, 10) = 5.04630E+01

RME1(3,12,10) = 1.93340E+01  
 RME1(3,13,10) = 1.10950E+01  
 RME1(3,14,10) = 7.52880E+00  
 RME1(3,15,10) = 5.59830E+00  
 RME1(3, 4,11) = 9.42750E-02  
 RME1(3, 5,11) = 2.58990E-01  
 RME1(3, 6,11) = 5.74630E-01  
 RME1(3, 7,11) = 1.20100E+00  
 RME1(3, 8,11) = 2.58350E+00  
 RME1(3, 9,11) = 6.37600E+00  
 RME1(3,10,11) = 2.36240E+01  
 RME1(3,11,11) = -1.74700E+02  
 RME1(3,12,11) = 5.87990E+01  
 RME1(3,13,11) = 2.24230E+01  
 RME1(3,14,11) = 1.28250E+01  
 RME1(3,15,11) = 8.68090E+00  
 RME1(3, 4,12) = 7.86350E-02  
 RME1(3, 5,12) = 2.09570E-01  
 RME1(3, 6,12) = 4.45070E-01  
 RME1(3, 7,12) = 8.71570E-01  
 RME1(3, 8,12) = 1.68970E+00  
 RME1(3, 9,12) = 3.45520E+00  
 RME1(3,10,12) = 8.21830E+00  
 RME1(3,11,12) = 2.95750E+01  
 RME1(3,12,12) = -2.09230E+02  
 RME1(3,13,12) = 6.77760E+01  
 RME1(3,14,12) = 2.57300E+01  
 RME1(3,15,12) = 1.46680E+01  
 RME1(3, 4,13) = 6.70770E-02  
 RME1(3, 5,13) = 1.74800E-01  
 RME1(3, 6,13) = 3.59820E-01  
 RME1(3, 7,13) = 6.74080E-01  
 RME1(3, 8,13) = 1.22400E+00  
 RME1(3, 9,13) = 2.25590E+00  
 RME1(3,10,13) = 4.44780E+00  
 RME1(3,11,13) = 1.02880E+01  
 RME1(3,12,13) = 3.61870E+01  
 RME1(3,13,13) = -2.46750E+02  
 RME1(3,14,13) = 7.73940E+01  
 RME1(3,15,13) = 2.92550E+01  
 RME1(3, 4,14) = 5.82180E-02  
 RME1(3, 5,14) = 1.49140E-01  
 RME1(3, 6,14) = 2.99950E-01  
 RME1(3, 7,14) = 5.44320E-01  
 RME1(3, 8,14) = 9.45240E-01  
 RME1(3, 9,14) = 1.63140E+00  
 RME1(3,10,14) = 2.89920E+00  
 RME1(3,11,14) = 5.56100E+00  
 RME1(3,12,14) = 1.25850E+01  
 RME1(3,13,14) = 4.34580E+01  
 RME1(3,14,14) = -2.87270E+02  
 RME1(3,15,14) = 8.76520E+01  
 RME1(3, 4,15) = 5.12330E-02  
 RME1(3, 5,15) = 1.29500E-01  
 RME1(3, 6,15) = 2.55840E-01  
 RME1(3, 7,15) = 4.53370E-01  
 RME1(3, 8,15) = 7.62330E-01  
 RME1(3, 9,15) = 1.25790E+00  
 RME1(3,10,15) = 2.09330E+00  
 RME1(3,11,15) = 3.61920E+00  
 RME1(3,12,15) = 6.79460E+00  
 RME1(3,13,15) = 1.51090E+01  
 RME1(3,14,15) = 5.13900E+01  
 RME1(3,15,15) = -3.30790E+02

C G-F TRANSITION:  
 RME1(4, 5, 4) = 1.77200E+01

RME1(4, 6, 4) = 5.25090E+00  
RME1(4, 7, 4) = 2.69850E+00  
RME1(4, 8, 4) = 1.72450E+00  
RME1(4, 9, 4) = 1.23510E+00  
RME1(4, 10, 4) = 9.47600E-01  
RME1(4, 11, 4) = 7.60920E-01  
RME1(4, 12, 4) = 6.30990E-01  
RME1(4, 13, 4) = 5.35870E-01  
RME1(4, 14, 4) = 4.63520E-01  
RME1(4, 15, 4) = 4.06800E-01  
RME1(4, 5, 5) = -2.25000E+01  
RME1(4, 6, 5) = 2.25640E+01  
RME1(4, 7, 5) = 7.82850E+00  
RME1(4, 8, 5) = 4.26610E+00  
RME1(4, 9, 5) = 2.80620E+00  
RME1(4, 10, 5) = 2.04360E+00  
RME1(4, 11, 5) = 1.58500E+00  
RME1(4, 12, 5) = 1.28250E+00  
RME1(4, 13, 5) = 1.06970E+00  
RME1(4, 14, 5) = 9.12640E-01  
RME1(4, 15, 5) = 7.92420E-01  
RME1(4, 5, 6) = 2.01870E+00  
RME1(4, 6, 6) = -4.02490E+01  
RME1(4, 7, 6) = 2.81160E+01  
RME1(4, 8, 6) = 1.02940E+01  
RME1(4, 9, 6) = 5.75420E+00  
RME1(4, 10, 6) = 3.83880E+00  
RME1(4, 11, 6) = 2.82030E+00  
RME1(4, 12, 6) = 2.20050E+00  
RME1(4, 13, 6) = 1.78850E+00  
RME1(4, 14, 6) = 1.49690E+00  
RME1(4, 15, 6) = 1.28080E+00  
RME1(4, 5, 7) = 6.36100E-01  
RME1(4, 6, 7) = 4.25990E+00  
RME1(4, 7, 7) = -6.03180E+01  
RME1(4, 8, 7) = 3.43500E+01  
RME1(4, 9, 7) = 1.28550E+01  
RME1(4, 10, 7) = 7.27030E+00  
RME1(4, 11, 7) = 4.88400E+00  
RME1(4, 12, 7) = 3.60450E+00  
RME1(4, 13, 7) = 2.82140E+00  
RME1(4, 14, 7) = 2.29880E+00  
RME1(4, 15, 7) = 1.92780E+00  
RME1(4, 5, 8) = 3.28470E-01  
RME1(4, 6, 8) = 1.38160E+00  
RME1(4, 7, 8) = 7.11540E+00  
RME1(4, 8, 8) = -8.31380E+01  
RME1(4, 9, 8) = 4.12540E+01  
RME1(4, 10, 8) = 1.55790E+01  
RME1(4, 11, 8) = 8.85540E+00  
RME1(4, 12, 8) = 5.96740E+00  
RME1(4, 13, 8) = 4.41330E+00  
RME1(4, 14, 8) = 3.45990E+00  
RME1(4, 15, 8) = 2.82250E+00  
RME1(4, 5, 9) = 2.08880E-01  
RME1(4, 6, 9) = 7.21280E-01  
RME1(4, 7, 9) = 2.34700E+00  
RME1(4, 8, 9) = 1.06040E+01  
RME1(4, 9, 9) = -1.08840E+02  
RME1(4, 10, 9) = 4.88210E+01  
RME1(4, 11, 9) = 1.84910E+01  
RME1(4, 12, 9) = 1.05290E+01  
RME1(4, 13, 9) = 7.10230E+00  
RME1(4, 14, 9) = 5.25620E+00  
RME1(4, 15, 9) = 4.12280E+00  
RME1(4, 5, 10) = 1.48690E-01  
RME1(4, 6, 10) = 4.60710E-01

RME1(4, 7,10) = 1.23320E+00  
 RME1(4, 8,10) = 3.53600E+00  
 RME1(4, 9,10) = 1.47330E+01  
 RME1(4,10,10) = -1.37480E+02  
 RME1(4,11,10) = 5.70480E+01  
 RME1(4,12,10) = 2.16050E+01  
 RME1(4,13,10) = 1.23010E+01  
 RME1(4,14,10) = 8.29600E+00  
 RME1(4,15,10) = 6.13850E+00  
 RME1(4, 5,11) = 1.13460E-01  
 RME1(4, 6,11) = 3.28540E-01  
 RME1(4, 7,11) = 7.89550E-01  
 RME1(4, 8,11) = 1.86530E+00  
 RME1(4, 9,11) = 4.94920E+00  
 RME1(4,10,11) = 1.95060E+01  
 RME1(4,11,11) = -1.69070E+02  
 RME1(4,12,11) = 6.59310E+01  
 RME1(4,13,11) = 2.49300E+01  
 RME1(4,14,11) = 1.41770E+01  
 RME1(4,15,11) = 9.55330E+00  
 RME1(4, 5,12) = 9.07080E-02  
 RME1(4, 6,12) = 2.50890E-01  
 RME1(4, 7,12) = 5.63460E-01  
 RME1(4, 8,12) = 1.19580E+00  
 RME1(4, 9,12) = 2.61750E+00  
 RME1(4,10,12) = 6.58690E+00  
 RME1(4,11,12) = 2.49240E+01  
 RME1(4,12,12) = -2.03650E+02  
 RME1(4,13,12) = 7.54690E+01  
 RME1(4,14,12) = 2.84690E+01  
 RME1(4,15,12) = 1.61630E+01  
 RME1(4, 5,13) = 7.49670E-02  
 RME1(4, 6,13) = 2.00660E-01  
 RME1(4, 7,13) = 4.30330E-01  
 RME1(4, 8,13) = 8.53470E-01  
 RME1(4, 9,13) = 1.67900E+00  
 RME1(4,10,13) = 3.48950E+00  
 RME1(4,11,13) = 8.44910E+00  
 RME1(4,12,13) = 3.09880E+01  
 RME1(4,13,13) = -2.41200E+02  
 RME1(4,14,13) = 8.56610E+01  
 RME1(4,15,13) = 3.22250E+01  
 RME1(4, 5,14) = 6.35040E-02  
 RME1(4, 6,14) = 1.65880E-01  
 RME1(4, 7,14) = 3.44130E-01  
 RME1(4, 8,14) = 6.51630E-01  
 RME1(4, 9,14) = 1.19820E+00  
 RME1(4,10,14) = 2.23890E+00  
 RME1(4,11,14) = 4.48110E+00  
 RME1(4,12,14) = 1.05360E+01  
 RME1(4,13,14) = 3.77000E+01  
 RME1(4,14,14) = -2.81740E+02  
 RME1(4,15,14) = 9.65060E+01  
 RME1(4, 5,15) = 5.48260E-02  
 RME1(4, 6,15) = 1.40550E-01  
 RME1(4, 7,15) = 2.84430E-01  
 RME1(4, 8,15) = 5.20870E-01  
 RME1(4, 9,15) = 9.14350E-01  
 RME1(4,10,15) = 1.59710E+00  
 RME1(4,11,15) = 2.87510E+00  
 RME1(4,12,15) = 5.59200E+00  
 RME1(4,13,15) = 1.28470E+01  
 RME1(4,14,15) = 4.50600E+01  
 RME1(4,15,15) = -3.25280E+02

C H-G TRANSITION:  
 RME1(5, 6, 5) = 2.72140E+01

RME1(5, 7, 5) = 7.45730E+00  
 RME1(5, 8, 5) = 3.64220E+00  
 RME1(5, 9, 5) = 2.24990E+00  
 RME1(5, 10, 5) = 1.57310E+00  
 RME1(5, 11, 5) = 1.18630E+00  
 RME1(5, 12, 5) = 9.40500E-01  
 RME1(5, 13, 5) = 7.72520E-01  
 RME1(5, 14, 5) = 6.51350E-01  
 RME1(5, 15, 5) = 5.60300E-01  
 RME1(5, 6, 6) = -2.98490E+01  
 RME1(5, 7, 6) = 3.30640E+01  
 RME1(5, 8, 6) = 1.08660E+01  
 RME1(5, 9, 6) = 5.70590E+00  
 RME1(5, 10, 6) = 3.65590E+00  
 RME1(5, 11, 6) = 2.61200E+00  
 RME1(5, 12, 6) = 1.99720E+00  
 RME1(5, 13, 6) = 1.59880E+00  
 RME1(5, 14, 6) = 1.32250E+00  
 RME1(5, 15, 6) = 1.12110E+00  
 RME1(5, 6, 7) = 2.37410E+00  
 RME1(5, 7, 7) = -5.14380E+01  
 RME1(5, 8, 7) = 3.96420E+01  
 RME1(5, 9, 7) = 1.39590E+01  
 RME1(5, 10, 7) = 7.58760E+00  
 RME1(5, 11, 7) = 4.95900E+00  
 RME1(5, 12, 7) = 3.58760E+00  
 RME1(5, 13, 7) = 2.76640E+00  
 RME1(5, 14, 7) = 2.22800E+00  
 RME1(5, 15, 7) = 1.85140E+00  
 RME1(5, 6, 8) = 6.99500E-01  
 RME1(5, 7, 8) = 4.86810E+00  
 RME1(5, 8, 8) = -7.49390E+01  
 RME1(5, 9, 8) = 4.69160E+01  
 RME1(5, 10, 8) = 1.70590E+01  
 RME1(5, 11, 8) = 9.44250E+00  
 RME1(5, 12, 8) = 6.24060E+00  
 RME1(5, 13, 8) = 4.54820E+00  
 RME1(5, 14, 8) = 3.52540E+00  
 RME1(5, 15, 8) = 2.85010E+00  
 RME1(5, 6, 9) = 3.44840E-01  
 RME1(5, 7, 9) = 1.49470E+00  
 RME1(5, 8, 9) = 7.96580E+00  
 RME1(5, 9, 9) = -1.01020E+02  
 RME1(5, 10, 9) = 5.48700E+01  
 RME1(5, 11, 9) = 2.02750E+01  
 RME1(5, 12, 9) = 1.13330E+01  
 RME1(5, 13, 9) = 7.53780E+00  
 RME1(5, 14, 9) = 5.51750E+00  
 RME1(5, 15, 9) = 4.29100E+00  
 RME1(5, 6, 10) = 2.12130E-01  
 RME1(5, 7, 10) = 7.50780E-01  
 RME1(5, 8, 10) = 2.50910E+00  
 RME1(5, 9, 10) = 1.16910E+01  
 RME1(5, 10, 10) = -1.29900E+02  
 RME1(5, 11, 10) = 6.34950E+01  
 RME1(5, 12, 10) = 2.36530E+01  
 RME1(5, 13, 10) = 1.32910E+01  
 RME1(5, 14, 10) = 8.87100E+00  
 RME1(5, 15, 10) = 6.50930E+00  
 RME1(5, 6, 11) = 1.47360E-01  
 RME1(5, 7, 11) = 4.66180E-01  
 RME1(5, 8, 11) = 1.27560E+00  
 RME1(5, 9, 11) = 3.74640E+00  
 RME1(5, 10, 11) = 1.60520E+01  
 RME1(5, 11, 11) = -1.61660E+02  
 RME1(5, 12, 11) = 7.27850E+01  
 RME1(5, 13, 11) = 2.72170E+01

RME1(5, 14, 11) = 1.53330E+01  
 RME1(5, 15, 11) = 1.02520E+01  
 RME1(5, 6, 12) = 1.10410E-01  
 RME1(5, 7, 12) = 3.25440E-01  
 RME1(5, 8, 12) = 7.96860E-01  
 RME1(5, 9, 12) = 1.92030E+00  
 RME1(5, 10, 12) = 5.20740E+00  
 RME1(5, 11, 12) = 2.10520E+01  
 RME1(5, 12, 12) = -1.96350E+02  
 RME1(5, 13, 12) = 8.27370E+01  
 RME1(5, 14, 12) = 3.09790E+01  
 RME1(5, 15, 12) = 1.74700E+01  
 RME1(5, 6, 13) = 8.70370E-02  
 RME1(5, 7, 13) = 2.44490E-01  
 RME1(5, 8, 13) = 5.58050E-01  
 RME1(5, 9, 13) = 1.20460E+00  
 RME1(5, 10, 13) = 2.68490E+00  
 RME1(5, 11, 13) = 6.89240E+00  
 RME1(5, 12, 13) = 2.66960E+01  
 RME1(5, 13, 13) = -2.34000E+02  
 RME1(5, 14, 13) = 9.33470E+01  
 RME1(5, 15, 13) = 3.49480E+01  
 RME1(5, 6, 14) = 7.11510E-02  
 RME1(5, 7, 14) = 1.93060E-01  
 RME1(5, 8, 14) = 4.19960E-01  
 RME1(5, 9, 14) = 8.45380E-01  
 RME1(5, 10, 14) = 1.68920E+00  
 RME1(5, 11, 14) = 3.56930E+00  
 RME1(5, 12, 14) = 8.80160E+00  
 RME1(5, 13, 14) = 3.29840E+01  
 RME1(5, 14, 14) = -2.74610E+02  
 RME1(5, 15, 14) = 1.04610E+02  
 RME1(5, 6, 15) = 5.97550E-02  
 RME1(5, 7, 15) = 1.57980E-01  
 RME1(5, 8, 15) = 3.31920E-01  
 RME1(5, 9, 15) = 6.36860E-01  
 RME1(5, 10, 15) = 1.18710E+00  
 RME1(5, 11, 15) = 2.25030E+00  
 RME1(5, 12, 15) = 4.57310E+00  
 RME1(5, 13, 15) = 1.09350E+01  
 RME1(5, 14, 15) = 3.99170E+01  
 RME1(5, 15, 15) = -3.18190E+02

C I-H TRANSITION:

RME1(6, 7, 6) = 3.87110E+01  
 RME1(6, 8, 6) = 9.90570E+00  
 RME1(6, 9, 6) = 4.61860E+00  
 RME1(6, 10, 6) = 2.76000E+00  
 RME1(6, 11, 6) = 2.60000E+00  
 RME1(6, 7, 7) = -3.78590E+01  
 RME1(6, 8, 7) = 4.55660E+01  
 RME1(6, 9, 7) = 1.42540E+01  
 RME1(6, 10, 7) = 7.22410E+00  
 RME1(6, 11, 7) = 4.50280E+00  
 RME1(6, 7, 8) = 2.72970E+00  
 RME1(6, 8, 8) = -6.34980E+01  
 RME1(6, 9, 8) = 5.31590E+01  
 RME1(6, 10, 8) = 1.80360E+01  
 RME1(6, 11, 8) = 9.53800E+00  
 RME1(6, 12, 8) = -6.09830E+00  
 RME1(6, 7, 9) = 7.57200E-01  
 RME1(6, 8, 9) = 5.47990E+00  
 RME1(6, 9, 9) = -9.05600E+01  
 RME1(6, 10, 9) = 6.14650E+01  
 RME1(6, 11, 9) = 2.17300E+01  
 RME1(6, 12, 9) = 1.17660E+01  
 RME1(6, 7, 10) = 3.55900E-01

```

RME1(6, 8,10) = 1.60020E+00
RME1(6, 9,10) = 8.82050E+01
RME1(6,10,10) = -1.20000E+02
RME1(6,11,10) = 7.04630E+01
RME1(6,12,10) = 2.54780E+01
RME1(6, 7,11) = 2.12000E-01
RME1(6, 8,11) = 7.74700E-01
RME1(6, 9,11) = 2.66250E+00
RME1(6,10,11) = 1.27800E+01
RME1(6,11,11) = -1.52120E+02
RME1(6,12,11) = 8.01380E+01
RME1(6, 8,12) = 4.69900E-01
RME1(6, 9,12) = 1.31310E+00
RME1(6,10,12) = 3.94800E+00
RME1(6,11,12) = 1.73870E+01
RME1(6,12,12) = -1.87060E+02

```

C K-I TRANSITION:

```

RME1(7, 8, 7) = 5.20000E+01
RME1(7,11, 7) = 5.03000E+00
RME1(7, 8, 8) = -4.64760E+01
RME1(7,11, 8) = 1.03000E+01
RME1(7, 8,11) = 6.00000E-01
RME1(7,11,11) = -1.40010E+02

```

RETURN  
END

```

SUBROUTINE RADMATX2
IMPLICIT REAL*8 (A-H,O-Z)
COMMON/RADIAL/RME2
DIMENSION RME2(10,20,20)

```

C THE DATA FORMAT IS RME2(L1,PN1,PN2); L1-L2=+1

C P-S TRANSITION:

```

RME2(1, 3, 3) = -5.24460E+00
RME2(1, 4, 3) = -1.79310E-01
RME2(1, 5, 3) = -1.60130E-02
RME2(1, 6, 3) = 8.80620E-03
RME2(1, 7, 3) = 1.34420E-02
RME2(1, 8, 3) = 1.35570E-02
RME2(1, 9, 3) = 1.25430E-02
RME2(1,10, 3) = 1.13150E-02
RME2(1,11, 3) = 1.01430E-02
RME2(1,12, 3) = 9.09840E-03
RME2(1,13, 3) = 8.18920E-03
RME2(1,14, 3) = 7.40360E-03
RME2(1,15, 3) = 6.72510E-03
RME2(1, 3, 4) = 4.25890E+00
RME2(1, 4, 4) = -1.18480E+01
RME2(1, 5, 4) = -7.11340E-01
RME2(1, 6, 4) = -1.97560E-01
RME2(1, 7, 4) = -8.34570E-02
RME2(1, 8, 4) = -4.31970E-02
RME2(1, 9, 4) = -2.52570E-02
RME2(1,10, 4) = -1.60330E-02
RME2(1,11, 4) = -1.08030E-02
RME2(1,12, 4) = -7.61800E-03
RME2(1,13, 4) = -5.56940E-03
RME2(1,14, 4) = -4.19310E-03
RME2(1,15, 4) = -3.23510E-03
RME2(1, 3, 5) = 1.04630E+00
RME2(1, 4, 5) = 9.78740E+00
RME2(1, 5, 5) = -2.08420E+01
RME2(1, 6, 5) = -1.48290E+00
RME2(1, 7, 5) = -4.77560E-01

```

RME2(1, 8, 5) = -2.32710E-01  
RME2(1, 9, 5) = -1.38370E-01  
RME2(1, 10, 5) = -9.25230E-02  
RME2(1, 11, 5) = -6.68360E-02  
RME2(1, 12, 5) = -5.09760E-02  
RME2(1, 13, 5) = -4.04690E-02  
RME2(1, 14, 5) = -3.31250E-02  
RME2(1, 15, 5) = -2.77710E-02  
RME2(1, 3, 6) = 5.53900E-01  
RME2(1, 4, 6) = 2.19490E+00  
RME2(1, 5, 6) = 1.72720E+01  
RME2(1, 6, 6) = -3.22470E+01  
RME2(1, 7, 6) = -2.48100E+00  
RME2(1, 8, 6) = -8.46130E-01  
RME2(1, 9, 6) = -4.31750E-01  
RME2(1, 10, 6) = -2.66600E-01  
RME2(1, 11, 6) = -1.83910E-01  
RME2(1, 12, 6) = -1.36340E-01  
RME2(1, 13, 6) = -1.06260E-01  
RME2(1, 14, 6) = -8.59080E-02  
RME2(1, 15, 6) = -7.14120E-02  
RME2(1, 3, 7) = 3.65410E-01  
RME2(1, 4, 7) = 1.12670E+00  
RME2(1, 5, 7) = 3.67390E+00  
RME2(1, 6, 7) = 2.67310E+01  
RME2(1, 7, 7) = -4.60680E+01  
RME2(1, 8, 7) = -3.70020E+00  
RME2(1, 9, 7) = -1.29890E+00  
RME2(1, 10, 7) = -6.77160E-01  
RME2(1, 11, 7) = -4.25110E-01  
RME2(1, 12, 7) = -2.97110E-01  
RME2(1, 13, 7) = -2.22570E-01  
RME2(1, 14, 7) = -1.74960E-01  
RME2(1, 15, 7) = -1.42460E-01  
RME2(1, 3, 8) = 2.67540E-01  
RME2(1, 4, 8) = 7.34010E-01  
RME2(1, 5, 8) = 1.84370E+00  
RME2(1, 6, 8) = 5.48660E+00  
RME2(1, 7, 8) = 3.81720E+01  
RME2(1, 8, 8) = -6.23060E+01  
RME2(1, 9, 8) = -5.13950E+00  
RME2(1, 10, 8) = -1.83450E+00  
RME2(1, 11, 8) = -9.67720E-01  
RME2(1, 12, 8) = -6.12820E-01  
RME2(1, 13, 8) = -4.31170E-01  
RME2(1, 14, 8) = -3.24690E-01  
RME2(1, 15, 8) = -2.56310E-01  
RME2(1, 3, 9) = 2.08180E-01  
RME2(1, 4, 9) = 5.34820E-01  
RME2(1, 5, 9) = 1.18730E+00  
RME2(1, 6, 9) = 2.70510E+00  
RME2(1, 7, 9) = 7.63340E+00  
RME2(1, 8, 9) = 5.15950E+01  
RME2(1, 9, 9) = -8.09630E+01  
RME2(1, 10, 9) = -6.79790E+00  
RME2(1, 11, 9) = -2.45200E+00  
RME2(1, 12, 9) = -1.30260E+00  
RME2(1, 13, 9) = -8.28960E-01  
RME2(1, 14, 9) = -5.85380E-01  
RME2(1, 15, 9) = -4.42060E-01  
RME2(1, 3, 10) = 1.68610E-01  
RME2(1, 4, 10) = 4.15690E-01  
RME2(1, 5, 10) = 8.59870E-01  
RME2(1, 6, 10) = 1.72420E+00  
RME2(1, 7, 10) = 3.71050E+00  
RME2(1, 8, 10) = 1.01140E+01  
RME2(1, 9, 10) = 6.70020E+01

RME2(1,10,10) = -1.02040E+02  
RME2(1,11,10) = -8.67500E+00  
RME2(1,12,10) = -3.15090E+00  
RME2(1,13,10) = -1.68120E+00  
RME2(1,14,10) = -1.07310E+00  
RME2(1,15,10) = -7.59340E-01  
RME2(1, 3,11) = 1.40520E-01  
RME2(1, 4,11) = 3.36950E-01  
RME2(1, 5,11) = 6.66340E-01  
RME2(1, 6,11) = 1.24110E+00  
RME2(1, 7,11) = 2.34420E+00  
RME2(1, 8,11) = 4.85990E+00  
RME2(1, 9,11) = 1.29300E+01  
RME2(1,10,11) = 8.43930E+01  
RME2(1,11,11) = -1.25530E+02  
RME2(1,12,11) = -1.07700E+01  
RME2(1,13,11) = -3.93070E+00  
RME2(1,14,11) = -2.10320E+00  
RME2(1,15,11) = -1.34480E+00  
RME2(1, 3,12) = 1.19640E-01  
RME2(1, 4,12) = 2.81290E-01  
RME2(1, 5,12) = 5.39460E-01  
RME2(1, 6,12) = 9.58220E-01  
RME2(1, 7,12) = 1.67760E+00  
RME2(1, 8,12) = 3.04680E+00  
RME2(1, 9,12) = 6.15290E+00  
RME2(1,10,12) = 1.60790E+01  
RME2(1,11,12) = 1.03770E+02  
RME2(1,12,12) = -1.51450E+02  
RME2(1,13,12) = -1.30840E+01  
RME2(1,14,12) = -4.79150E+00  
RME2(1,15,12) = -2.56850E+00  
RME2(1, 3,13) = 1.03580E-01  
RME2(1, 4,13) = 2.40030E-01  
RME2(1, 5,13) = 4.50290E-01  
RME2(1, 6,13) = 7.74100E-01  
RME2(1, 7,13) = 1.29030E+00  
RME2(1, 8,13) = 2.16880E+00  
RME2(1, 9,13) = 3.83170E+00  
RME2(1,10,13) = 7.58960E+00  
RME2(1,11,13) = 1.95630E+01  
RME2(1,12,13) = 1.25130E+02  
RME2(1,13,13) = -1.79780E+02  
RME2(1,14,13) = -1.56160E+01  
RME2(1,15,13) = -5.73290E+00  
RME2(1, 3,14) = 9.08890E-02  
RME2(1, 4,14) = 2.08310E-01  
RME2(1, 5,14) = 3.84420E-01  
RME2(1, 6,14) = 6.45420E-01  
RME2(1, 7,14) = 1.03970E+00  
RME2(1, 8,14) = 1.66190E+00  
RME2(1, 9,14) = 2.71450E+00  
RME2(1,10,14) = 4.69900E+00  
RME2(1,11,14) = 9.16990E+00  
RME2(1,12,14) = 2.33810E+01  
RME2(1,13,14) = 1.48480E+02  
RME2(1,14,14) = -2.10530E+02  
RME2(1,15,14) = -1.83650E+01  
RME2(1, 3,15) = 8.06370E-02  
RME2(1, 4,15) = 1.83240E-01  
RME2(1, 5,15) = 3.33920E-01  
RME2(1, 6,15) = 5.50760E-01  
RME2(1, 7,15) = 8.65480E-01  
RME2(1, 8,15) = 1.33570E+00  
RME2(1, 9,15) = 2.07270E+00  
RME2(1,10,15) = 3.31450E+00  
RME2(1,11,15) = 5.64840E+00

RME2(1,12,15) = 1.08940E+01  
 RME2(1,13,15) = 2.75330E+01  
 RME2(1,14,15) = 1.73810E+02  
 RME2(1,15,15) = -2.43700E+02

C D-P TRANSITION:

RME2(2, 3, 3) = -6.67490E+00  
 RME2(2, 4, 3) = -1.50350E+00  
 RME2(2, 5, 3) = -7.13760E-01  
 RME2(2, 6, 3) = -4.39720E-01  
 RME2(2, 7, 3) = -3.08170E-01  
 RME2(2, 8, 3) = -2.32920E-01  
 RME2(2, 9, 3) = -1.84880E-01  
 RME2(2, 10, 3) = -1.51870E-01  
 RME2(2, 11, 3) = -1.27930E-01  
 RME2(2, 12, 3) = -1.09870E-01  
 RME2(2, 13, 3) = -9.58090E-02  
 RME2(2, 14, 3) = -8.45900E-02  
 RME2(2, 15, 3) = -7.54550E-02  
 RME2(2, 3, 4) = 8.83250E+00  
 RME2(2, 4, 4) = -1.23150E+01  
 RME2(2, 5, 4) = -3.09460E+00  
 RME2(2, 6, 4) = -1.54110E+00  
 RME2(2, 7, 4) = -9.74390E-01  
 RME2(2, 8, 4) = -6.94260E-01  
 RME2(2, 9, 4) = -5.30890E-01  
 RME2(2, 10, 4) = -4.25190E-01  
 RME2(2, 11, 4) = -3.51780E-01  
 RME2(2, 12, 4) = -2.98110E-01  
 RME2(2, 13, 4) = -2.57340E-01  
 RME2(2, 14, 4) = -2.25420E-01  
 RME2(2, 15, 4) = -1.99810E-01  
 RME2(2, 3, 5) = 3.74890E-01  
 RME2(2, 4, 5) = 1.84220E+01  
 RME2(2, 5, 5) = -1.93880E+01  
 RME2(2, 6, 5) = -5.00390E+00  
 RME2(2, 7, 5) = -2.52640E+00  
 RME2(2, 8, 5) = -1.60990E+00  
 RME2(2, 9, 5) = -1.15300E+00  
 RME2(2, 10, 5) = -8.85250E-01  
 RME2(2, 11, 5) = -7.11370E-01  
 RME2(2, 12, 5) = -5.90290E-01  
 RME2(2, 13, 5) = -5.01590E-01  
 RME2(2, 14, 5) = -4.34060E-01  
 RME2(2, 15, 5) = -3.81090E-01  
 RME2(2, 3, 6) = 1.70570E-01  
 RME2(2, 4, 6) = 6.71120E-01  
 RME2(2, 5, 6) = 3.06760E+01  
 RME2(2, 6, 6) = -2.79070E+01  
 RME2(2, 7, 6) = -7.25040E+00  
 RME2(2, 8, 6) = -3.67240E+00  
 RME2(2, 9, 6) = -2.34390E+00  
 RME2(2, 10, 6) = -1.68070E+00  
 RME2(2, 11, 6) = -1.29160E+00  
 RME2(2, 12, 6) = -1.03900E+00  
 RME2(2, 13, 6) = -8.63070E-01  
 RME2(2, 14, 6) = -7.34210E-01  
 RME2(2, 15, 6) = -6.36110E-01  
 RME2(2, 3, 7) = 1.08290E-01  
 RME2(2, 4, 7) = 2.88660E-01  
 RME2(2, 5, 7) = 9.46780E-01  
 RME2(2, 6, 7) = 4.56730E+01  
 RME2(2, 7, 7) = -3.78740E+01  
 RME2(2, 8, 7) = -9.84080E+00  
 RME2(2, 9, 7) = -4.98080E+00  
 RME2(2, 10, 7) = -3.17610E+00  
 RME2(2, 11, 7) = -2.27570E+00

RME2(2,12, 7) = -1.74820E+00  
RME2(2,13, 7) = -1.40600E+00  
RME2(2,14, 7) = -1.16810E+00  
RME2(2,15, 7) = -9.93930E-01  
RME2(2, 3, 8) = 7.81850E-02  
RME2(2, 4, 8) = 1.80720E-01  
RME2(2, 5, 8) = 3.82470E-01  
RME2(2, 6, 8) = 1.19770E+00  
RME2(2, 7, 8) = 6.34350E+01  
RME2(2, 8, 8) = -4.92930E+01  
RME2(2, 9, 8) = -1.27780E+01  
RME2(2,10, 8) = -6.45260E+00  
RME2(2,11, 8) = -4.10640E+00  
RME2(2,12, 8) = -2.93770E+00  
RME2(2,13, 8) = -2.25410E+00  
RME2(2,14, 8) = -1.81160E+00  
RME2(2,15, 8) = -1.50420E+00  
RME2(2, 3, 9) = 6.04820E-02  
RME2(2, 4, 9) = 1.30120E-01  
RME2(2, 5, 9) = 2.35240E-01  
RME2(2, 6, 9) = 4.50580E-01  
RME2(2, 7, 9) = 1.42150E+00  
RME2(2, 8, 9) = 8.39680E+01  
RME2(2, 9, 9) = -6.21630E+01  
RME2(2,10, 9) = -1.60640E+01  
RME2(2,11, 9) = -8.08850E+00  
RME2(2,12, 9) = -5.13510E+00  
RME2(2,13, 9) = -3.66650E+00  
RME2(2,14, 9) = -2.80910E+00  
RME2(2,15, 9) = -2.25510E+00  
RME2(2, 3,10) = 4.88670E-02  
RME2(2, 4,10) = 1.00770E-01  
RME2(2, 5,10) = 1.68540E-01  
RME2(2, 6,10) = 2.71170E-01  
RME2(2, 7,10) = 4.92210E-01  
RME2(2, 8,10) = 1.61650E+00  
RME2(2, 9,10) = 1.07280E+02  
RME2(2,10,10) = -7.64840E+01  
RME2(2,11,10) = -1.96990E+01  
RME2(2,12,10) = -9.88900E+00  
RME2(2,13,10) = -6.26210E+00  
RME2(2,14,10) = -4.46200E+00  
RME2(2,15,10) = -3.41300E+00  
RME2(2, 3,11) = 4.06920E-02  
RME2(2, 4,11) = 8.16280E-02  
RME2(2, 5,11) = 1.30450E-01  
RME2(2, 6,11) = 1.92990E-01  
RME2(2, 7,11) = 2.88240E-01  
RME2(2, 8,11) = 5.06950E-01  
RME2(2, 9,11) = 1.78180E+00  
RME2(2,10,11) = 1.33360E+02  
RME2(2,11,11) = -9.22580E+01  
RME2(2,12,11) = -2.36840E+01  
RME2(2,13,11) = -1.18540E+01  
RME2(2,14,11) = -7.48770E+00  
RME2(2,15,11) = -5.32410E+00  
RME2(2, 3,12) = 3.46460E-02  
RME2(2, 4,12) = 6.81820E-02  
RME2(2, 5,12) = 1.05800E-01  
RME2(2, 6,12) = 1.49170E-01  
RME2(2, 7,12) = 2.03410E-01  
RME2(2, 8,12) = 2.86380E-01  
RME2(2, 9,12) = 4.94570E-01  
RME2(2,10,12) = 1.91690E+00  
RME2(2,11,12) = 1.62220E+02  
RME2(2,12,12) = -1.09480E+02  
RME2(2,13,12) = -2.80190E+01

RME2(2,14,12) = -1.39850E+01  
 RME2(2,15,12) = -8.81190E+00  
 RME2(2, 3,13) = 3.00080E-02  
 RME2(2, 4,13) = 5.82390E-02  
 RME2(2, 5,13) = 8.85420E-02  
 RME2(2, 6,13) = 1.21070E-01  
 RME2(2, 7,13) = 1.56940E-01  
 RME2(2, 8,13) = 1.99850E-01  
 RME2(2, 9,13) = 2.65580E-01  
 RME2(2,10,13) = 4.54940E-01  
 RME2(2,11,13) = 2.02130E+00  
 RME2(2,12,13) = 1.93860E+02  
 RME2(2,13,13) = -1.28160E+02  
 RME2(2,14,13) = -3.27050E+01  
 RME2(2,15,13) = -1.62800E+01  
 RME2(2, 3,14) = 2.63480E-02  
 RME2(2, 4,14) = 5.06040E-02  
 RME2(2, 5,14) = 7.58010E-02  
 RME2(2, 6,14) = 1.01480E-01  
 RME2(2, 7,14) = 1.27460E-01  
 RME2(2, 8,14) = 1.53850E-01  
 RME2(2, 9,14) = 1.82390E-01  
 RME2(2,10,14) = 2.25870E-01  
 RME2(2,11,14) = 3.87980E-01  
 RME2(2,12,14) = 2.09480E+00  
 RME2(2,13,14) = 2.28270E+02  
 RME2(2,14,14) = -1.48290E+02  
 RME2(2,15,14) = -3.77420E+01  
 RME2(2, 3,15) = 2.33940E-02  
 RME2(2, 4,15) = 4.45690E-02  
 RME2(2, 5,15) = 6.60190E-02  
 RME2(2, 6,15) = 8.70490E-02  
 RME2(2, 7,15) = 1.07030E-01  
 RME2(2, 8,15) = 1.25090E-01  
 RME2(2, 9,15) = 1.40020E-01  
 RME2(2,10,15) = 1.51100E-01  
 RME2(2,11,15) = 1.67250E-01  
 RME2(2,12,15) = 2.93620E-01  
 RME2(2,13,15) = 2.13700E+00  
 RME2(2,14,15) = 2.65460E+02  
 RME2(2,15,15) = -1.69870E+02

C F-D TRANSITION:

RME2(3, 4, 3) = 1.00470E+01  
 RME2(3, 5, 3) = 3.32660E+00  
 RME2(3, 6, 3) = 1.81760E+00  
 RME2(3, 7, 3) = 1.20590E+00  
 RME2(3, 8, 3) = 8.84760E-01  
 RME2(3, 9, 3) = 6.89960E-01  
 RME2(3,10, 3) = 5.60120E-01  
 RME2(3,11, 3) = 4.68080E-01  
 RME2(3,12, 3) = 3.99700E-01  
 RME2(3,13, 3) = 3.47070E-01  
 RME2(3,14, 3) = 3.05430E-01  
 RME2(3,15, 3) = 2.71760E-01  
 RME2(3, 4, 4) = -1.59620E+01  
 RME2(3, 5, 4) = 1.35960E+01  
 RME2(3, 6, 4) = 5.12770E+00  
 RME2(3, 7, 4) = 2.92940E+00  
 RME2(3, 8, 4) = 1.98590E+00  
 RME2(3, 9, 4) = 1.47600E+00  
 RME2(3,10, 4) = 1.16110E+00  
 RME2(3,11, 4) = 9.49110E-01  
 RME2(3,12, 4) = 7.97480E-01  
 RME2(3,13, 4) = 6.84100E-01  
 RME2(3,14, 4) = 5.96350E-01  
 RME2(3,15, 4) = 5.26690E-01

RME2(3, 4, 5) = 1.86750E+00  
RME2(3, 5, 5) = -3.01440E+01  
RME2(3, 6, 5) = 1.77680E+01  
RME2(3, 7, 5) = 6.95340E+00  
RME2(3, 8, 5) = 4.06320E+00  
RME2(3, 9, 5) = 2.76020E+00  
RME2(3, 10, 5) = 2.06310E+00  
RME2(3, 11, 5) = 1.62990E+00  
RME2(3, 12, 5) = 1.33690E+00  
RME2(3, 13, 5) = 1.12660E+00  
RME2(3, 14, 5) = 9.68940E-01  
RME2(3, 15, 5) = 8.46710E-01  
RME2(3, 4, 6) = 6.31830E-01  
RME2(3, 5, 6) = 4.09330E+00  
RME2(3, 6, 6) = -4.69590E+01  
RME2(3, 7, 6) = 2.25510E+01  
RME2(3, 8, 6) = 8.92190E+00  
RME2(3, 9, 6) = 5.20480E+00  
RME2(3, 10, 6) = 3.56960E+00  
RME2(3, 11, 6) = 2.67360E+00  
RME2(3, 12, 6) = 2.11560E+00  
RME2(3, 13, 6) = 1.73790E+00  
RME2(3, 14, 6) = 1.46670E+00  
RME2(3, 15, 6) = 1.26320E+00  
RME2(3, 4, 7) = 3.43270E-01  
RME2(3, 5, 7) = 1.39640E+00  
RME2(3, 6, 7) = 7.00710E+00  
RME2(3, 7, 7) = -6.66460E+01  
RME2(3, 8, 7) = 2.79380E+01  
RME2(3, 9, 7) = 1.10680E+01  
RME2(3, 10, 7) = 6.45870E+00  
RME2(3, 11, 7) = 4.42980E+00  
RME2(3, 12, 7) = 3.31820E+00  
RME2(3, 13, 7) = 2.62630E+00  
RME2(3, 14, 7) = 2.15820E+00  
RME2(3, 15, 7) = 1.82220E+00  
RME2(3, 4, 8) = 2.26100E-01  
RME2(3, 5, 8) = 7.58660E-01  
RME2(3, 6, 8) = 2.39860E+00  
RME2(3, 7, 8) = 1.06220E+01  
RME2(3, 8, 8) = -8.92730E+01  
RME2(3, 9, 8) = 3.39250E+01  
RME2(3, 10, 8) = 1.34070E+01  
RME2(3, 11, 8) = 7.80860E+00  
RME2(3, 12, 8) = 5.34830E+00  
RME2(3, 13, 8) = 4.00240E+00  
RME2(3, 14, 8) = 3.16600E+00  
RME2(3, 15, 8) = 2.60090E+00  
RME2(3, 4, 9) = 1.64990E-01  
RME2(3, 5, 9) = 4.98900E-01  
RME2(3, 6, 9) = 1.30170E+00  
RME2(3, 7, 9) = 3.64100E+00  
RME2(3, 8, 9) = 1.49420E+01  
RME2(3, 9, 9) = -1.14870E+02  
RME2(3, 10, 9) = 4.05100E+01  
RME2(3, 11, 9) = 1.59450E+01  
RME2(3, 12, 9) = 9.26000E+00  
RME2(3, 13, 9) = 6.32920E+00  
RME2(3, 14, 9) = 4.72930E+00  
RME2(3, 15, 9) = 3.73700E+00  
RME2(3, 4, 10) = 1.28170E-01  
RME2(3, 5, 10) = 3.63470E-01  
RME2(3, 6, 10) = 8.54190E-01  
RME2(3, 7, 10) = 1.97270E+00  
RME2(3, 8, 10) = 5.12350E+00  
RME2(3, 9, 10) = 1.99690E+01  
RME2(3, 10, 10) = -1.43440E+02

RME2(3,11,10) = 4.76890E+01  
 RME2(3,12,10) = 1.86850E+01  
 RME2(3,13,10) = 1.08160E+01  
 RME2(3,14,10) = 7.37490E+00  
 RME2(3,15,10) = 5.50090E+00  
 RME2(3, 4,11) = 1.03830E-01  
 RME2(3, 5,11) = 2.82060E-01  
 RME2(3, 6,11) = 6.21120E-01  
 RME2(3, 7,11) = 1.29170E+00  
 RME2(3, 8,11) = 2.77120E+00  
 RME2(3, 9,11) = 6.84600E+00  
 RME2(3,10,11) = 2.57040E+01  
 RME2(3,11,11) = -1.75010E+02  
 RME2(3,12,11) = 5.54640E+01  
 RME2(3,13,11) = 2.16290E+01  
 RME2(3,14,11) = 1.24780E+01  
 RME2(3,15,11) = 8.48710E+00  
 RME2(3, 4,12) = 8.66610E-02  
 RME2(3, 5,12) = 2.28350E-01  
 RME2(3, 6,12) = 4.81260E-01  
 RME2(3, 7,12) = 9.37350E-01  
 RME2(3, 8,12) = 1.81070E+00  
 RME2(3, 9,12) = 3.69650E+00  
 RME2(3,10,12) = 8.80810E+00  
 RME2(3,11,12) = 3.21470E+01  
 RME2(3,12,12) = -2.09560E+02  
 RME2(3,13,12) = 6.38340E+01  
 RME2(3,14,12) = 2.47800E+01  
 RME2(3,15,12) = 1.42490E+01  
 RME2(3, 4,13) = 7.39600E-02  
 RME2(3, 5,13) = 1.90550E-01  
 RME2(3, 6,13) = 3.89200E-01  
 RME2(3, 7,13) = 7.25070E-01  
 RME2(3, 8,13) = 1.31140E+00  
 RME2(3, 9,13) = 2.41050E+00  
 RME2(3,10,13) = 4.74830E+00  
 RME2(3,11,13) = 1.10100E+01  
 RME2(3,12,13) = 3.92980E+01  
 RME2(3,13,13) = -2.47100E+02  
 RME2(3,14,13) = 7.27980E+01  
 RME2(3,15,13) = 2.81370E+01  
 RME2(3, 4,14) = 6.42180E-02  
 RME2(3, 5,14) = 1.62640E-01  
 RME2(3, 6,14) = 3.24540E-01  
 RME2(3, 7,14) = 5.85630E-01  
 RME2(3, 8,14) = 1.01270E+00  
 RME2(3, 9,14) = 1.74250E+00  
 RME2(3,10,14) = 3.09060E+00  
 RME2(3,11,14) = 5.92610E+00  
 RME2(3,12,14) = 1.34500E+01  
 RME2(3,13,14) = 4.71580E+01  
 RME2(3,14,14) = -2.87640E+02  
 RME2(3,15,14) = 8.23550E+01  
 RME2(3, 4,15) = 5.65310E-02  
 RME2(3, 5,15) = 1.41270E-01  
 RME2(3, 6,15) = 2.76900E-01  
 RME2(3, 7,15) = 4.87880E-01  
 RME2(3, 8,15) = 8.16790E-01  
 RME2(3, 9,15) = 1.34340E+00  
 RME2(3,10,15) = 2.23010E+00  
 RME2(3,11,15) = 3.85060E+00  
 RME2(3,12,15) = 7.22970E+00  
 RME2(3,13,15) = 1.61200E+01  
 RME2(3,14,15) = 5.57270E+01  
 RME2(3,15,15) = -3.31180E+02

C G-F TRANSITION:

RME2(4, 5, 4) = 1.77190E+01  
RME2(4, 6, 4) = 5.25110E+00  
RME2(4, 7, 4) = 2.69870E+00  
RME2(4, 8, 4) = 1.72470E+00  
RME2(4, 9, 4) = 1.23530E+00  
RME2(4,10, 4) = 9.47740E-01  
RME2(4,11, 4) = 7.61030E-01  
RME2(4,12, 4) = 6.31090E-01  
RME2(4,13, 4) = 5.35970E-01  
RME2(4,14, 4) = 4.63600E-01  
RME2(4,15, 4) = 4.06880E-01  
RME2(4, 5, 5) = -2.25010E+01  
RME2(4, 6, 5) = 2.25600E+01  
RME2(4, 7, 5) = 7.82840E+00  
RME2(4, 8, 5) = 4.26630E+00  
RME2(4, 9, 5) = 2.80640E+00  
RME2(4,10, 5) = 2.04380E+00  
RME2(4,11, 5) = 1.58520E+00  
RME2(4,12, 5) = 1.28270E+00  
RME2(4,13, 5) = 1.06980E+00  
RME2(4,14, 5) = 9.12770E-01  
RME2(4,15, 5) = 7.92540E-01  
RME2(4, 5, 6) = 2.02010E+00  
RME2(4, 6, 6) = -4.02500E+01  
RME2(4, 7, 6) = 2.81090E+01  
RME2(4, 8, 6) = 1.02930E+01  
RME2(4, 9, 6) = 5.75420E+00  
RME2(4,10, 6) = 3.83890E+00  
RME2(4,11, 6) = 2.82050E+00  
RME2(4,12, 6) = 2.20070E+00  
RME2(4,13, 6) = 1.78870E+00  
RME2(4,14, 6) = 1.49710E+00  
RME2(4,15, 6) = 1.28090E+00  
RME2(4, 5, 7) = 6.36560E-01  
RME2(4, 6, 7) = 4.26300E+00  
RME2(4, 7, 7) = -6.03200E+01  
RME2(4, 8, 7) = 3.43410E+01  
RME2(4, 9, 7) = 1.28540E+01  
RME2(4,10, 7) = 7.27010E+00  
RME2(4,11, 7) = 4.88400E+00  
RME2(4,12, 7) = 3.60460E+00  
RME2(4,13, 7) = 2.82160E+00  
RME2(4,14, 7) = 2.29890E+00  
RME2(4,15, 7) = 1.92800E+00  
RME2(4, 5, 8) = 3.28730E-01  
RME2(4, 6, 8) = 1.38260E+00  
RME2(4, 7, 8) = 7.12070E+00  
RME2(4, 8, 8) = -8.31410E+01  
RME2(4, 9, 8) = 4.12410E+01  
RME2(4,10, 8) = 1.55760E+01  
RME2(4,11, 8) = 8.85480E+00  
RME2(4,12, 8) = 5.96720E+00  
RME2(4,13, 8) = 4.41330E+00  
RME2(4,14, 8) = 3.46000E+00  
RME2(4,15, 8) = 2.82250E+00  
RME2(4, 5, 9) = 2.09060E-01  
RME2(4, 6, 9) = 7.21800E-01  
RME2(4, 7, 9) = 2.34870E+00  
RME2(4, 8, 9) = 1.06120E+01  
RME2(4, 9, 9) = -1.08840E+02  
RME2(4,10, 9) = 4.88040E+01  
RME2(4,11, 9) = 1.84880E+01  
RME2(4,12, 9) = 1.05280E+01  
RME2(4,13, 9) = 7.10180E+00  
RME2(4,14, 9) = 5.25600E+00  
RME2(4,15, 9) = 4.12280E+00  
RME2(4, 5,10) = 1.48810E-01

RME2(4, 6,10) = 4.61060E-01  
RME2(4, 7,10) = 1.23400E+00  
RME2(4, 8,10) = 3.53830E+00  
RME2(4, 9,10) = 1.47440E+01  
RME2(4,10,10) = -1.37480E+02  
RME2(4,11,10) = 5.70270E+01  
RME2(4,12,10) = 2.16010E+01  
RME2(4,13,10) = 1.22990E+01  
RME2(4,14,10) = 8.29530E+00  
RME2(4,15,10) = 6.13820E+00  
RME2(4, 5,11) = 1.13560E-01  
RME2(4, 6,11) = 3.28790E-01  
RME2(4, 7,11) = 7.90120E-01  
RME2(4, 8,11) = 1.86650E+00  
RME2(4, 9,11) = 4.95240E+00  
RME2(4,10,11) = 1.95200E+01  
RME2(4,11,11) = -1.69080E+02  
RME2(4,12,11) = 6.59050E+01  
RME2(4,13,11) = 2.49250E+01  
RME2(4,14,11) = 1.41750E+01  
RME2(4,15,11) = 9.55230E+00  
RME2(4, 5,12) = 9.07910E-02  
RME2(4, 6,12) = 2.51090E-01  
RME2(4, 7,12) = 5.63870E-01  
RME2(4, 8,12) = 1.19660E+00  
RME2(4, 9,12) = 2.61910E+00  
RME2(4,10,12) = 6.59100E+00  
RME2(4,11,12) = 2.49420E+01  
RME2(4,12,12) = -2.03650E+02  
RME2(4,13,12) = 7.54380E+01  
RME2(4,14,12) = 2.84620E+01  
RME2(4,15,12) = 1.61600E+01  
RME2(4, 5,13) = 7.50360E-02  
RME2(4, 6,13) = 2.00830E-01  
RME2(4, 7,13) = 4.30650E-01  
RME2(4, 8,13) = 8.54060E-01  
RME2(4, 9,13) = 1.68010E+00  
RME2(4,10,13) = 3.49160E+00  
RME2(4,11,13) = 8.45430E+00  
RME2(4,12,13) = 3.10100E+01  
RME2(4,13,13) = -2.41210E+02  
RME2(4,14,13) = 8.56250E+01  
RME2(4,15,13) = 3.22170E+01  
RME2(4, 5,14) = 6.35640E-02  
RME2(4, 6,14) = 1.66020E-01  
RME2(4, 7,14) = 3.44390E-01  
RME2(4, 8,14) = 6.52090E-01  
RME2(4, 9,14) = 1.19890E+00  
RME2(4,10,14) = 2.24030E+00  
RME2(4,11,14) = 4.48380E+00  
RME2(4,12,14) = 1.05420E+01  
RME2(4,13,14) = 3.77270E+01  
RME2(4,14,14) = -2.81750E+02  
RME2(4,15,14) = 9.64640E+01  
RME2(4, 5,15) = 5.48790E-02  
RME2(4, 6,15) = 1.40760E-01  
RME2(4, 7,15) = 2.84640E-01  
RME2(4, 8,15) = 5.21240E-01  
RME2(4, 9,15) = 9.14950E-01  
RME2(4,10,15) = 1.59810E+00  
RME2(4,11,15) = 2.87690E+00  
RME2(4,12,15) = 5.59530E+00  
RME2(4,13,15) = 1.28550E+01  
RME2(4,14,15) = 4.50920E+01  
RME2(4,15,15) = -3.25280E+02

C H-G TRANSITION:

RME2(5, 6, 5) = 2.72140E+01  
RME2(5, 7, 5) = 7.45730E+00  
RME2(5, 8, 5) = 3.64320E+00  
RME2(5, 9, 5) = 2.24990E+00  
RME2(5, 10, 5) = 1.57310E+00  
RME2(5, 11, 5) = 1.18630E+00  
RME2(5, 12, 5) = 9.40500E-01  
RME2(5, 13, 5) = 7.72520E-01  
RME2(5, 14, 5) = 6.51350E-01  
RME2(5, 15, 5) = 5.60300E-01  
RME2(5, 6, 6) = -2.98490E+01  
RME2(5, 7, 6) = 3.30640E+01  
RME2(5, 8, 6) = 1.08660E+01  
RME2(5, 9, 6) = 5.70590E+00  
RME2(5, 10, 6) = 3.65590E+00  
RME2(5, 11, 6) = 2.61200E+00  
RME2(5, 12, 6) = 1.99720E+00  
RME2(5, 13, 6) = 1.59880E+00  
RME2(5, 14, 6) = 1.32250E+00  
RME2(5, 15, 6) = 1.12110E+00  
RME2(5, 6, 7) = 2.37410E+00  
RME2(5, 7, 7) = -5.14390E+01  
RME2(5, 8, 7) = 3.96420E+01  
RME2(5, 9, 7) = 1.39590E+01  
RME2(5, 10, 7) = 7.58760E+00  
RME2(5, 11, 7) = 4.95900E+00  
RME2(5, 12, 7) = 3.58760E+00  
RME2(5, 13, 7) = 2.76640E+00  
RME2(5, 14, 7) = 2.22800E+00  
RME2(5, 15, 7) = 1.85140E+00  
RME2(5, 6, 8) = 6.99500E-01  
RME2(5, 7, 8) = 4.86810E+00  
RME2(5, 8, 8) = -7.49390E+01  
RME2(5, 9, 8) = 4.69160E+01  
RME2(5, 10, 8) = 1.70590E+01  
RME2(5, 11, 8) = 9.44250E+00  
RME2(5, 12, 8) = 6.24060E+00  
RME2(5, 13, 8) = 4.54820E+00  
RME2(5, 14, 8) = 3.52540E+00  
RME2(5, 15, 8) = 2.85010E+00  
RME2(5, 6, 9) = 3.44840E-01  
RME2(5, 7, 9) = 1.49470E+00  
RME2(5, 8, 9) = 7.96580E+00  
RME2(5, 9, 9) = -1.01020E+02  
RME2(5, 10, 9) = 5.48700E+01  
RME2(5, 11, 9) = 2.02750E+01  
RME2(5, 12, 9) = 1.13330E+01  
RME2(5, 13, 9) = 7.53780E+00  
RME2(5, 14, 9) = 5.51750E+00  
RME2(5, 15, 9) = 4.29010E+00  
RME2(5, 6, 10) = 2.12140E-01  
RME2(5, 7, 10) = 7.50780E-01  
RME2(5, 8, 10) = 2.50910E+00  
RME2(5, 9, 10) = 1.16910E+01  
RME2(5, 10, 10) = -1.29900E+02  
RME2(5, 11, 10) = 6.34950E+01  
RME2(5, 12, 10) = 2.36530E+01  
RME2(5, 13, 10) = 1.32910E+01  
RME2(5, 14, 10) = 8.87100E+00  
RME2(5, 15, 10) = 6.50930E+00  
RME2(5, 6, 11) = 1.47360E-01  
RME2(5, 7, 11) = 4.66180E-01  
RME2(5, 8, 11) = 1.27560E+00  
RME2(5, 9, 11) = 3.74640E+00  
RME2(5, 10, 11) = 1.60520E+01  
RME2(5, 11, 11) = -1.61660E+02  
RME2(5, 12, 11) = 7.27850E+01

```

RME2(5,13,11) = 2.72170E+01
RME2(5,14,11) = 1.53330E+01
RME2(5,15,11) = 1.02520E+01
RME2(5, 6,12) = 1.10410E-01
RME2(5, 7,12) = 3.25440E-01
RME2(5, 8,12) = 7.96860E-01
RME2(5, 9,12) = 1.92030E+00
RME2(5,10,12) = 5.20740E+00
RME2(5,11,12) = 2.10520E+01
RME2(5,12,12) = -1.96350E+02
RME2(5,13,12) = 8.27360E+01
RME2(5,14,12) = 3.09790E+01
RME2(5,15,12) = 1.74700E+01
RME2(5, 6,13) = 8.70370E-02
RME2(5, 7,13) = 2.44490E-01
RME2(5, 8,13) = 5.58060E-01
RME2(5, 9,13) = 1.20460E+00
RME2(5,10,13) = 2.68500E+00
RME2(5,11,13) = 6.89250E+00
RME2(5,12,13) = 2.66960E+01
RME2(5,13,13) = -2.34000E+02
RME2(5,14,13) = 9.33460E+01
RME2(5,15,13) = 3.49480E+01
RME2(5, 6,14) = 7.11510E-02
RME2(5, 7,14) = 1.93060E-01
RME2(5, 8,14) = 4.19970E-01
RME2(5, 9,14) = 8.45390E-01
RME2(5,10,14) = 1.68920E+00
RME2(5,11,14) = 3.56930E+00
RME2(5,12,14) = 8.80170E+00
RME2(5,13,14) = 3.29840E+01
RME2(5,14,14) = -2.74610E+02
RME2(5,15,14) = 1.04610E+02
RME2(5, 6,15) = 5.95760E-02
RME2(5, 7,15) = 1.57980E-01
RME2(5, 8,15) = 3.31920E-01
RME2(5, 9,15) = 6.36870E-01
RME2(5,10,15) = 1.18710E+00
RME2(5,11,15) = 2.25030E+00
RME2(5,12,15) = 4.57310E+00
RME2(5,13,15) = 1.09350E+01
RME2(5,14,15) = 3.99170E+01
RME2(5,15,15) = -3.18190E+02

```

C I-H TRANSITION:

```

RME2(6, 7, 6) = 3.87110E+01
RME2(6, 8, 6) = 9.90570E+00
RME2(6, 9, 6) = 4.61860E+00
RME2(6,10, 6) = 2.76000E+00
RME2(6,11, 6) = 2.60000E+00
RME2(6, 7, 7) = -3.78590E+01
RME2(6, 8, 7) = 4.55660E+01
RME2(6, 9, 7) = 1.42540E+01
RME2(6,10, 7) = 7.22410E+00
RME2(6,11, 7) = 4.50280E+00
RME2(6, 7, 8) = 2.72970E+00
RME2(6, 8, 8) = -6.34980E+01
RME2(6, 9, 8) = 5.31590E+01
RME2(6,10, 8) = 1.80360E+01
RME2(6,11, 8) = 9.53800E+00
RME2(6,12, 8) = -6.09830E+00
RME2(6, 7, 9) = 7.57200E-01
RME2(6, 8, 9) = 5.47990E+00
RME2(6, 9, 9) = -9.05600E+01
RME2(6,10, 9) = 6.14650E+01
RME2(6,11, 9) = 2.17300E+01
RME2(6,12, 9) = 1.17660E+01

```

```
RME2(6, 7,10) = 3.55900E-01
RME2(6, 8,10) = 1.60020E+00
RME2(6, 9,10) = 8.82050E+01
RME2(6,10,10) = -1.20000E+02
RME2(6,11,10) = 7.04630E+01
RME2(6,12,10) = 2.54780E+01
RME2(6, 7,11) = 2.12000E-01
RME2(6, 8,11) = 7.74700E-01
RME2(6, 9,11) = 2.66250E+00
RME2(6,10,11) = 1.27800E+01
RME2(6,11,11) = -1.52120E+02
RME2(6,12,11) = 8.01380E+01
RME2(6, 8,12) = 4.69900E-01
RME2(6, 9,12) = 1.31310E+00
RME2(6,10,12) = 3.94800E+00
RME2(6,11,12) = 1.73870E+01
RME2(6,12,12) = -1.87060E+02
```

C K-I TRANSITION:

```
RME2(7, 8, 7) = 5.20000E+01
RME2(7,11, 7) = 5.03000E+00
RME2(7, 8, 8) = -4.64760E+01
RME2(7,11, 8) = 1.03000E+01
RME2(7, 8,11) = 6.00000E-01
RME2(7,11,11) = -1.40010E+02
```

```
RETURN
END
```

**CODE C: Line Shape Construction and Instrument Convolution**

```

*****LINSHAPE.FOR*****
C
C          LINE SHAPE CONSTRUCTION
C          AND INSTRUMENT FUNCTION CONVOLUTION PROGRAM
C
C          LAST UPDATE: 20 MAY 1994
C
C          MISSION RESEARCH CORPORATION
C          1 TARA BLVD SUITE 302
C          NASHUA NH 03062-2801
C
C
C          SPEC:      SWITCH FOR INSTRUMENT FUNCTION (SPEX SPECTROMETER, CVF
C                           INTERFEROMETER, OR GENERIC).*
C          INSTFNT:   TRIANGULAR OR RECTANGULAR INSTRUMENT FUNCTION. *
C          DELAMDA:   FWHM SUPPLIED ON INPUT FOR TRIANGULAR/RECTANGULAR INST. FN.* *
C          ENAMEW:    OUTPUT FILE FOR CONVOLVED SPECTRA. *
C          NAMEIN1:   SPIN 1 OUTPUT FILE FROM CODE-B. *
C          NAMEIN2:   SPIN 2 OUTPUT FILE FROM CODE-B. *
C
C          I,J,N,M:  LOOP INDICES. *
C          NP:        ARRAY SIZE LIMIT. *
C          NUMLINE:   NUMBER OF TRANSITIONS (LINES) LOADED INTO PROGRAM. *
C          NINC:      NUMBER OF SAMPLES IN THE SPECTRUM. *
C          DIV:       LOOP INDICE (STEP) DETERMINE FROM EXTERNAL RESOLUTION. *
C
C          PI:        3.1415927
C          HP,C0:     PLANCK'S CONSTANT AND SPEED OF LIGHT. *
C          FPI:       FOUR PI STERADIANS. *
C          LINE:      LINE POSITION (MICRON). *
C          A:         EINSTEIN A-COEFFICIENT (S-1). *
C          POP:       RELATIVE POPULATION OF THE UPPER STATE OF THE TRANSITION. *
C          DENS:      TOTAL ATOM DENSITY SUPPLIED ON INPUT (CM-3). *
C          DDN:       ELECTRON DENSITY SUPPLIED BY CODE-B INPUT FILE. *
C          TE:        ELECTRON TEMPERATURE SUPPLIED BY CODE-B INPUT FILE. *
C          TEL:       ELECTRONIC TEMPERATURE SUPPLIED BY CODE-B INPUT FILE. *
C          EWDTH:     HALF-WIDTH AT HALF MAX OF STARK WIDTH (CM-1). *
C          A/C0:      ROUGH APPROXIMATION OF NATURAL LINE WIDTH (CM-1) *
C          LORLINE:   CALCULATED LORENTZ ARRAY AT EACH LINE (CM-1). *
C          TOTRAD:   SUMMATION OF ALL LORENTZ ARRAYS FOR TOTAL CONTRIBUTION. *
C          WAVLEN:   WAVELENGTH ARRAY (MICRON). *
C          F:         WAVENUMBER SPACE VARIABLE (CM-1). *
C          FO:        LINE POSITION IN WAVENUMBER SPACE (CM-1). *
C          XCONVL:    WAVELENGTH ARRAY PASSED BACK FROM CONVOLUTION SUBROUTINE. *
C          YCONVL:    CONVOLVED SPECTRUM ARRAY PASSED BACK FROM CONVOLUTION
C                           SUBROUTINE. *
C          R:         INTERNAL RESOLUTION FOR LORENTZ ARRAYS (MICRON). *
C          REXT:      EXTERNAL RESOLUTION FOR CONVOLVED OUTPUT (MICRON). *
C          ENRGY:     ENERGY OF TRANSITION (ERG). *
C          INTENS:    POPULATION, A-COEFFICIENT, AND TRANSITION ENERGY. *
C          NUMER:     VARIABLE USED FOR OPTIMIZATION. *
C          HWHM2:    VARIABLE USED FOR OPTIMIZATION. *
C
C          SUBROUTINES: LORENTZ, CONVOLV.
C          REAL FUNCTIONS: SPEX, CVF.
C
C*****

```

PROGRAM LINSHAP7  
IMPLICIT NONE

INTEGER I,J,N,M,NUMLINE,NP,NINC,DIV  
CHARACTER\*1 SPEC,INSTFNT

```

CHARACTER*12 ENAMEW, NAMEIN1, NAMEIN2
REAL PI, HP, C0, HC, FPI
REAL DELAMDA, WVST, WVEN, R, REXT, WAVLEN, F, F0, XCONVL, LINE -
REAL YCONVL, LORLINE, TOTRAD, INTENS
REAL DDN, TE, TEL, A, POP, EWDTH, ENRGY, HWHM, SLIT, PTHLEN
REAL PARTFUNC, Z, DENS
PARAMETER (NP=50000) ! ARRAY SIZE LIMIT
PARAMETER (PI=3.14159D0) ! PI
PARAMETER (HP=6.6261961D-27) ! PLANCK'S CONST ERG*S
PARAMETER (C0=2.997925D+10) ! SPEED OF LIGHT CMS-1
PARAMETER (HC=HP*C0) ! ERGCM
PARAMETER (FPI=4.D0*PI) ! 4PI SR
DIMENSION YCONVL(NP), XCONVL(-300:NP)
DIMENSION LORLINE(NP), TOTRAD(-300:NP)
DIMENSION WAVLEN(-300:NP), F(-300:NP)
DIMENSION LINE(50000), A(50000), POP(50000), EWDTH(50000)
COMMON/SPEX/ SLIT

9001 FORMAT(1X,F8.4,2X,1P,E12.3)
9000 FORMAT(1X,F9.6,5X,1PE10.4)

OPEN (10,FILE='LINSHAPE.SET', STATUS = 'OLD')

READ(10,'(A12)') NAMEIN1 ! SPIN 1 CODE-B OUTPUT FILE
READ(10,'(A12)') NAMEIN2 ! SPIN 2 CODE-B OUTPUT FILE
READ(10,'(A12)') ENAMEW ! CONVOLVED SPECTRA (OUTPUT)
READ(10,*) DENS ! TOTAL ATOM DENSITY (CM-3)
READ(10,*) PTHLEN ! PATH LENGTH (CM)
READ(10,*) WVST ! STARTING WAVELENGTH (MICRONS)
READ(10,*) WVEN ! ENDING WAVELENGTH (MICRONS)
READ(10,*) R ! INTERNAL RESOLUTION (MICRONS)
READ(10,*) REXT ! EXTERNAL RESOLUTION (MICRONS)
READ(10,'(A1)') SPEC ! SWITCH FOR INSTRUMENT FUNCTION
READ(10,*) SLIT ! SLIT WIDTH IN MILLIMETERS
READ(10,*) DELAMDA ! FWHM IN MICRONS
READ(10,'(A1)') INSTFNT ! TRIANGULAR OR RECTANGULAR INSTR. FN.

OPEN (11,FILE = NAMEIN1, STATUS = 'OLD')
OPEN (12,FILE = NAMEIN2, STATUS = 'OLD')
OPEN (13,FILE = ENAMEW, STATUS = 'UNKNOWN')
OPEN (14,FILE = 'UNCONVL.DAT', STATUS = 'UNKNOWN')

NINC=NINT((WVEN-WVST)/R)
DIV=INT(REXT/R)
IF(NINC.GT.NP)THEN
    WRITE(*,*) ' NINC > ',NP,' SPECTRAL RANGE IS TOO BIG'
    GO TO 9999
ENDIF

C ARRAY INITIALIZATION:

DO 1000 I=1,NINC
    WAVLEN(I)=WVST+FLOAT(I)*R ! WAVELENGTH ARRAY (MICRONS)
    TOTRAD(I)=0.E0 ! RADIANCE ARRAY (WCM-3SR-1MICRON-1)
1000 CONTINUE
DO 1001 I=NINC,1,-1
    F(I)=1.D+4/WAVLEN(I) ! WAVENUMBER ARRAY (CM-1)
1001 CONTINUE

WRITE(*,*) ' READING SPIN 1 LINE FILES... ! SPIN 1

READ(11,*) DDN ! ELECTRON DENSITY.
READ(11,*) TE ! ELECTRON TEMPERATURE.
READ(11,*) TEL ! ELECTRONIC TEMPERATURE.
DDN=DDN ! THIS INFO IS LABELLING INFO FOR STARK OUTPUT.
TE=TE ! VARIABLES ARE RESTORED FOR A CLEAN COMPILE

```

```

I=1
1090 READ(11,* ,END=1100) LINE(I),A(I),POP(I),EWDTH(I)
I=I+1
GOTO 1090
1100 N=I-1
Z=PARTFUNC(TEL)

DO 1300 I=1,N
IF (LINE(I).EQ.-1.) GOTO 1301
EWDTH(I)=MAX(0.D0,EWDTH(I)) ! SEE EWIDHT=-2. FLAG IN CODE-B MAIN
HWHM=EWDTH(I)+A(I)/C0 ! HWHM NATURAL LINE WIDTH LOWER LIMIT
FO=1.D4/LINE(I) ! CONVERSION FROM MICRONS TO WAVENUMBER
LINE(I)=LINE(I)*1D-04 ! CONVERSION FROM MICRONS TO CM
ENRGY=HC/LINE(I) ! ENERGY OF TRANSITION (ERG)
INTENS=1.D-7*ENRGY*A(I)*POP(I)*PTHLEN*DENS/(Z*FPI)
! WCM-2JSR-1 (1E-7W/ERGS-1)

CALL LORENTZ(F(1),FO,INTENS,HWHM,LORLINE,NINC)

DO 1200 J=1,NINC ! SUM ALL LORENTZ DISTRIBUTIONS
LORLINE(J)=LORLINE(J)*1.D4/(WAVLEN(J))**2
TOTRAD(J)=TOTRAD(J)+LORLINE(J)
1200 CONTINUE

1300 CONTINUE
1301 CONTINUE

WRITE(*,*) ' READING SPIN 2 LINE FILES...' ! SPIN 2

READ(12,*) DDN ! ELECTRON DENSITY.
READ(12,*) TE ! ELECTRON TEMPERATURE.
READ(12,*) TEL ! ELECTRONIC TEMPERATURE.
DDN=DDN ! THIS INFO IS LABELLING INFO OF STARK OUTPUT
TE=TE ! VARIABLES ARE RESTORED FOR A CLEAN COMPILE

I=1
1390 READ(12,* ,END=1400) LINE(I),A(I),POP(I),EWDTH(I)
I=I+1
GOTO 1390
1400 M=I-1
Z=PARTFUNC(TEL)

DO 1600 I=1,M
IF (LINE(I).EQ.-1.) GO TO 1601
EWDTH(I)=MAX(0.D0,EWDTH(I)) ! SEE EWIDHT=-2. FLAG IN CODE-B MAIN
HWHM=EWDTH(I)+A(I)/C0 ! HWHM NATURAL LINE WIDTH LOWER LIMIT
FO=1.D4/LINE(I) ! CONVERSION FROM MICRONS TO WAVENUMBER
LINE(I)=LINE(I)*1D-4 ! CONVERSION FROM MICRONS TO CM
ENRGY=HC/LINE(I) ! ENERGY OF TRANSITION (ERG)
INTENS=1.D-7*ENRGY*A(I)*POP(I)*PTHLEN*DENS/(Z*FPI)
! WCM-2JSR-1 (1E-7W/ERGS-1)

CALL LORENTZ(F(1),FO,INTENS,HWHM,LORLINE,NINC)

DO 1500 J=1,NINC
LORLINE(J)=LORLINE(J)*1.D4/(WAVLEN(J))**2
TOTRAD(J)=TOTRAD(J)+LORLINE(J)
1500 CONTINUE

1600 CONTINUE
1601 CONTINUE

NUMLINE=N+M
WRITE(*,*) ' NUMBER OF SPIN 1 LINES= ',N
WRITE(*,*) ' NUMBER OF SPIN 2 LINES= ',M
WRITE(*,*) ' SUM OVER STATES (PARTITION FUNCTION)= '
WRITE(*,*) ' TOTAL NUMBER OF LINES= ',NUMLINE

```

```

      WRITE(*,*) ' CONVOLVING...'
      CALL CONVOLVE(WAVLEN,TOTRAD,XCONVL,YCONVL,NINC,
&               DELAMDA,SPEC,INSTFNT)

      DO 1900 I=1,NINC,DIV
         WRITE(13,9000) XCONVL(I), YCONVL(I)
         WRITE(14,9000) WAVLEN(I), TOTRAD(I)
1900   CONTINUE

      9999  CONTINUE

      CLOSE(11)
      CLOSE(12)
      CLOSE(13)
      CLOSE(14)

      STOP
      END

```

```

SUBROUTINE LORENTZ(F,F0,INTENS,HWHM,LORLINE,NINC)
C*****
C
C THIS SUBROUTINE PASSES BACK A LORENTZIAN DISTRIBUTION FOR A
C SINGLE LINE.
C
C NINC      NUMBER OF SAMPLES IN THE SPECTRUM.
C F:        WAVENUMBER SPACE VARIABLE (CM-1).
C F0:       LINE POSITION IN WAVENUMBER SPACE (CM-1).
C INTENS:   POPULATION, A-COEFFICIENT, AND TRANSITION ENERGY.
C NUMER:    VARIABLE USED FOR OPTIMIZATION.
C HWHM2:    VARIABLE USED FOR OPTIMIZATION.
C LORLINE:  CALCULATED LORENTZ ARRAY AT EACH LINE (CM-1).
C
C*****

```

```

IMPLICIT NONE
INTEGER I,NINC
REAL PI,HWHM,HWHM2,F,F0,LORLINE,NUMER,INTENS
DIMENSION LORLINE(*),F(*)
PARAMETER (PI=3.14159D0)

NUMER=INTENS*HWHM/PI           ! LOOP OPTIMIZATION VARIABLE
HWHM2=HWHM**2                 ! HWHM SQUARED. UNITS: CM-1

DO 1000 I=1,NINC
LORLINE(I)=NUMER/((F(I)-F0)**2+HWHM2) ! LORENTZ DISTRIBUTION.
1000 CONTINUE

RETURN
END

```

```

REAL FUNCTION SPEX(WAVLEN)
C*****
C THIS FUNCTION RETURNS THE VALUE OF FWHM FOR THE SPEX INSTRUMENT
C*****
C
REAL SLIT,FWHM,WAVLEN
COMMON/SPEX/ SLIT

IF (WAVLEN.LT.8.0) THEN
   FWHM=SLIT*(-.000585*WAVLEN+.0142)
ELSE IF (WAVLEN.LT.16.) THEN
   FWHM=SLIT*(-.000585*WAVLEN+.0284)
ELSE
   FWHM=SLIT*(-.000585D0*WAVLEN+.0426D0)

```

```

END IF
SPEX=FWHM

RETURN
END

REAL FUNCTION CVF (WAVLEN)
C*****
C THIS FUNCTION RETURNS FWHM FOR THE EXCEDE III CVF4 INSTRUMENT *
C*****
IF (WAVLEN.LT.4.2E0) THEN
  FWHM=(-.00304709E0*WAVLEN+.0357227E0)*WAVLEN
ELSE IF (WAVLEN.LT.7.35E0) THEN
  FWHM=(-.00231325E0*WAVLEN+.0406235E0)*WAVLEN
ELSE IF (WAVLEN.LT.12.85E0) THEN
  FWHM=(-.00079086E0*WAVLEN+.037995E0)*WAVLEN
ELSE
  FWHM=(-.000236616E0*WAVLEN+.03491286E0)*WAVLEN
ENDIF
CVF=FWHM

RETURN
END

SUBROUTINE CONVOLVE (WAVLEN, TOTRAD, XCONVL, YCONVL, NINC,
$ DELAMDA, SPEC, INSTFNT)
C*****
C THIS SUBROUTINE CONVOLVES THE SUPERPOSED LORENTZIAN DISTRIBUTIONS WITH *
C EITHER A TRIANGULAR OR RECTANGULAR INSTRUMENT FUNCTION. *
C*****
PARAMETER (INTVL=15000)
CHARACTER*1 SPEC, INSTFNT
DIMENSION YCONVL (INTVL), XCONVL (-300:INTVL), B (-300:INTVL)
DIMENSION X (-300:INTVL), Y (-300:INTVL)
DIMENSION WAVLEN (-300:INTVL), TOTRAD (-300:INTVL)
COMMON/SPEX/ SLIT

DO 100 I=1,NINC
  X(I)=WAVLEN(I)
  Y(I)=TOTRAD(I)
  XCONVL(I)=X(I)
100   CONTINUE

C IF SPEC = S THEN CALCULATE FWHM FOR SPEX INSTRUMENT
C IF SPEC = C THEN CALCULATE FWHM FOR CVF INSTRUMENT

IF (SPEC.EQ.'S') THEN
  FWHM1=SPEX(X(1))
ELSE IF (SPEC.EQ.'C') THEN
  FWHM1=CVF(X(1))
ELSE
  FWHM1=DELAMDA
END IF

DELX1=X(2)-X(1)
NPT1=INT(FWHM1/DELX1)
DO 120 M1=0,-NPT1,-1
  X(M1)=X(1)+FLOAT(M1-1)*DELX1
  XCONVL(M1)=X(M1)
  Y(M1)=0.E0
120   CONTINUE

IF (SPEC.EQ.'S') THEN
  FWHMN=SPEX(X(NINC))

```

```

    ELSE IF (SPEC.EQ.'C') THEN
        FWHMN=CVF(X(NINC))
    ELSE
        FWHMN=DELAMDA
    END IF

    DELXN=X(NINC)-X(NINC-1)
    NPTN=INT(FWHMN/DELXN)
    DO 130 MN=NINC+1,NINC+NPTN
        X(MN)=X(NINC)+(MN-NINC)*DELXN
        XCONVL(MN)=X(MN)
        Y(MN)=0.D0
130    CONTINUE

```

C CONVOLUTION WITH THE INSTRUMENT FUNCTION:

```

    DO 1000 I=1,NINC
        IENDR=0
        IENDL=0
        BJSUM=0.D0

        IF (SPEC.EQ.'S') THEN
            FWHM=SPEX(X(I))
        ELSE IF (SPEC.EQ.'C') THEN
            FWHM=CVF(X(I))
        ELSE
            FWHM=DELAMDA
        END IF

```

C CALCULATION FOR THE RIGHT SIDE OF THE INSTRUMENT FUNCTION:

```

    DO 150 J=I,NINC+200
        B(J)=0.D0
        DELX=ABS(X(I)-XCONVL(J))

```

C TRIANGULAR INSTRUMENT FUNCTION:

```

        IF (INSTFNT.EQ.'T') THEN
            IF (DELX.GT.FWHM) GO TO 155
            B(J)=1.D0-(DELX/FWHM)
        ENDIF

```

C RECTANGULAR INSTRUMENT FUNCTION:

```

        IF (INSTFNT.EQ.'R') THEN
            IF (DELX.GT.FWHM) GO TO 155
            B(J)=1.D0
        ENDIF

```

C SPEX INSTRUMENT FUNCTION:

```

        IF (INSTFNT.EQ.'S') THEN
            IF (DELX.GT.FWHM) GO TO 155
            B(J)=1.D0-(DELX/FWHM)
        ENDIF

```

```

        IENDR=IENDR+1
        BJSUM=BJSUM+B(J)

```

150 CONTINUE

C CALCULATION FOR THE LEFT SIDE OF THE INSTRUMENT FUNCTION

```

155    DO 160 J=I-1,-NINC-200,-1
        B(J)=0.D0
        DELX=ABS(X(I)-XCONVL(J))

```

C TRIANGULAR INSTRUMENT FUNCTION:

```

        IF (INSTFNT.EQ.'T') THEN
            IF (DELX.GT.FWHM) GO TO 190
            B(J)=1.D0-(DELX/FWHM)

```

```

        ENDIF

C RECTANGULAR INSTRUMENT FUNCTION:
    IF (INSTFNT.EQ.'R') THEN
        IF (DELX.GT.FWHM) GO TO 190
        B(J)=1.D0
    ENDIF

C SPEX INSTRUMENT FUNCTION:
    IF (INSTFNT.EQ.'S') THEN
        IF (DELX.GT.FWHM) GO TO 190
        B(J)=1.D0-(DELX/FWHM)
    ENDIF

    IENDL=IENDL+1
    BJSUM=BJSUM+B(J)
160    CONTINUE

C NORMALIZATION OF WEIGHTING FACTORS
190    DO 200 K=I-IENDL,I+IENDR-1
        B(K)=B(K)/BJSUM
200    CONTINUE

C CONVOLUTION:
    YCONVL(I)=0.D0
    DO 300 L=I-IENDL,I+IENDR-1
        YCONVL(I)=YCONVL(I)+Y(L)*B(L)
300    CONTINUE
1000   CONTINUE

    RETURN
    END

FUNCTION PARTFUNC(TEL)
INTEGER S,N,L
INTEGER NMAX,NMIN,LMAX,LMIN
REAL F,PARTFUNC
REAL KB,H,C,HC,KT,TEL,G
DIMENSION F(30,30,0:3)
COMMON/TERMS/F

PARAMETER (KB=1.38066E-16)      ! BOLTZMANN CONST ERG/K.
PARAMETER (H=6.62608E-27)      ! PLANCK'S CONST ERGS.
PARAMETER (C=2.99792E+10)      ! SPEED OF LIGHT CM/S.
PARAMETER (HC=H*C)

CALL BASIS                      ! FILL ENERGY MATRIX WITH VALUES.

KT=KB*TEL                      ! ELECTRONIC TEMPERATURE * BOLTZ CONST.
PARTFUNC=0.0                      ! PARTITION FUNCTION VARIABLE INITIALIZATION.

DO 1000 S=0,2

    IF(S.EQ.0) THEN
        NMAX=2                  ! THE LOOP INDICES ARE 'HARD WIRED' BECAUSE
        NMIN=2                  ! OF THE DIFFERENCE IN SIZE OF THE BASIS SETS
        LMAX=1                  ! WITH RESPECT TO SINGLETS, TRIPLETS AND
        LMIN=1                  ! QUINTETS.
    END IF
    IF(S.EQ.1) THEN
        NMAX=11                 ! LOOP INDICES FOR THE SPIN 1 BASIS STATES.
        NMIN=2
        LMAX=7
        LMIN=0
    END IF

```

```

END IF
IF(S.EQ.2) THEN
  NMAX=11           ! LOOP INDICES FOR THE SPIN 2-BASIS STATES.
  NMIN=3
  LMAX=7
  LMIN=0
END IF

G=(2.D0*(FLOAT(S))+1.D0)*(2.D0*(FLOAT(S))+1.D0) ! DEGENERACY.
DO 1200 L=LMAX,LMIN,-1 ! FORMAT FOR CODE-B
  DO 1100 N=NMAX,NMIN,-1 ! INPUT.
    IF(N.LE.L) GOTO 1200 ! 'L=N-1'
    IF(N.EQ.2.AND.L.EQ.0) GOTO 1200 ! NO 2S STATE.
    IF(N.GE.9.AND.L.EQ.LMAX) GOTO 1100 ! NO 2S STATE.
    PARTFUNC=PARTFUNC+G*EXP(-HC*F(N,L,S)/KT)

1100   CONTINUE
1200   CONTINUE
1000   CONTINUE

RETURN
END

```

```

SUBROUTINE BASIS
*****
C
C THIS SUBROUTINE FILLS THE ARRAY, F(N,L,S), WITH THE ENERGY LEVELS OF
C ATOMIC OXYGEN INCLUDING TRIPLETS, QUINTETS, AND THE THREE LOWEST
C SINGLETS, I.E., 2P4(1D), 2P4(1S), AND 3S(1D). THE ARRAY INDICES ARE
C PRINCIPAL QUANTUM NUMBER, THE VECTOR SUM OF THE ORBITAL MAGNETIC
C QUANTUM NUMBER, AND SPIN.
C
*****
REAL F
DIMENSION F(30,30,0:3)
COMMON/TERMS/F

F(2,1,0) = 33792.5830      ! 2P4 (1D)
F(2,1,1) = 77.9750        ! 2P4 (3P)
F(2,2,0) = 15867.8620      ! 2P4 (1S)

F(3,0,1) = 76794.9780
F(3,0,2) = 73768.2000
F(3,1,1) = 88630.9770
F(3,1,2) = 86629.0890
F(3,2,0) = 102662.0260      ! 3S (1D)
F(3,2,1) = 97488.4760
F(3,2,2) = 97420.7480

F(4,0,1) = 96225.0490
F(4,0,2) = 95476.7280
F(4,1,1) = 99681.0510
F(4,1,2) = 99094.0650
F(4,2,2) = 102865.5620
F(4,2,1) = 102908.4200
F(4,3,2) = 102968.2490
F(4,3,1) = 102968.3430

F(5,0,1) = 102411.9950
F(5,0,2) = 102116.6980
F(5,1,1) = 103870.0200
F(5,1,2) = 103626.2730
F(5,2,1) = 105409.0080
F(5,2,2) = 105385.3850
F(5,3,1) = 105441.7240
F(5,3,2) = 105441.6450
F(5,4,1) = 105446.2900

```

$F(5, 4, 2) = 105446.2900$   
 $F(6, 0, 1) = 105165.2320$   
 $F(6, 0, 2) = 105019.3070$   
 $F(6, 1, 1) = 105912.0310$   
 $F(6, 1, 2) = 105788.6840$   
 $F(6, 2, 1) = 106765.8030$   
 $F(6, 2, 2) = 106751.4620$   
 $F(6, 3, 1) = 106785.2010$   
 $F(6, 3, 2) = 106785.1600$   
 $F(6, 4, 1) = 106787.8910$   
 $F(6, 4, 2) = 106787.8910$   
 $F(6, 5, 1) = 106788.5800$   
 $F(6, 5, 2) = 106788.5800$   
  
 $F(7, 0, 1) = 106627.9340$   
 $F(7, 0, 2) = 106545.3540$   
 $F(7, 1, 1) = 107072.0000$   
 $F(7, 1, 2) = 106982.0000$   
 $F(7, 2, 1) = 107582.7770$   
 $F(7, 2, 2) = 107573.4870$   
 $F(7, 3, 1) = 107595.1470$   
 $F(7, 3, 2) = 107595.1400$   
 $F(7, 4, 1) = 107596.9600$   
 $F(7, 4, 2) = 107596.9600$   
 $F(7, 5, 1) = 107597.3600$   
 $F(7, 5, 2) = 107597.3600$   
 $F(7, 6, 1) = 107597.4800$   
 $F(7, 6, 2) = 107597.4800$   
  
 $F(8, 0, 1) = 107497.2240$   
 $F(8, 0, 2) = 107446.0360$   
 $F(8, 1, 1) = 107778.0000$   
 $F(8, 1, 2) = 107720.0000$   
 $F(8, 2, 1) = 108114.0000$   
 $F(8, 2, 2) = 108106.0790$   
 $F(8, 3, 1) = 108120.7900$   
 $F(8, 3, 2) = 108120.7900$   
 $F(8, 4, 1) = 108122.0200$   
 $F(8, 4, 2) = 108122.0200$   
 $F(8, 5, 1) = 108122.2900$   
 $F(8, 5, 2) = 108122.2900$   
 $F(8, 6, 1) = 108122.3800$   
 $F(8, 6, 2) = 108122.3800$   
 $F(8, 7, 1) = 108122.4100$   
 $F(8, 7, 2) = 108122.4100$   
  
 $F(9, 0, 1) = 108056.0000$   
 $F(9, 0, 2) = 108021.4000$   
 $F(9, 1, 1) = 108244.0000$   
 $F(9, 1, 2) = 108205.0000$   
 $F(9, 2, 1) = 108476.7000$   
 $F(9, 2, 2) = 108470.2000$   
 $F(9, 3, 1) = 108481.1100$   
 $F(9, 3, 2) = 108481.1100$   
 $F(9, 4, 1) = 108481.9800$   
 $F(9, 4, 2) = 108481.9800$   
 $F(9, 5, 1) = 108482.1800$   
 $F(9, 5, 2) = 108482.1800$   
 $F(9, 6, 1) = 108482.2400$   
 $F(9, 6, 2) = 108482.2400$   
  
 $F(10, 0, 1) = 108436.3000$   
 $F(10, 0, 2) = 108412.0000$   
 $F(10, 1, 1) = 108568.0000$   
 $F(10, 1, 2) = 108541.0000$   
 $F(10, 2, 1) = 108736.1000$

F(10,2,2) = 108731.5000  
F(10,3,1) = 108738.8200  
F(10,3,2) = 108738.8200  
F(10,4,1) = 108739.4600  
F(10,4,2) = 108739.4600  
F(10,5,1) = 108739.6100  
F(10,5,2) = 108739.6100  
F(10,6,1) = 108739.6500  
F(10,6,2) = 108739.6500

F(11,0,1) = 108705.5000  
F(11,0,2) = 108688.4000  
F(11,1,1) = 108803.0000  
F(11,1,2) = 108782.0000  
F(11,2,1) = 108927.2000  
F(11,2,2) = 108924.7300  
F(11,3,1) = 108929.4800  
F(11,3,2) = 108929.4800  
F(11,4,1) = 108929.9600  
F(11,4,2) = 108929.9600  
F(11,5,1) = 108930.0700  
F(11,5,2) = 108930.0700  
F(11,6,1) = 108930.1100  
F(11,6,2) = 108930.1100

RETURN  
END

**This Page Intentionally Left Blank**

**APPENDIX C**

**APOSTLE OUTPUT**  
**LINE POSITIONS, EINSTEIN COEFFICIENTS**

OI Triplet Transitions ( $\lambda$ , Einstein Coefficient, and transition assignment)

2.0536	1.579E+05	8p- 4d	4.0356	1.161E+08	5g- 4f
2.0550	8.621E+05	10d- 5p	4.0972	7.645E+05	5d- 4f
2.0680	3.311E+05	11s- 5p	4.2212	1.017E+05	8p- 5d
2.1337	1.611E+07	7f- 4d	4.5414	1.545E+06	8d- 6p
2.1459	1.109E+05	7p- 5s	4.5609	9.367E+06	4p- 3d
2.1605	1.755E+07	7g- 4f	4.5743	9.502E+06	7f- 5d
2.1671	1.757E+05	7d- 4f	4.5976	8.834E+03	11p- 7s
2.1708	1.265E+06	9d- 5p	4.6218	1.334E+06	11f- 6d
2.1900	4.640E+05	10s- 5p	4.6399	1.491E+07	7g- 5f
2.3563	1.983E+06	8d- 5p	4.6489	1.682E+07	7h- 5g
2.3889	6.807E+05	9s- 5p	4.6536	9.759E+04	7f- 5g
2.4018	2.548E+05	7p- 4d	4.6625	1.907E+06	11g- 6f
2.5795	2.838E+07	6f- 4d	4.6643	4.691E+05	9s- 6p
2.6181	3.735E+07	6g- 4f	4.6681	2.038E+06	11h- 6g
2.6333	3.325E+05	6d- 4f	4.6685	5.916E+04	11d- 6f
2.6934	3.421E+06	7d- 5p	4.6694	2.577E+04	11f- 6g
2.7489	7.059E+03	11p- 6s	4.6696	2.421E+06	11i- 6h
2.7569	1.065E+06	8s- 5p	4.6699	6.479E+03	11g- 6h
2.8405	2.105E+06	11f- 5d	4.6706	2.949E+05	7d- 5f
2.8571	5.062E+05	6p- 5s	4.9087	2.082E+04	11p- 6d
2.8668	2.592E+06	11g- 5f	5.0684	1.813E+06	10f- 6d
2.8691	5.178E+04	11d- 5f	5.1170	2.673E+06	10g- 6f
2.8704	1.808E+06	11h- 5g	5.1237	3.019E+06	10h- 6g
2.8709	1.322E+04	11f- 5g	5.1254	2.063E+06	10i- 6h
2.8935	3.932E+07	4p- 4s	5.1258	3.831E+04	10f- 6g
2.9388	1.266E+04	10p- 6s	5.1258	8.458E+04	10d- 6f
2.9464	3.333E+04	11p- 5d	5.1259	1.015E+04	10g- 6h
3.0032	2.865E+06	10f- 5d	5.1545	1.651E+04	10p- 7s
3.0324	3.641E+06	10g- 5f	5.2445	2.339E+05	7p- 6s
3.0355	7.270E+04	10d- 5f	5.3902	3.386E+05	11d- 7p
3.0364	2.686E+06	10h- 5g	5.5488	2.906E+04	10p- 6d
3.0372	1.918E+04	10f- 5g	5.8299	2.557E+06	9f- 6d
3.0985	7.330E+07	4d- 4p	5.8935	3.932E+06	9g- 6f
3.1656	4.569E+04	10p- 5d	5.9022	4.811E+06	9h- 6g
3.2481	2.584E+04	9p- 6s	5.9044	3.779E+06	9i- 6h
3.2551	4.049E+06	9f- 5d	5.9053	1.755E+04	9g- 6h
3.2892	5.379E+06	9g- 5f	5.9059	6.139E+04	9f- 6g
3.2939	4.304E+06	9h- 5g	5.9119	1.280E+05	9d- 6f
3.2949	1.072E+05	9d- 5f	5.9854	2.846E+06	7d- 6p
3.2951	2.964E+04	9f- 5g	6.0092	4.879E+05	10d- 7p
3.3166	4.504E+05	11d- 6p	6.0133	1.915E+05	7p- 5d
3.3293	4.850E+05	6p- 4d	6.1218	1.552E+05	11s- 7p
3.4533	6.930E+06	6d- 5p	6.1879	3.683E+04	9p- 7s
3.5274	6.562E+04	9p- 5d	6.3084	7.743E+05	8s- 6p
3.5410	6.379E+05	10d- 6p	6.4978	1.994E+07	5d- 5p
3.5798	2.192E+05	11s- 6p	6.7650	4.388E+04	9p- 6d
3.6259	1.846E+06	7s- 5p	6.8586	8.910E+06	5p- 5s
3.6617	1.227E+07	5s- 4p	7.1190	7.505E+05	9d- 7p
3.6876	6.010E+06	8f- 5d	7.2664	1.615E+07	6f- 5d
3.7309	8.518E+06	8g- 5f	7.3298	2.260E+05	10s- 7p
3.7369	7.724E+06	8h- 5g	7.3801	3.768E+06	8f- 6d
3.7390	5.017E+04	8f- 5g	7.4255	8.955E+05	11f- 7d
3.7421	1.694E+05	8d- 5f	7.4285	3.019E+07	6g- 5f
3.8274	6.449E+04	8p- 6s	7.4500	5.442E+07	6h- 5g
3.8991	9.541E+05	9d- 6p	7.4688	2.378E+05	6f- 5g
3.9474	5.793E+07	5f- 4d	7.4804	6.153E+06	8g- 6f
3.9615	3.118E+05	10s- 6p	7.4917	1.379E+06	11g- 7f

7.4940	8.524E+06	8h- 6g	12.2627	6.280E+05	11f- 8d
7.4974	8.489E+06	8i- 6h	12.3189	1.028E+07	7g- 6f
7.4994	3.525E+04	8g- 6h	12.3538	1.762E+07	7h- 6g
7.5013	1.770E+06	11h- 7g	12.3583	1.010E+06	11g- 8f
7.5024	1.099E+05	8f- 6g	12.3625	2.892E+07	7i- 6h
7.5033	1.750E+06	11i- 7h	12.3704	9.047E+04	7g- 6h
7.5041	1.563E+04	11g- 7h	12.3755	1.429E+06	11h- 8g
7.5042	3.878E+03	11h- 7i	12.3790	1.749E+06	11i- 8h
7.5046	3.585E+04	11f- 7g	12.3810	1.153E+04	11h- 8i
7.5072	6.215E+04	11d- 7f	12.3813	2.605E+04	11g- 8h
7.5256	2.099E+05	8d- 6f	12.3845	4.452E+04	11f- 8g
7.5524	5.891E+05	6d- 5f	12.3876	2.320E+05	7f- 6g
7.6583	1.050E+04	11p- 8s	12.4006	6.381E+04	11d- 8f
7.7207	4.041E+06	6s- 5p	12.5380	3.789E+05	7d- 6f
8.1952	1.387E+04	11p- 7d	13.3869	1.325E+04	11p- 9s
8.6502	1.216E+06	10f- 7d	13.3905	2.825E+06	6p- 6s
8.6951	1.152E+05	8p- 7s	13.3909	6.118E+04	9p- 8s
8.7017	2.724E+05	11d- 8p	13.9684	1.623E+06	7s- 6p
8.7389	1.925E+06	10g- 7f	14.3123	6.605E+05	9d- 8p
8.7516	2.610E+06	10h- 7g	14.5138	1.031E+04	11p- 8d
8.7543	2.836E+06	10i- 7h	14.6370	2.327E+05	11d- 9p
8.7556	6.881E+03	10h- 7i	15.1235	3.841E+04	9p- 7d
8.7558	2.551E+04	10g- 7h	15.1906	1.863E+05	10s- 8p
8.7576	5.503E+04	10f- 7g	16.0046	8.474E+05	10f- 8d
8.7646	9.097E+04	10d- 7f	16.1637	1.397E+06	10g- 8f
9.3390	2.165E+04	10p- 8s	16.1920	2.083E+06	10h- 8g
9.5969	1.288E+06	8d- 7p	16.1980	2.791E+06	10i- 8h
9.8795	8.190E+04	8p- 6d	16.2014	2.195E+04	10h- 8i
10.1500	2.055E+04	10p- 7d	16.2030	4.497E+04	10g- 8h
10.1626	3.561E+05	9s- 7p	16.2127	7.132E+04	10f- 8g
10.3993	3.435E+06	5p- 4d	16.2520	9.628E+04	10d- 8f
10.4373	4.046E+05	10d- 8p	18.5869	2.439E+06	8f- 7d
10.7817	1.212E+05	11s- 8p	18.9799	4.195E+06	8g- 7f
11.1317	1.705E+06	9f- 7d	19.0357	6.922E+06	8h- 7g
11.2761	2.802E+06	9g- 7f	19.0469	1.096E+07	8i- 7h
11.2966	4.107E+06	9h- 7g	19.0545	3.927E+04	8h- 7i
11.3010	5.133E+06	9i- 7h	19.0600	1.040E+05	8g- 7h
11.3033	1.448E+04	9h- 7i	19.0902	1.769E+05	8f- 7g
11.3043	4.699E+04	9g- 7h	19.2733	2.407E+05	8d- 7f
11.3103	9.254E+04	9f- 7g	19.5313	3.459E+04	10p- 9s
11.3436	1.422E+05	9d- 7f	19.5780	2.811E+06	7d- 7p
11.7127	7.100E+06	6d- 6p	19.8798	1.363E+06	6p- 5d
12.0577	5.766E+06	7f- 6d			

OI Quintet Transitions ( $\lambda$ , Einstein Coefficient, and transition assignment)

2.0554	2.660E+05	7p- 5s	4.2834	3.770E+04	8p- 5d
2.0600	7.568E+04	8p- 4d	4.3152	3.400E+06	8d- 6p
2.0644	3.061E+06	9d- 5p	4.4710	2.048E+04	11p- 7s
2.0896	8.208E+05	10s- 5p	4.4789	8.249E+05	9s- 6p
2.1143	2.758E+07	7f- 4d	4.5254	1.585E+07	7f- 5d
2.1604	2.926E+07	7g- 4f	4.5913	2.244E+06	11f- 6d
2.1714	3.497E+05	7d- 4f	4.6397	2.486E+07	7g- 5f
2.2322	4.720E+06	8d- 5p	4.6489	2.803E+07	7h- 5g
2.2753	1.212E+06	9s- 5p	4.6536	1.629E+05	7f- 5g
2.4293	1.177E+05	7p- 4d	4.6624	3.180E+06	11g- 6f
2.5334	7.951E+06	7d- 5p	4.6681	3.396E+06	11h- 6g
2.5513	4.811E+07	6f- 4d	4.6694	4.302E+04	11f- 6g
2.6180	1.919E+06	8s- 5p	4.6696	4.034E+06	11i- 6h
2.6181	6.225E+07	6g- 4f	4.6699	1.080E+04	11g- 6h
2.6433	6.568E+05	6d- 4f	4.6738	1.148E+05	11d- 6f
2.6515	1.648E+08	4d- 4p	4.6908	5.740E+05	7d- 5f
2.6577	1.825E+04	11p- 6s	4.9248	6.316E+03	11p- 6d
2.7233	1.103E+06	6p- 5s	5.0109	3.691E+04	10p- 7s
2.7645	6.729E+07	4p- 4s	5.0318	3.039E+06	10f- 6d
2.8216	3.593E+06	11f- 5d	5.0950	4.713E+05	7p- 6s
2.8395	3.144E+04	10p- 6s	5.1169	4.456E+06	10g- 6f
2.8667	4.321E+06	11g- 5f	5.1237	5.032E+06	10h- 6g
2.8704	3.013E+06	11h- 5g	5.1254	3.438E+06	10i- 6h
2.8709	2.208E+04	11f- 5g	5.1258	6.395E+04	10f- 6g
2.8710	1.021E+05	11d- 5f	5.1259	1.692E+04	10g- 6h
2.9441	1.351E+04	11p- 5d	5.1379	1.635E+05	10d- 6f
2.9820	4.877E+06	10f- 5d	5.1474	7.692E+05	11d- 7p
3.0323	6.069E+06	10g- 5f	5.5880	8.536E+03	10p- 6d
3.0364	4.476E+06	10h- 5g	5.6029	6.054E+06	7d- 6p
3.0372	3.202E+04	10f- 5g	5.6847	4.145E+07	5d- 5p
3.0396	1.429E+05	10d- 5f	5.7159	1.094E+06	10d- 7p
3.1390	6.104E+04	9p- 6s	5.7815	4.259E+06	9f- 6d
3.1690	1.808E+04	10p- 5d	5.8603	2.765E+05	11s- 7p
3.1887	1.042E+06	11d- 6p	5.8934	6.553E+06	9g- 6f
3.1998	1.548E+07	6d- 5p	5.9022	8.019E+06	9h- 6g
3.2303	6.868E+06	9f- 5d	5.9044	6.298E+06	9i- 6h
3.2891	8.967E+06	9g- 5f	5.9053	2.924E+04	9g- 6h
3.2939	7.173E+06	9h- 5g	5.9059	1.025E+05	9f- 6g
3.2951	4.949E+04	9f- 5g	5.9346	2.463E+05	9d- 6f
3.3019	2.101E+05	9d- 5f	5.9761	7.404E+06	4p- 3d
3.3084	2.679E+07	5s- 4p	6.0254	7.811E+04	9p- 7s
3.3981	1.458E+06	10d- 6p	6.0337	1.388E+06	8s- 6p
3.4210	2.279E+05	6p- 4d	6.2633	7.390E+04	7p- 5d
3.4257	3.400E+06	7s- 5p	6.6244	1.513E+07	5p- 5s
3.4486	3.804E+05	11s- 6p	6.7195	1.656E+06	9d- 7p
3.5466	2.513E+04	9p- 5d	6.8798	1.263E+04	9p- 6d
3.6558	1.027E+07	8f- 5d	6.9930	4.077E+05	10s- 7p
3.7027	1.428E+05	8p- 6s	7.1440	2.631E+07	6f- 5d
3.7292	2.146E+06	9d- 6p	7.1786	8.168E+06	6s- 5p
3.7308	1.420E+07	8g- 5f	7.3029	6.210E+06	8f- 6d
3.7369	1.288E+07	8h- 5g	7.3747	1.487E+06	11f- 7d
3.7390	8.375E+04	8f- 5g	7.4281	5.031E+07	6g- 5f
3.7531	3.308E+05	8d- 5f	7.4500	9.070E+07	6h- 5g
3.8120	5.436E+05	10s- 6p	7.4690	3.968E+05	6f- 5g
3.8819	9.602E+07	5f- 4d	7.4802	1.025E+07	8g- 6f
4.0354	1.935E+08	5g- 4f	7.4852	2.262E+04	11p- 8s
4.1371	1.496E+06	5d- 4f	7.4916	2.298E+06	11g- 7f

7.4940	1.421E+07	8h- 6g	13.8941	4.941E+05	11d- 9p
7.4974	1.415E+07	8i- 6h	14.4509	3.433E+05	10s- 8p
7.4994	5.875E+04	8g- 6h	14.7946	1.608E+03	11p- 8d
7.5013	2.950E+06	11h- 7g	15.8042	1.384E+06	10f- 8d
7.5024	1.834E+05	8f- 6g	15.8350	1.031E+04	9p- 7d
7.5033	2.917E+06	11i- 7h	16.1637	2.327E+06	10g- 8f
7.5041	2.604E+04	11g- 7h	16.1920	3.471E+06	10h- 8g
7.5042	6.463E+03	11h- 7i	16.1980	4.651E+06	10i- 8h
7.5046	5.984E+04	11f- 7g	16.2014	3.659E+04	10h- 8i
7.5211	1.192E+05	11d- 7f	16.2030	7.494E+04	10g- 8h
7.5705	4.029E+05	8d- 6f	16.2127	1.190E+05	10f- 8g
7.6346	1.144E+06	6d- 5f	16.3744	1.817E+05	10d- 8f
8.2746	2.970E+03	11p- 7d	16.9065	6.013E+06	7d- 7p
8.3006	5.972E+05	11d- 8p	18.2714	3.888E+06	8f- 7d
8.5132	2.247E+05	8p- 7s	18.9796	6.988E+06	8g- 7f
8.5812	2.006E+06	10f- 7d	18.9933	7.629E+05	10d- 9p
8.7388	3.209E+06	10g- 7f	19.0357	1.154E+07	8h- 7g
8.7516	4.349E+06	10h- 7g	19.0469	1.826E+07	8i- 7h
8.7543	4.727E+06	10i- 7h	19.0545	6.545E+04	8h- 7i
8.7556	1.147E+04	10h- 7i	19.0600	1.733E+05	8g- 7h
8.7558	4.252E+04	10g- 7h	19.0902	2.953E+05	8f- 7g
8.7576	9.184E+04	10f- 7g	19.2456	6.566E+04	10p- 9s
8.8000	1.735E+05	10d- 7f	19.5718	4.573E+05	8d- 7f
8.8962	2.786E+06	8d- 7p			
9.1327	4.475E+04	10p- 8s			
9.6209	6.627E+05	9s- 7p			
9.8863	8.728E+05	10d- 8p			
10.3248	2.640E+04	8p- 6d			
10.3263	2.172E+05	11s- 8p			
10.3358	4.444E+03	10p- 7d			
10.3866	1.408E+07	6d- 6p			
11.0178	2.783E+06	9f- 7d			
11.2760	4.669E+06	9g- 7f			
11.2966	6.845E+06	9h- 7g			
11.3010	8.555E+06	9i- 7h			
11.3033	2.413E+04	9h- 7i			
11.3043	7.832E+04	9g- 7h			
11.3103	1.545E+05	9f- 7g			
11.4278	2.699E+05	9d- 7f			
11.8529	9.279E+06	7f- 6d			
12.1448	1.034E+06	11f- 8d			
12.3183	1.712E+07	7g- 6f			
12.3538	2.936E+07	7h- 6g			
12.3583	1.683E+06	11g- 8f			
12.3625	4.820E+07	7i- 6h			
12.3704	1.508E+05	7g- 6h			
12.3755	2.382E+06	11h- 8g			
12.3790	2.914E+06	11i- 8h			
12.3810	1.922E+04	11h- 8i			
12.3813	4.341E+04	11g- 8h			
12.3845	7.430E+04	11f- 8g			
12.3878	3.873E+05	7f- 6g			
12.4387	1.212E+05	11d- 8f			
12.6851	7.309E+05	7d- 6f			
12.9975	4.796E+06	6p- 6s			
13.1456	3.026E+06	5p- 4d			
13.1475	2.679E+04	11p- 9s			
13.1759	1.170E+05	9p- 8s			
13.2158	3.135E+06	7s- 6p			
13.3298	1.396E+06	9d- 8p			